Department of Dermatology, Allergology and Venereology, Helsinki University Hospital and Päijät-Häme Central Hospital
Doctoral Programme in Clinical Research, University of Helsinki

DIAGNOSIS AND TREATMENT OF PREMALIGNANT CHANGES OF PHOTODAMAGED SKIN:
Novel Hyperspectral Imaging and New Therapeutical Aspects

Academic Dissertation

Noora Neittaanmäki-Perttu

To be presented with the permission of the Faculty of Medicine of the University of Helsinki for public examination at the Skin and Allergy Hospital Auditorium, Meilahdentie 2, Helsinki on May 29th at 12 o'clock, noon

Supervised by:
Professor Erna Snellman, M.D., PhD.

Department of Dermatology,

Tampere University and Tampere University Hospital, Tampere, Finland

and

Professor Olli Saksela, M.D., PhD.

Department of Dermatology, Allergology and Venereology, University of Helsinki and Helsinki University Central Hospital

Supervisery group:

Professor Annamari Ranki, M.D., PhD

Department of Dermatology, Allergology and Venereology, University of Helsinki and Helsinki University Central Hospital

and

Mari Grönroos, M.D., PhD

Department of Dermatology and Allergology,

Päijät-Häme Central Hospital, Lahti, Finland

Reviewed by:

Professor Veli-Matti Kähäri, M.D., PhD.

Department of Dermatology,

University of Turku and Turku University Hospital

and

Professor Raimo Suhonen, M.D, PhD.

University of Kuopio, Finland

Opponent:

Professor Olle Larkö, M.D., PhD.

Sahlgrenska Akademin, Göteborgs Universitet, Sweden

ISBN 978-951-51-1215-6 (baberback)

ISBN 978-951-51-1216-3 (PDF)

http://ethesis.helsinki.fi

Hansaprint 2015

To my father

TABLE OF CONTENTS

LIST OF ORIGINAL PUBLICATIONS

This thesis is based on the following publications that are referred to in the text by their Roman numerals.

I Delineating margins of lentigo maligna using a hyperspectral imaging system. **Neittaanmäki-Perttu N**, Grönroos M, Jeskanen L, Pölönen I, Ranki A, Saksela O, Snellman E. *Acta DV* 2015; 95: 549–552.

II Detecting field cancerization using a hyperspectral imaging system. **Neittaanmäki-Perttu N**, Grönroos M, Tani T, Pölönen I, Ranki A, Saksela O, Snellman E. *Lasers Surg Med* 2013;45(7):410-7.

This publication was also part of Ilkka Pölönen's PhD dissertation: Discovering knowledge in various applications with a novel hyperspectral imager, University of Jyväskylä 2013.

III Daylight photodynamic therapy for actinic keratoses: A randomized double-blinded non-sponsored prospective study comparing aminolevulinic acid nanoemulsion (BF-200) with methyl-5-aminolaevulinate. **Neittaanmäki-Perttu N**, Karppinen TT, Grönroos M, Tani T, Snellman E. *Br J Dermatol* 2014; 171:1172–80.

IV Photodynamic therapy of actinic keratoses: a randomized prospective non-sponsored study on cost-effectiveness comparing conventional LED and daylight-mediated treatment. **Neittaanmäki-Perttu N**, Grönroos M, Karppinen TT, Snellman E, Rissanen P. Submitted to peer review.

In addition, unpublished data are presented.

LIST OF ABBREVIATIONS

AFL	ablative fractional laser
AK	actinic keratosis
BCC	basal cell carcinoma
BF-200 ALA	5-aminolaevulinic acid nanoemulsion
CE	cost-effectiveness
CEA	cost-effectiveness analysis
DFMO	difluoromethylornithine
DL-PDT	daylight photodynamic therapy
FD	fluorescence diagnosis
FOV	field of view
GR	grenz-ray
HAL	hexylaminolaevulinate
HE	haematoxylin and eosin
HIS	hyperspectral imaging system
ICER	incremental cost-effectiveness ratio
IPL	intense pulsed light
LM	lentigo maligna
LMM	lentigo maligna melanoma
LN	liquid nitrogen
MAL	methylaminolaevulinate
MED	minimal erythema dose
MMS	Mohs micrographic surgery
MMP	matrix metalloproteinases
NMSC	non-melanoma skin cancer
OCT	optical coherence tomography
ODC	ornithine decarboxylase
PBG	porphobilinogen

PBGD	porphobilinogen deaminase
PDT	photodynamic therapy
PpIX	protoporphyrin IX
p53	p53 tumor suppressor gene
QALY	quality adjusted life year
RAS	rat sarcoma
RDEB	recessive dystrophic epidermolysis bullosa
RCM	reflectance confocal microscopy
ROS	reactive oxygen species
SCC	squamous cell carcinoma
cSCC	cutaneous squamous cell carcinoma
SPF	sun protection factor
SSE	staged surgical excision
UVR	ultra-violet radiation
UV	ultra violet
5-ALA	5-aminolaevulinic acid
95%CI	95% confidence interval

ABSTRACT

Background and purpose: As the skin cancer burden continues to increase, there is an urgent need for novel methods for the early detection of skin cancers, and for new cost-effective treatments. The hyperspectral imaging system (HIS) is a novel technique, which offers the dual advantages of allowing the imaging of large skin areas rapidly and non-invasively. Daylight photodynamic therapy (DL-PDT), with the advantages of excellent tolerability and convenience, is an attaractive therapy for actinic keratoses (AK) and field cancerization.This thesis aimed to enable early and effective treatment of common premalignancies of photo-damaged skin.The first purpose of this thesis was to evaluate the feasibility of HIS in the detection of field cancerized skin and in the detection of ill-defined borders of lentigo maligna (LM) and lentigo maligna melanoma (LMM). In addition, this thesis aimed to further develop the treatment of field cancerized skin with photodynamic therapy using a novel photosensitizer in combination with daylight (DL-PDT), and to evaluate the cost-effectiveness of DL-PDT.

Methods: This thesis included four non-sponsored prospective clinical studies. The novel prototype HIS, used in studies **I-II**, was developed for the study at the VTT Technical Research Centre of Finland. The technique enabled *in vivo* imaging of the skin prior to surgical procedures and produced abundance maps of the affected skin areas. The results were verified by histopathology. Study **III** was a randomized double-blinded intra-individual split-face trial comparing novel photosensitizer formulation, 5-aminolaevulinate nanoemulsion (BF-200 ALA) with methyl-5-aminolaevulinate (MAL) in DL-PDT of AKs. In addition to blinded clinical and histological treatment efficacy, tolerability of the treatment was assessed. Study **IV** evaluated the cost-effectiveness of MAL-DL-PDT compared to conventional MAL-LED-PDT.

Results: In studies **I-II** HIS showed its feasibility in both the detection of subclinical borders of ill-defined lentigo malignas (LM) and lentigo maligna melanomas (LMM), and in the detection of early subclinical actinic keratoses (AK). In study **I** HIS accurately detected 20 of 23 (87%) of the LM/LMM borders as confirmed by histology. HIS was useful i.e. detected the lesion borders more accurately than a clinician using Wood's light in 11 of 23 (47.8%) cases. Six re-excisions could have been avoided with HIS. In 3/23 cases (13%) HIS was not in concordance with the histopathology, while in two cases HIS showed lesion extensions which were not verified histologically (wrong positive) and in one case HIS missed the subclinical extension (wrong negative). In study **II** with 12 patients and 52 clinical AKs, HIS accurately detected all the clinical lesions in addition to numerous areas of subclinical damage. HIS findings matched the histopathological findings in all 33 biopsied areas (AK, n=28, photo-damaged skin, n=5), revealing 16 subclinical lesions of which 10 were not detected by fluorescence diagnosis.

In study **III** (13 patients, 177 lesions) in a per patient (half-face) analysis BF-200 ALA cleared thin AKs more effectively than did MAL (p=0.027). In per lesion analysis the complete clearance rates were 84.5% for BF-200 ALA, and 74.2% for MAL (p=ns). The area response rates, including also the new appeared lesions

(i.e.preventive effect), were 79.8% for BF-200 ALA and 65.6% for MAL, p=0.044. Histologically, DL-PDT effectively cleared all the signs of dysplasia in 61.5% lesions treated with BF-200 ALA and in 38.5% with MAL (p=ns). The mean decrease in p53 expression was 54.4% with BF-200 ALA, 34 % with MAL (p=ns). DL-treatment was nearly painless with both photosensitizers. BF-200 ALA and MAL DL-treatments were similarly tolerated as regards to adverse reactions.

In study **IV** 70 patients (210 target lesions) randomized to receive DL-PDT or LED-PDT with MAL, at six months the patient complete response rates were 15 of 35 (42.9%) and 24 of 35 (68.6%), (p=0.030) and lesion clearance rates were 72.4% and 89.2%, respectively (p=0.0025). DL-PDT required significantly less time at the clinic (p<0.0001) and could be used with lower total costs (€132) compared to conventional LED-PDT (€170), p=0.022. However, in terms of cost-effectiveness MAL-DL-PDT was found to give less value for money compared to MAL-LED-PDT. The incrementl cost-effectiveness ratio (ICER) showed a monetary gain of €147 per unit of effectiveness lost. Thus, the use of DL-PDT instead of LED-PDT would decrease the healing probability but only low incremental cost savings would be achieved. The costs per complete responder were €308 for MAL DL-PDT and €248 for MAL LED-PDT, p= 0.004.

Conclusions: The more accurate pre-surgical assessment of the subclinical borders of LM and LMM with HIS could lead to fewer re-excixions, which furthermore could reduce the burden to both patients and clinics. In addition, the early non-invasive detection of skin field cancerization could enhance the treatment process by revealing the as yet subclinical areas in need of treatment, and could possibly aid the monitoring of treatment efficacy. Even though HIS was found to be useful in these two indications, more studies are warranted to qualify the optimal mathematical algorithms for diagnostic use. The use of a novel photosensitizer formulation, BF-200 ALA, in DL-PDT could lead to lower costs and increase the efficacy. Interestingly, the efficacy of DL-PDT with BF-200 ALA was approaching the efficacy achieved with conventional LED-PDT. As field cancerized skin should be treated as a chronic disease requiring repeated treatments, DL-PDT offers a painless and convenient option for this purpose. However, DL-PDT with MAL provided less value for money compared to conventional MAL-PDT. The cost-effectiveness of BF-200 ALA in DL-PDT for AKs needs further studies.

TIIVISTELMÄ

Ihosyöpien määrä on jatkuvassa räjähdysmäisessä kasvussa maailmanlaajuisesti. Tämä kuormittaa terveydenhuoltoa merkittävästi. Taudinmäärityksen kehittäminen, siten että ihosyövät pystytään tunnistamaan jo varhaisessa vaiheessa sekä hoitoalueiden aiempaa tarkempi määrittäminen lisähoitojen välttämiseksi, ovat keskeisiä keinoja rajoittaa hoitokustannuksia. Lisäksi on tarve uusille, helposti toteutettaville ja kustannusvaikuttaville hoitomuodoille.

Väitöstyössä tutkittiin uutta Suomessa kehitettyä hyperspektritekniikkaa ihon okasolusyövän varhaisasteiden, ns. subkliinisten aktiinikeratoosien, tunnistamisessa, sekä huonosti rajautuvien ihon pintamelanoomien, ns. lentigo malignojen, rajojen määrittämisessä lisäleikkausten välttämiseksi. Väitöstyössä selvitettiin myös uuden päivänvalolla toteutettavan fotodynaamisen hoidon (päivänvalo-PDT) tehoa ja turvallisuutta, sekä kustannusvaikuttavuutta ihon okasolusyövän esiasteiden eli aktiinikeratoosien hoidossa. Tutkimuksessa tutkittiin kahta iholle levitettävää valoherkistäjävoidetta, joista toista ei aiemmin ole käytetty tällä indikaatiolla. Tutkimuksella haluttiin kehittää ihosyöpien varhaisvaiheiden hoitoprosessia resursseja ja kustannuksia säästäväksi, sekä löytää uusia, hyvin siedettyjä mutta tehokkaita hoitomuotoja. Väitöskirjatyöhön sisältyi neljä prospektiivista kliinistä tutkimusta.

Hyperspektrikuvantaminen todettiin hyödylliseksi varhaisten, silmälle vielä näkymättömien, aktiinikeratoosien havaitsemisessa. Lisäksi hyperspektrikuvantamisen avulla kyettiin havaitsemaan silmälle näkymättömiä lentigo maligna-kasvainten rajoja. Tämä auttaa entistä tarkemmin määrittämään hoitoalueet ja saattaa mahdollistaa entistä tarkemman hoidon seurannan. Turhilta lisäleikkauksilta saatetaan välttyä. Päivänvalo-PDT osoittautui tehokkaaksi, turvalliseksi ja paremmin siedetyksi kuin perinteinen fotodynaaminen hoito (keinovalo-PDT), missä valolähteenä on keinovalo. Päivänvalo-PDT vei vähemmän sekä poliklinikan henkilökunnan että potilaan aikaa. Keinovalo-PDT osoittautui kuitenkin kustannustehokkaammaksi kuin päivänvalohoito, kun lääkkeenä oli perinteinen valoherkistäjä, metyyliaminolevulinaatti (MAL). Uusi valoherkistäjälääkkeet, aminolevulinaatti nanoemulsio (BF-200 ALA), osoittautui tehokkaaksi ja turvallisia aktiinikeratoosien päivänvalo-PDT:ssa.

Hyperspektrikuvantaminen on lupaava uusi tekniikka silmälle näkymättömien ihosyöpien varhaisvaiheiden havaitsemissa sekä hoitoa tarvitsevan ihosyöpäalueen määrittämisessä. Päivänvalo-PDT mahdollistaa laajojen valovaurioalueiden hoidon tehokkaasti ja kivuttomasti. Uusien tehokkaiden valoherkistäjien käyttö saattaa parantaa hoitotehoa, laskea hoitokustannuksia ja siten lisätä hoidon kustannustehokkuutta.

INTRODUCTION

Skin cancers are the most common cancers in fair-skinned populations worldwide (*Kozma et al 2014,)*. An increase in skin cancer incidence has been a significant problem around the world, especially in countries with high levels of ultra-violet radiation (UVR) exposure, but also in northern countries. Currently, in Sweden skin cancers are a cause of greater mortality than traffic accidents (*Eriksson et al 2014*). The high incidence rates also bring a significant economical burden, ***Figure 1*** (*Gordon et al 2014, Erikson et al 2014*). Due to aging of populations and increases in cumulative and habitual UVR-exposure, skin cancer incidence will continue to increase sharply in upcoming years (*Gordon et al 2014, Mayer et al 2014*). Consequently, the health care costs of skin cancer treatments are expected to expand dramatically. In Sweden the direct health care costs for skin cancers have increased by 23% over a 6-year period (2005-2011) causing approx.102 million euros total annual costs (*Eriksson et al 2014*). As the cost of treatment for metastatic skin cancers are very high and economically poor value for money more focus should be put on prevention and the treatment of skin cancers at their very early stages (*Gordon et al 2014*).

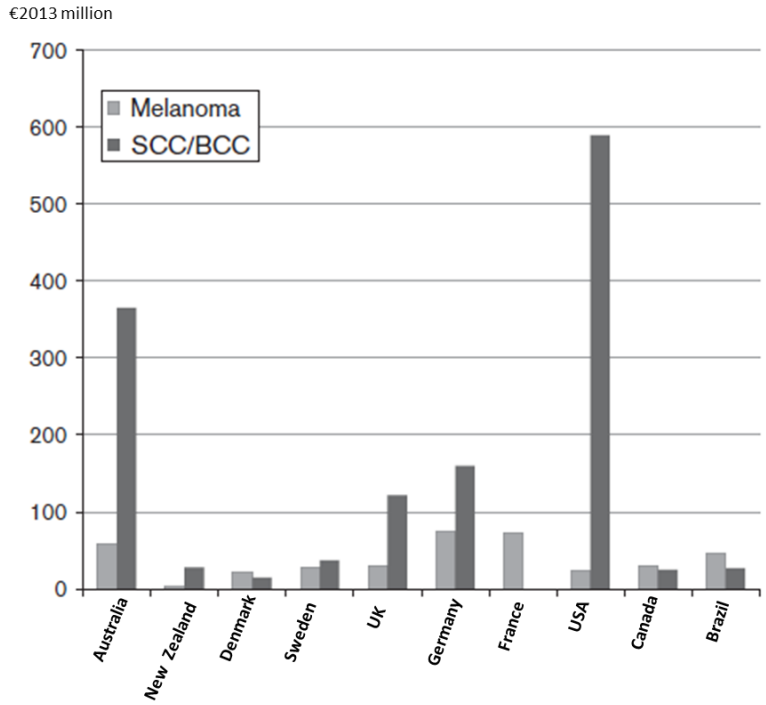

Figure 1. Annual direct health care costs of skin cancer burden (million euros 2013). SCC=squamous cell carcinoma, BCC= basal cell carcinoma. From *Gordon et al 2014*, with the permission of Wolters Kluwer Health.

Actinic keratoses (AK), regarded as early stage precursors of cutaneous squamous cell carcinoma (cSCC), are the most common premalignancies among humans and the third most frequent reason for visiting a dermatologist (*Salasche 2000, Quaedvlieg et al 2006).* AK prevalence among the elderly varies from approx. 11-34% in the Northern hemisphere up to 50% in Australia (*Frost et al 2000, Memon et al 2000, Schaefer et al 2014).* The total annual direct costs for AKs vary from 18 million euros in Sweden in 2011 to up to1.2

billion USD in the US in 2004 (*Neidecker et al 2009, Eriksson et al 2014*). AKs typically occur as multiple lesions in sun-damaged skin areas, typically in facial or scalp areas (*Callen et al 1997)*. As 25-75% of AK patients require repeated treatments, AKs should be treated as a chronic disease (*Ceilley et al 2013*). Thus, an ideal AK treatment has high clinical response rates with low recurrence with minimal side effects, good cosmetic outcome and low costs.

AKs are the earliest clinically detectable areas of skin undergoing carcinogenesis. Skin field cancerization refers to the presence of early invisible changes on photo-damaged skin surrounding the visible AKs (*Braakhuis et al 2003).* Despite the relatively low transformation risk for a single AK lesion to develop into cSCC, the presence of multiple lesions in a sun-damaged field over several years increases the risk for the development of invasive and potentially metastatic cSCCs (*Dodson et a 1991).* Current guidelines recommend the use of field-directed therapies also targeting subclinical, non-apparent AKs instead of ablative lesion-targeted therapies (*Braathen et al 2012, Stockfleth 2012, Ceilley et al 2013, Micali et al 2014*). Photodynamic therapy (PDT) offers several advantages in the treatment of AKs. Large field areas can be treated with high clearance rates, short treatment and adverse reaction periods, and excellent cosmetic outcome (*Braathen et al 2012)*. Novel photosensitizers and the development of better tolerated treatment processes like daylight-PDT (DL-PDT), make PDT an even more appealing treatment choice (*Szeimies et al 2010*[2]*, Wiegell et al 2008)*.

Lentigo maligna (LM) and lentigo maligna melanoma (LMM) are the most common melanoma subtypes in the facial area, and like AKs, are also related to chronic sun-exposure. Their location in sun-damaged skin poses both diagnostic and therapeutic challenges. The presence of benign pigmented lesions in sun-damaged skin in the vicinity of LM is difficult to diagnose both clinically and histologically. In addition, the amelanotic subclinical extension of the lesions often leads to higher recurrence rates than for other melanomas (*McKenna et al 2006*).

Histopathology, based on the detection of characteristics of sliced tissue using light microscopy, is the gold standard for the diagnosis of skin cancer. However, being an invasive and slow procedure, it has its limitations. Recently, many non-invasive diagnostic methods have emerged for skin cancer detection (*Calin et al 2013)*.

This thesis represents hyperspectral imaging as a novel non-invasive tool for the detection of field cancerized skin and ill-defined borders of lentigo malignas. In addition, this thesis aims to further develop PDT using a novel photosensitizer formulation in combination with daylight for the treatment of field cancerized skin. These approaches aim to enable early and effective treatment of common (pre)malignancies of photo-damaged skin. Furhermore, this thesis evaluates the cost-effectiveness of DL-PDT and LED-PDT.

REVIEW OF THE LITERATURE

1. ACTINIC KERATOSES AND FIELD CANCERIZATION

1.1 Definitions and clinical characteristics

Aktinic keratosis (AK) was first described byDubreuilh in 1896 as "the seed of cancer". The histological continuum from AK (at that time named keratosis senilis) to cutaneous squamous cell carcinoma (cSCC) was first introduced by Freudenthal in 1926. In 1938 Sutton claimed that AK is an early superficial cSCC (*Heaphy et al 2000)*. In 1958 Pinkus renamed keratosis senilis, actinic keratosis, meaning a thickened/scaly growth caused by electromagnetic irradiation. Since *field cancerization* was first presented in the upper gastro-intestinal tract in 1953, similar findings of multifocal precancerous changes surrounding the primary tumor have been described in several organs including the skin, oropharynx, esophagus, stomach, lung, colon, anus, cervix and bladder (*Vatve et al 2007*).

To date AKs are regarded as the earliest clinically detectable areas of dysplastic keratinocytes in the continuum towards invasive and potentially metastatic cSCCs (*Callen et al 1997, Ulrich C 2009*), *Figure 2*. Histologically, AKs represent dysplastic intraepithelial keratinocytes lacking dermal invasion (*Cockerell 2000*). Clinically AKs appear as rough, scaly, skin-colored, erythematous or pigmented lesions of varying diameter (mm-cm) on sun-exposed skin areas. The differential diagnosis include cSCC, basal cell carcinoma (BCC), Bowens disease, seborrheic keratoses, stucco keratoses, lichenoid keratoses, porokeratosis, arsenical keratoses, early keratoacanthoma, acantholytic acantoma, verruca vulgaris, acrokeratosis verruciformis, psoriasis, seborrheic dermatitis, lichen planus, discoid lupus erythematosus and in the case of pigmented lesions also lentigo maligna must be considered (*Venna et al 2005, Lee et al 2014*).

Field cancerization defines a larger skin area where visible AKs are surrounded by early clinically undetectable changes with genetic oncogenic alterations spread over the sun-damaged field. Field cancerization involves a risk for multiple keratinocytic skin cancers (*Braakhuis et al 2003, Braathen et al 2012*).

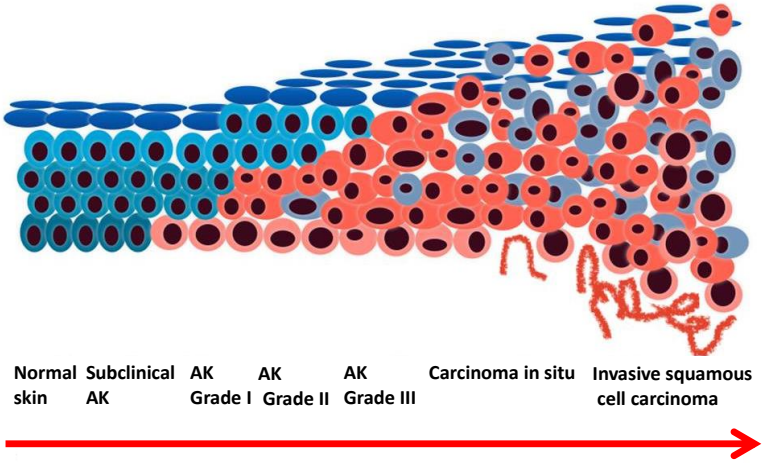

Figure 2. The skin cancer progression model: actinic keratoses (AK) represent the earliest clinically detectable phase in the continuum from sun-damaged skin towards invasive cutaneous squamous cell carcinoma (cSCC). Figure by Dr Giovanni Pellacani, edited with permission.

1.2 Prevalence and incidence

Non-melanoma skin cancers (NMSC) i.e. cSCC and BCC are the most common cancers in fair-skinned populations with an annual incidence of 3.5 million in the United States alone (*Kozma et al 2014*). The majority of NMSCs are BCCs, but 20% are cSCCs that are capable of metastasing and causing death (*Salasche 2000*). In Denmark, the age-standardized incidence rate for NMSC was 119/100 000 for men and 117/100 000 in women in 2006-2010 (*Bentzen et al 2013*). Patients with multiple AKs but no previous NMSCs have very high risk of developing cSCCs (3,198/100000 person years) (*Foote et al 2001*). In Finland the age-standardize incidence of cSCCs is 96/100 000 person years (*Finnish Cancer Registry statistics 2011*).

AK prevalence (proportion of individuals with at least one AK in the population) is clearly associated with latitude ranging from 2.7% (16-70 yrs.)-11.5% (60-70 yrs.) in Germany (*Schaefer et al 2014)*, to 5.9% in women and 15.4% in men over 40 years and 18.2% in women and 34.1% in men over 70 years in northern England (*Memon et al 2000*), to approx. 11-25% among adults in Ireland and northern USA (*Frost et al 1994*), to 50% (30-69 yrs.) in Australia (*Frost et al 2000*) with higher prevalences in men and increases with age in both sexes. In Austria, AK prevalence among dermatologic outpatients (≥30 yrs.) is as high as 31% (*Eder et al 2014*). Previous AK dramatically increases the risk for further AKs. Annual incidence (proportion of individuals in the population who develop a new AK) was 84% in men and 69% in women with AK present at the baseline examination, and 15% in men and 7% in women without previous AK (*Frost et al 2000*). In South Florida, the number of AKs treated by dermatologists was approx. 4500 per 100 000

per year in the population aged 0-65 years and approx. 110 000 per 100 000 per year in the population older than 65 (*Nestor et al 2012*). The incidence of AKs or carcinoma in situs is not registered in Finland.

High incidence rates of AKs raise a significant economic issue. AKs tend to have high recurrence rates requiring repeated treatments and thus, multiple office visits (*Warino et al 2006*). In 2011 in Sweden the direct costs for AKs, including mostly the outpatient care, were 18 million euros accounting for over 10% of all the skin cancer costs *(Eriksson et al 2014)*. In 2004 in the US the estimated total annual direct costs of AKs including office visits, drugs, hospital costs were 1.2 billion USD and indirect costs including lost workdays, restricted activity days and caregiver lost workdays were 295 million USD (*Neidecker et al 2009*).

Etiology and risk factors

The most important factor in NMSC development is solar UV radiation (UVR), absorbed by the keratinocyte DNA, which can act as a tumor initiator and promoter. The UVR spectrum contains UVC (200–290 nm), UVB (290–320 nm) and UVA (320–400 nm). UVC is mostly absorbed by the Earth's ozone layer, ***Figure 3*** (*D'Orazio et al 2013, Kozma et al 2014)*. Both UVB (290-320 nm), penetrating the superficial dermis, and UVA (320-400 nm) penetrating the deep dermis, can cause DNA damage leading to carcinogenesis. UVR can cause direct DNA-damage or indirect oxidative damage via reactive oxygen species (ROS). In addition, UVR causes immunosuppression by inducing immunosuppressive molecules and by affecting cells in the adaptive immune system (*Chen et al 2013*). UV-radiation also stimulates inflammation via cyclooxygenase 2 (COX-2), a cascade which stimulates the proliferation of (pre)malignant keratinocytes (*Maltusch et al 2011, Elmets et al 2014*). AKs and cSCCs are caused by chronic cumulative UV-radiation while BCCs develop due to acute intermittent UV damage (*Kraft et al 2014*).

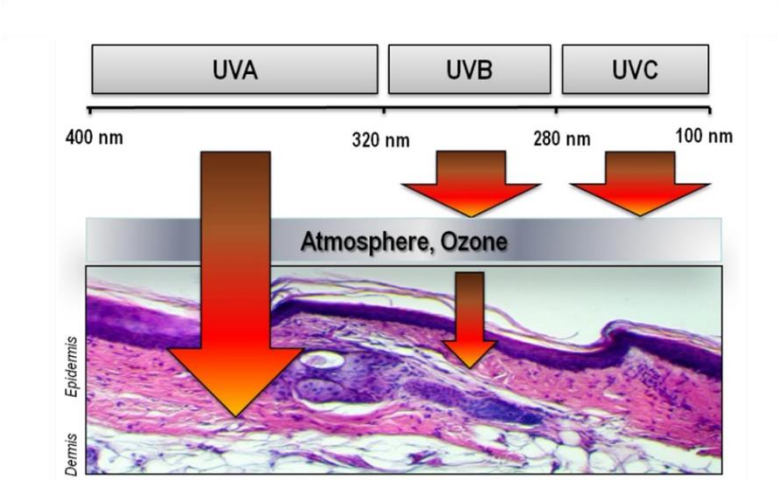

Figure 3. UVR penetration in the skin. From *D'Orazio et al 2013*, with permission.

In 1993, Campbell and colleagues found UV-induced mutations in the p53 tumor suppressor gene to be an early event in the development of cSCCs (*Cockerell 2000, Heaphy et al 2000*). The p53 gene, located in chromosome 17, regulates the cell cycle, DNA repair and apoptosis after DNA damage. Mutations in p53 lead to impaired cell repair and resistance to apoptosis and thus, proliferation of mutant keratinocytes with elevated expression of mutated p53 protein (*Holmes et al 2007, Kozma et al 2014)*. Mutations in p53 occur in 50% of all human cancers, and in almost all carcinomas (*Benjamin et al 2007*). Mutations in p53 have been documented in 0-60% of AKs, in 15-96% of cSCCs, and also in chronically sun-exposed skin supporting the theory of a continuum from healthy skin through DNA-damage to AK, invasive cSCC, and finally potentially mortal metastasis (*Callen et al 1997, Einspahr et al 1997*). In addition, mutations of RAS (rat sarcoma) proto-oncogenes (HRAS, NRAS, KRAS) and of BRM tumor suppressor gene frequently occur in cSCCs (*Kraft et al 2014, Chen et al 2013*). Recently also novel biomarkers including matrix metalloproteinases (MMP) have been found to be involved in the development of AKs and cSCCs (*Kivisaari et al 2008, Kivisaari et al 2013, de Oliveira et al 2015*).

AKs serve as biomarkers for individuals at risk for the development of an invasive cSCC (*Salasche 2000*). Fair skin type (*Fitzpatrick 1988*), red or blonde hair, blue eyes, sunburns in childhood, solar lentigines, wrinkles and elastosis, freckles on the arms, old age, male sex, low educational level, outdoor occupation, residency in a tropical country, photosensitizing drugs (thiazile diuretics, amiodarone, diltiazem) increase the risk for AK (*Traianou et al 2012, Schaefer et al 2014)*. Patients with solid organ transplantation and immunosuppressive medication (azathioprine, calcineurin inhibitors) have a 250 times as high risk for AK than do immunocompetent patients (*Tessari et al 2012*). Dark skin protects against actinic damage due to its higher concentration of UV absorbing epidermal melanin (*Holmes et al 2007*). Some genetic syndromes such as albinism (lack of melanin), xeroderma pigmentosum (impaired DNA repair) and epidermodysplasia verruciformis (decreased cell-mediated immunity) increase the risk for AKs and cSCCs (*Kraft et al 2014)*. Also patients with recessive dystrophic epidermolysis bullosa (RDEB) have increased risk for cSSC (*Kivisaari et al 2008*). Exposure to X-ray or psoralen ultra-violet A (PUVA) therapy induces the risk for AK (*Zalaudek et al 2014*). Also human papilloma virus (HPV) seems to play a role in the pathogenesis of AK and NMSC (*Forslund et al 2003*). Chemical carcinogens like smoking and arsenic increase the risk for cSCC (*Chen et al 2013*).

1.3 Histopathology and immunohistochemistry

The diagnosis of AK is mainly clinical. Histopathological sampling is used in order to rule out invasive cSCC. The accuracy of clinical diagnosis of AK (positive predictive value) among dermatologists varies between 74% and 94% (*Holmes et al 2007, Tschen et al 2006*). AKs representing induration or inflammation, diameter >1 cm, rapid enlargement, bleeding, erythema or ulceration should be considered for histopathological verification. Other characteristics arising suspicion of progression into cSCC include pigmentation, palpability, pain, pruritus and hyperkeratosis (*Quaedvlieg et al 2006)*.

AK and cSCC are indistinguishable by cytology alone, and thus the histological diagnosis also requires architectural characteristics. Histological criteria for AK include pleomorphic atypical keratinocytes: nuclei that are hyperchromatic, an increased mitotic rate, and disordered maturation; an irregularly achantotic epidermis; irregular dermo-epidermal junction; and alternating hyperkeratosis, parakeratosis and orthokeratosis. Usually signs of photoaging: elastosis in the dermis, destruction of its fibrillar structure, and perivascular or lichenoid inflammation is present, ***Figure 4.*** AKs can be graded, analogously to cervical intraepithelial neoplasia, as grade I (mild, atypia of basal keratinocytes of the lower one third of the epidermis), grade II (intermediate; atypia of keratinocytes of at least the lower two thirds of the epidermis), and grade III (severe; diffuse atypical keratinocyte proliferation involving the full epidermal thickness) (*Cockerell 2000, Tsatsou et al 2012*). Histological variants of AK include pigmented, acantholytic, bowenoid, and hyperplastic AKs with a common characteristic of atypical keratinocytes confined to the epidermis (*Tsatsou et al 2012)*. Bowen's disease is an intraepithelial cSCC defined by full-thickness severe squamous atypia, where the cells are in complete disorder ("windblown appearance"). Parakeratosis consisting of atypical cells is prominent. In conntrast to AKs, the atypical infiltrate replaces the epithelium of adnexal structures. When atypical keratinocytes invade basal membrane down to the dermis, forming lobules of atypical epithelium, the lesion is defined as invasive cSCC (*Elder et al 2013*).

Sun-damaged skin includes dermal elastosis and atrophy, but only minor cytologic atypia, epidermal thickening and inflammation (*Carpenter et al 2004*). The skin adjacent to AKs often has many similar histological characteristics to an AK and has been suggested to represent very early AKs (*Einspahr et al 2014*). Early field cancerized areas represent genetically abnormal, but not yet histologically detectable, altered cells (*Braakhuis et al 2003*).

Molecular markers, like p53, a marker for apoptosis and cell cycle arrest; and Ki67, a marker for cell proliferation, can be used in the detection of early carcinogesis. These markers are detectable before the occurrence of histologically detectable cellular changes, and increase as the carcinogenesis progresses (*Carpenter et al 2004)*. In immunohistochemical stainings, p53 overexpression is seen as accumulated epidermal patches, ***Figure 4***. Increased p53 expression, as an indicator of mutated p53, has been reported in 0-80% of AKs and in 0-92% of cSCCs, but also in lower amounts in apparently normal sun-exposed skin. The variability of the methods used (frozen vs.fixed tissue) and antibodies explain the variability of the results. Some, but not all, immunohistochemical stainings distinguish between the mutant and wild-type p53 protein (*Einspahr et al 1997*). In addition, immunohistochemical markers for inflammation (COX-2, CD3, CD8), and angiogenesis (CD31) are also involved in the carcinogenic process (*Maltusch et al 2011)*. Molecular markers can provide information about the mechanism of action and efficacy of the AK treatments (*Einspahr et al 1997, Carpenter et al 2004, Maltusch et al 2011*).

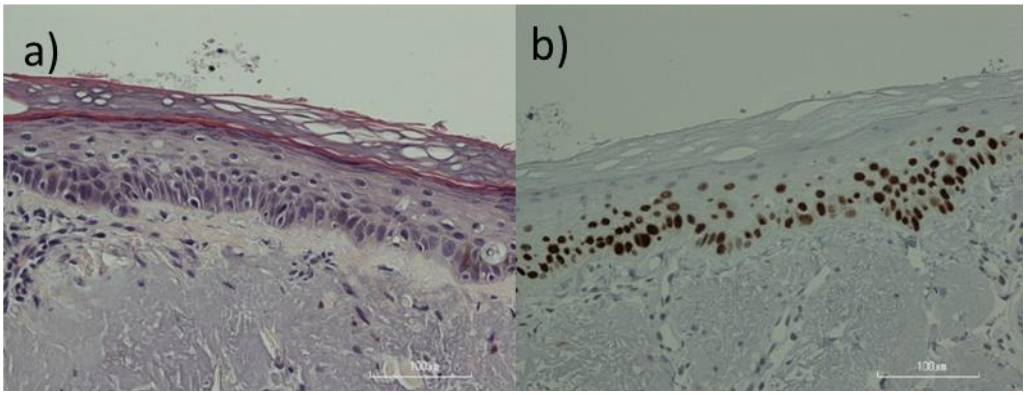

Figure 4, Grade II AK a) in HE-staining showing hyperkeratosis/parakeratosis, atypical keratinocytes in the lower two thirds of the epidermis and solar elatosis b) the same lesion with p53 immunostaining showing increased p53 expression. Figure by Taneli Tani, MD, PhD, with permission.

2. LENTIGO MALIGNA AND LENTIGO MALIGNA MELANOMA

2.1 Definitions and clinical characteristics

Lentigo maligna (LM) was first described by Hutchinson in 1912 as "the presence and overgrowth of atypical melanocytes at the dermal epidermal junction of chronically sun-damaged skin" (*Bosbous et al 2009*). Histologically, LM represents an *in situ* melanoma, which is limited to the epidermis and lacks dermal invasion. Lentigo maligna melanoma (LMM) represents the development of dermal invasion in an area of the LM (*Bosbous et al 2009*). LMM is one of the four histologic subtypes of invasive malignant melanoma, the others being superficial spreading, nodular and acral lentiginous (*Reed et al 2011*).

Typical clinical presentation of LM and LMM include a brown-gray to dark colored black macule with poorly defined borders on sun exposed skin areas, typically on the head and neck. Size and color may vary and the lesions tend to slowly enlarge over time (*Bosbous et al 2010*). A rare amelanotic LM type may resemble eczema, Bowen's disease or superficial BCC (*Reed et al 2011*). Previous treatments may alter the appearance of LM and lead to misdiagnosis (*Bosbous et al 2010*). Clinically in situ LM and invasive LMM are hard to distinguish (*Hazan et al 2008*). The presence of increasing variation in color, border irregularity, expanding lesion size, regression or nodules may predict tumor invasion (*McKenna et al 2006*). It is also often difficult to clinically distinguish LM from benign lentigos, thin seborrheic keratoses and pigmented AKs. In addition, differential diagnosis includes cSCC, pigmented BCC and dysplastic nevus (*Bosbous et al 2010*). LMs are characterized with a tendency to develop into subclinical peripheral disease, and an inadequacy of histological visualization leading to high recurrence rates (*McKenna et al 2006*).

LMs represent a prolonged horizontal growth phase and thus their progression to invasion is slow. However, also rapid progression to LMM has been reported (*McKenna et al 2006*). The prognosis of invasive LMM is

similar to that of other types of invasive melanomas (*Cox et al 1996, Kraft et al 2014*). The estimated lifetime risk for LM progression to invasive LMM varies between 5-50% with a higher risk associated with larger lesions (*Bosbous et al 2010, Erickson et al 2010*). It should be noted that initial partial biopsies may not provide accurate histological diagnoses. In partial removal or punch biopsy, there is 8-29% risk that an invasive component will be missed (*Kunishige et al 2012, Iorizzo et al 2013*).Thus, excisional biopsy is the most accurate technique to diagnose LM and LMM. However, in the cases of large lesions, clinicians are often forced to use punch biopsies for diagnostic use (*McLeod et al 2011*).

LM and LMM have higher recurrence rates than other melanoma subtypes (*Bosbous et al 2010*). Twenty-three percent of the initially inadequately excised LMs show an invasive component at the time of recurrence imposing the risk for metastatic disease. Furthermore, 33% of the recurrent primary LMMs appear at greater Breslow-thickness than the initial tumor (*DeBloom et al 2010)*. Thus, adequate initial removal of the lesions is crucial for the prognosis.

2.2 Prevalence and incidence

LM and LMM form the most common melanocytic malignancy of the head and neck regions *(Bosbous et al 2010*). Worldwide LMM subtype represents 4-15% of all invasive melanomas while higher incidence is seen for superficial spreading melanoma and nodular melanoma (*Swetter et al 2005, Youl et al 2013*). In California, LM is the most prevalent in situ subtype of melanoma (79-83%) and the incidence of both LM and LMM is rising above the other melanoma subtypes *(Swetter et al 2005)*. Also in Sweden, LM is the most prevalent in situ melanoma subtype with age-standardized incidence of 1.29/100000 in men and 1.53/100000 in women in 1993-98 (*Hemminki et al 2003*).In northern USA, age-and sex-adjusted LM incidence was 13.7 per 100 000 person years in 2004-2007 with a 7-fold increase since 1970s and with the highest incidence in men between 70 and 79 years (91.3 per 100000 person years) (*Mirzoyev et al 2014*). In Denmark over a15-year period between 1997 and 2011, LM incidence had markedly increased from 0.6 to 1.5 and from 0.5 to1.4 cases per 100 000 person years in women and men, respectively (*Toender et al 2014*). The increased incidence of *in situ* melanomas may partially be caused by a growing awareness of skin cancers and earlier removal of suspicious lesions (*Toender et al 2014)*.

There are no accurate costs data available for LM/LMM treatments. Invasive malignant melanoma is the cost driver of skin cancers with over 90 million total annual costs accounting for over 50% of all the skin cancer costs in Sweden, while the annual costs for in situ melanomas were only 1 million (0.6% of the total skin cancer costs) (*Eriksson et al 2014*). As the costs of the in situ disease are significantly lower than those of advanced or metastasized melanoma (*Alexandrescu 2009*), early detection and treatment are crucial.

2.3 Etiology and risk factors

UV-radiation induces increased melanin production and proliferation of melanocytes. UV-induced DNA damage leads to impaired cell cycle arrest and dysregulated proliferation of melanocytes (*Reed et al 2011*).

Unlike melanomas on the trunk, LMs are associated with NMSC and AK, markers of chronic UV-exposure, but not the number of nevi (*Gaudy-Marqueste et al 2009, Kvaskoff et al 2013*). In addition, BRAF mutations, commonly found in melanoma types associated with intermittent sun-exposure, are rare in LMMs (*Maldonado et al 2003, Sasaki et al 2004, Stadelmeyer et al 2014*). Familial risk for LM is low (*Hemminki et al 2003*). Interestingly, p53 mutations, present in AKs and NMSCs, are commonly seen in LMMs (*Purdue et al 2005*). These facts support a theory that LMs have a distinct etiologic and genetic pathway i.e. "chronic sun-exposure pathway" compared to other melanoma types, which are associated with the "nevus pathway" and intermittent sun-exposure. Thus LMs are likely to originate from acquired mutations due to chronic sun-damage on field cancerizated skin (*Gaudy-Marqueste et al 2009, Kvaskoff et al 2013, Kraft et al 2014).* In addition mutations in the KIT gene (encoding the stem cell factor receptor tyrosine kinase) may play a role in the pathogenesis of LM (*Kraft et al 2014).* In addition to chronic sun exposure, other risk factors for LM include fair skin type, low tanning ability, red or blonde hair, history of sunburns, and freckling at adolescence. LM risk increases in males and with old age (*Mirzoyev et al 2014)*. The average age of which LM/LMM occurs is 66-72 years which is higher than that of other melanoma subtypes (45-57 years) (*Bosbous et al 2010*). Thus LMs are considered to be "late onset" melanomas *(Kraft et al 2014).*

2.4 Histopathology and immunohistochemistry

In situ melanomas, including LM, represent the earliest histologically detectable stage of malignant melanoma (*Reed et al 2011*). LMs are characterized by atypical junctional melanocytic overgrowth and underlying photo-damage. The histological characteristics of LM include atypical melanocytes at the dermal-epidermal junction arranged in solitary units and small nests, pagetoid spread of atypical melanocytes, confluence of melanocytes replacing the basilar layer, solar elastosis, periadnexal extension of atypical melanocytes, epidermal atrophy and loss of the rete ridges, a dermal infiltrate composed of lymphocytes and melanophages and multinucleated melanocytes, ***Figure 5*** (*Flotte et al 1999*). LMM is defined when dermal invasion of atypical melanocytes is found (*Tannous et al 2000*).

Some dermatopathologists regard LM as the initial phase of a more aggressive form of malignant melanoma in situ (MIS), LM type (*Flotte et al 1999, Tannous et al 2000*). Compared to LM, MIS LM type has additional features such as individual cells invading the upper epidermis (pagetoid spread) and confluent growth. However, this distinction is rarely used in the literature and the treatment for LM and MIS LM type is similar.

Histological different diagnoses of LM include pigmented AK, seborrheic keratosis, pigmented BCC, porocarcinoma, pigmented epidermotrophic metastases and Paget's disease (*Wiltz et al 2007).* In parts of LM also benign lesions may be present, and thus partial biopsies may lead to sampling error and misdiagnosis *(Dalton et al 2005).*

The presence of LM on the sun-damaged skin poses a diagnostic challenge to dermatopathologists (*Reed et al 2011, Acker et al 1998*). The diffuse melanocytic overgrowth of sun-damaged skin makes it challenging to assess the peripheral margins of LM. Also benign melanocytes may extend along the hair follicles (*Hendi et al 2006*). The margin may also be obscured by benign lentigos, seborrheic keratoses and AKs (*Dalton et al 2005*). Morphometric analyses of melanocytes may help identify LM margins from sun-damaged skin. However, section artifacts and nuclear shrinking in formalin-fixed material are problematic (*Acker et al 1998*).

It is common that LMs continue histologically several mms to cms beyond the clinically defined border (*Breuninger et al 1999*). The goal of the surgery is "negative margins". "Positive or involved margins" are reported when histologic features of LM extend to the periphery of an excised specimen. The distance between specimen border and nearest histological findings of LM is called the histological margin (*Hazan et al 2008*). It should be noted that the guidelines for lesion removal are based on clinically measured margins and that the histological margins differ from those assessed clinically because of the shrinking of paraffin embeded specimens.

Several immunostains can be used to help detection of LM. *Melanoma antigen recognized by T-cells (MART-1, also named Mel-*A) is a cytoplasmic melanosome-associated transmembrane glycoprotein expressed by benign and malignant melanocytes, ***Figure 5***. It is considered as the most sensitive marker for melanoma (*McLeod et al 2011*). However, also normal sun chronically sun-exposed skin contains high numbers of MART-1 positive melanocytes (*Hendi et al 2006*). Also pigmented AKs, which can occur in the vicinity of LMs, stain positively with MART-1 which may be misleading for positive margins (*El Shabrawi-Caelen et al 2004*). However, in a more recent study MART-1 with azure-B counterstaining was successfully used to differentiate LM from pigmented AKs (*Wiltz et al 2007*). *S-100* is a calcium-binding protein present in melanoma cells, but also in various benign cells. Thus it has a low specificity and it is not widely used for LM detection (*Erickson et al 2010). Human melanoma black (HMB-45)* is a murine monoclonal antibody binding to melanosome-associated sialated glycoprotein (gp100) present in neoplastic, fetal and immature active melanocytes. HMB-45 is not widely used due to its poor sensitivity compared to other immunostainings (*McLeod et al 2011*). *Mel-5* is a murin monoclonal antibody that binds glycoprotein75 in mature melanocytes. It stains epidermal and basal melanocytes and can be used in the detection of LM borders, but it is not suitable for the detection of invasive LMM (*McLeod et al 2011*). In addition, *micropthalmic transcription factor (MITF),* a nuclear stain may be useful in LM margin detection (*McLeod et al 2011*).

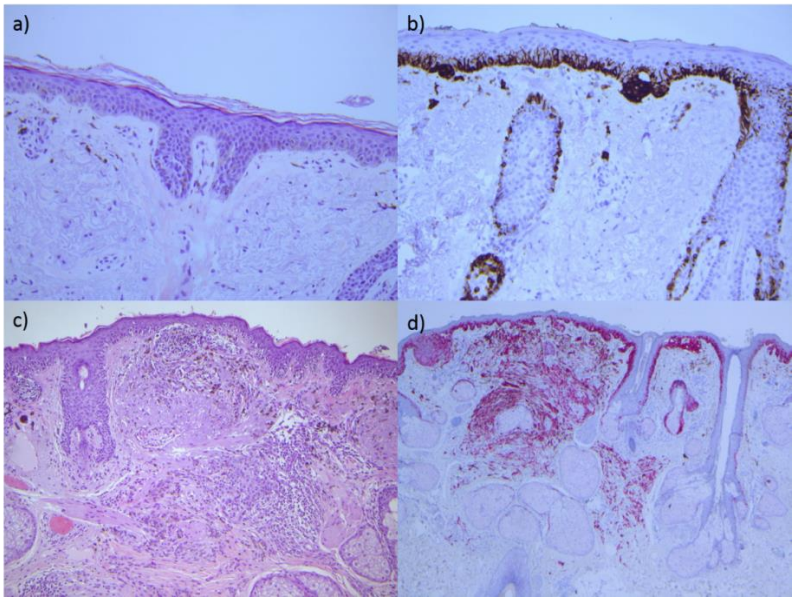

Figure 5 a) LM HE-staining showing atypical junctional melanocytes and nevoid nests, solar elastosis and b) LM immunostaining (MART-1) showing atypical junctional melanosytic proliferation and periadnexal extension, c) LMM Breslow 1.1 mm HE-staining showing epidermal characteristics of and LM and atypical melanocytic proliferation into the dermis, c) LMM Breslow 1.1 in MART-1/Melan A-staining shoving melanosytic proliferation in dermo-epidermal junction and into the dermis. Figure by Leila Jeskanen, MD, with permission.

3. NON-INVASIVE METHODS FOR SKIN CANCER DETECTION

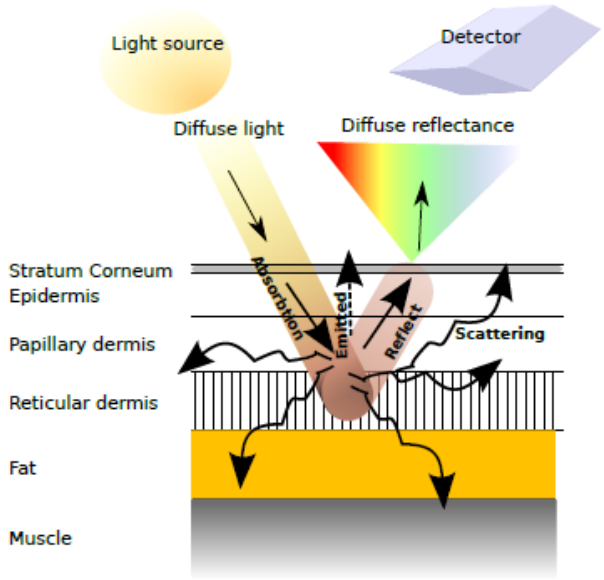

Figure 6. Light reflectance from the skin. Figure by Ilkka Pölönen, PhD, with permission.

Despite being the gold standard of cancer diagnosis, histopathology has its limitations. First of all, the processing of the samples is time consuming.The numerous and sometimes unnecessary invasive biopsies

can be burden to a patient. Additionally, the histological cross-sectional processing of the samples enables detection of only a tiny (approx.1%) part of the specimen (*Bosbous et al 2010*). The diagnosis is greatly dependent on the judgment of the pathologists (*Akbari et al 2011*). Typically patients have multiple lesions that are widespread on sun-damaged skin areas and visual inspection fails to detect the earliest changes. Non-invasive imaging techniques have emerged to aid clinical diagnosis and assessment of the early invisible changes and thus enable more accurate primary treatment and follow-up.

When it reaches the skin surface, some of light is reflected or scattered back while some light is absorbed and only a small percentage of the incident light penetrates deeper structures. The energy from the absorbed light activates specific fluorophores in the skin to emit fluorescence when returning back to rest stage (*Szepetiuk et al 2011*).Thus, by monitoring lights behavior in the skin, it is possible to obtain insights into the skin's structures, ***Figure 6***.

Various novel non-invasive imaging methods are based on either the detection of light reflectance, scattering or emitting (fluorescence) in the skin (*Calin et al 2013*). The commercially available devices are listed in ***Table 1***. The devices can be classified according to their resolution as follows: 1) primary; detects subcellular structures (melanosome, melanin, nucleioli), 2) secondary; detects at cellular resolution (melanocytes, keratinocytes), 3) tertiary; detects cellular aggregates (cell nests, collagen, and blood vessels), 4) quaternary; detects characteristics visible to the naked eye (*Marghoob et al 2003*). In addition this chapter introduces the principle of hyperspectral imaging. This novel method is not yet commercially available for skin cancer detection.

Method	Examples of commercial devices	Principle	Images	Analysis	Light source	FOV	Resolution	Imaging depth	Time aquired	Detection of clinical /subclinical AKs	Delineation of LM	Limitations
Fluorescence imaging	Philips Burton®, Dyaderm®, Visioscan® etc.	Detection of skin's auto fluorescence or exogenous fluorophores	Horizontal	Automated possible	UV light	Several cm^2	Macroscopic characteristics visible to the naked eye	Skin surface	Seconds to hours (exogenous fluorophores)	Yes/Yes	Yes	Non-spesific
Dermatoscopy	Dermlite® etc.	Magnified macroscopic images	Horizontal	User-dependent	Transillu-minating or polarized light	Several cm^2	Cellular aggregates	Papillary dermis	Seconds	Yes/Yes	Yes	User-dependent
Confocal microscopy	Vivascope®	Microscopic imaging in vivo	Horizontal	User-dependent	700/2500 nm laser	500x500µm^2, 8x8mm^2 mosaic composite images	Subcellular structures, Lateral 0.5-1µm, axial 3-4 µm	350 µm (papillary dermis)	5 min for 8x8 mm^2	Yes/Yes	Yes	User-dependent, small FOV, hyperkeratosis disrupts, limited imaging depth
Optical coherence tomography	HD-OCT Skintell®	"High resolution ultrasound with light"	Horizontal and vertical	User-dependent	1300 nm	1.8x1.5 mm^2	Subcellular structures, 3 µm in three dimensions	570 µm (superficial reticular dermis)	5-7 min	Yes/Yes	No	User-dependent, small FOV, crusting and ulceration disturbs
	Vivosight OCT®		Vertical	User-dependent	1300 nm	6x6mm^2	Cellular aggregates, 7.5 µm lateral, 10 µm axial	2mm (deep reticular dermis)	Several mnutes	Yes/?	No	Poor resolution compared to HD-OCT
Raman spectroscopy	Verisante aura®	Detects vibrational energies of tissue biomolecules due to laser beam excitation	No images provided	Automated	785nm laser	3.5 mm diameter	No images provided	200 µm (epidermis)	1s/FOV	Yes/?	No	No image provided, point measurement, small FOV
Multispectral imaging	SiaScope®	Detects skin chromophores at 5-8 different bands of wavelengths	Horizontal	User-dependent	400-1000 nm	12x12-24x24 mm^2	Cellular aggregates, 50-100 µm	2 mm (deep reticular dermis)	15 s	No	Possibly	User-dependent
	Melafind®	Takes 10 images at differed narrow bands of wavelengths	Horizontal	Automated	430-950nm	22x22 mm	Cellular aggregates, 20 µm	2.5 mm (reticular dermis/ subcutis)	3 s	No	Possibly	Spesificity?

Table 1.Commercially available devices for detection of premalignancies the photodamaged skin including actinic keratoses (AK) and lentigo malignas (LM). FOV=field of view.

3.1 Fluorescence detection

Fluorescence detection can be based either on the detection of natural fluorophores of the skin (e.g. elastin, collagen, melanin) (*Andersson-Engels et al 1991, Brancaleon et al 2001*), or the detection of fluorescence caused by exogenous fluorophores (*Tyrrell et al 2010*[1], *Calin et al 2013*).

Protoporphyrin IX (PpIX) exhibits red fluorescence when excited with blue light matching the 410 nm absorbance peak (*Tyrrell et al 2010*[1]). Fluorescence-based photo detection (PD) can be used to detect the areas of high PpIX accumulation corresponding to tissue with a high degree of dysplasia, and thus the detection of the field cancerized skin (*Ericson et al 2004*), ***Figure 7***. Fluorescence detection can be performed either by fluorescence imaging or fluorescence spectroscopy (*Calin et al 2013*). Several non-invasive devices like Wood's light (Philips Burton®, Somerset, USA) (*Fritsch et al 1998, Passos et al 2013*) , CCD fluorescence camera systems (i.e. Dyaderm®, Biocam GmbH, Regensburg Germany; Medeikonos® PDD/PDT, Medeikonos AB, Gothenburg, Sweden; Visioscan® VC98 and Visiopor® PP34, C+K

electronics, Cologne Germany) (*Tyrrell et al 2010[1], Wiegell et al 2008, Szepetiuk et al 2011*), fluorescence spectroscopy devices (*Hewett et al 2001, Juzeniene et al 2006*), as well as invasive fluorescence microscopy (*Dögnitz et al 2008*) can be used in the detection of PpIX fluorescence. Some devices like Wood's light provide subjective information while validated systems like CCD cameras can provide semi-quantitative information. PD can be used in the detection of areas in need of treatment, and to help manage the post-treatment follow-up (*Liutkeviciute-Navickiene et al 2009*). PpIX is the main component in porphyrin-based photodynamic therapy (PDT) and thus PD can be used to monitor the treatment effect (*Ericson et al 2004*). The intensity of the fluorescence can provide information on the selectivity of the photosensitizer (*Martin A et al 1995, Fritsch et al 1998*). Photobleaching i.e. photo-oxidation of the photosensitizer seen as diminished fluorescence intensity during PDT, indicates the level of cellular damage, and thus is predictive for treatment efficacy. Over 50-60% reduction in fluorescence intensity during treatment predicts complete clearance. In contrast, the intensity of total initial PpIX fluorescence alone fails to predict the treatment efficacy (*Tyrrell et al 2010[2]*). In daylight-photodynamic therapy (DL-PDT), PpIX is activated during its development, leading to low PpIX-fluorescence levels and no photobleaching (*Wiegell et al 2008*). There are several limitations in PD. The exogenous fluorescence detection procedure is time-consuming, due to hours of PpIX precursor application followed by imaging, and thus is not useful for daily clinical practices (*van der Beek et al 2012*). Although highly accumulated in cancerous tissues, also non-cancerous skin diseases like psoriasis accumulate PpIX (*Smits et al 2005*). In addition, PD is not useful in monitoring the progression of carcinogenesis as it fails to distinguish between between AKs and invasive cSCC (*Kleinpenning et al 2010*).

A UV lamp, Wood's light (320-400 nm, peak 365 nm), first described in the beginning of the 1900s, is also commonly used in the detection of ill-defined borders of LM/LMM in order to achieve more accurate primary excision margins. Melanin absorbs the majority of the UV radiation the skin is exposed to. Thus, in Wood's light examination, areas with increased amounts of epidermal melanin appear darker than the surrounding skin which in some cases may help define peripheral subclinical melanocytes, ***Figure 7*** (*Robinson JK 2004, Paraskevas et al 2005, Kimyai-Asadi et al 2007, Hazan et al 2008*).

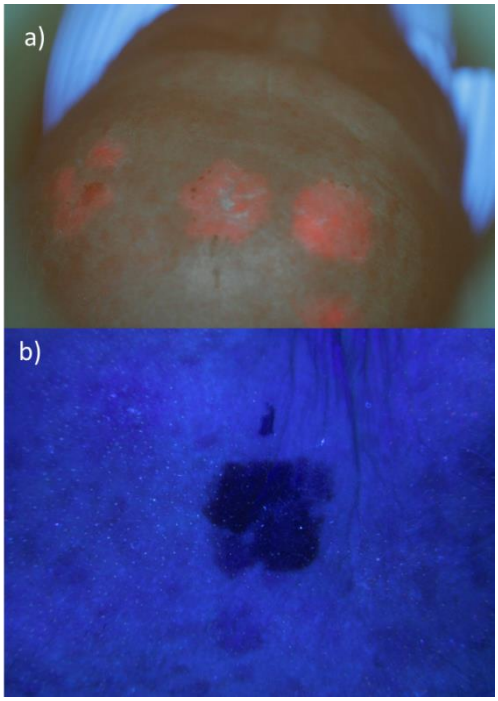

Figure 7 a) Field cancerization in Wood's light (PpIX fluorescence), b) lentigo maligna in Wood's light. Figures by Noora Neittaanmäki-Perttu with the permission of the patients.

3.2 Dermatoscopy

Dermatoscopy (i.e. epiluminescence microscopy, Dermlite® 3GenCA, USA, Molemax®, Derma Instruments Vienna Austria), using transilluminating or polarized light, provides x10 to x30 magnified images of the structures in epidermis and papillary dermis. Dermatoscopy was initially developed to aid melanoma diagnosis, but has also been introduced as a diagnostic tool for non-melanoma skin cancers (*Fargnoli et al 2012*). Dermatoscopy can be used in the detection of AKs (*Huerta-Brogeras et al 2012)* as well as in the detection of LM borders *(Robinson JK 2004)*.

Dermatoscopy can aid AK diagnosis with a sensitivity of 98.7% and specificity of 95% (*Huerta-Brogeras et al 2012).* However, the technique is based on morphologic features and is strongly user-dependent. Dermatoscopic criteria for AK include a pink-to red erythematous pseudonetwork, surface scale, follicular openings filled with keratotic plugs, vascular structures including linear-wavy vessels or coiled/dotted vessels around the hair follicles. Dermatoscopically AKs can be divided into three different grades: grade I red pseudonetwork, discrete white scales; grade II erythematous background, white to yellow keratotic enlarged follicular openings (strawberry sign); grade III white-yellow background with enlarged follicular openings filled with keratotic plugs, or white-yellow structureless areas due to marked hyperkeratosis, ***Figure 8***. The presence of advanced vascular structures (dotted, glomerular, hairpin or linear vessels) is a sign of more aggressive growth preceding SCC development (*Zalaudek et al 2014*).Hyperkeratotic AK have a light-pink-to-yellowish hue without visualization of the underlying structures. Pigmented AKs are seen as gray-to-black dots and globules around the follicular openings, annular granular structures, brown-to-gray

pseudo network, and rhomboidal structures, some of the dermatoscopic characteristics overlapping with those of lentigo maligna. Other differential diagnosis include Bowens disease with glomerular, irregular, linear or dotted vessels in small clusters, and a scaly surface; cSCC showing polymorphous vascular structures including glomerular "hairpin", dotted, linear or irregular vessels, white structure less areas, central keratin mass and ulceration; BCC showing arborizing vessels, ulceration, blue-gray globules, ovoid nests, leaf-like and spoke wheel areas; sebaceous hyperplasia showing crown vessels (*Huerta-Brogeras et al 2012, Fargnoli et al 2012).* Dermatoscopy has been used to monitor the treatment efficacy and for the diagnosis of recurrent lesions *(Kaçar et al 2012*). However, only limited histologically confirmed evidence is available and it is unclear whether dermatocopy is able to detect subclinical lesions. In one study, despite the complete histological clearance of 33/34 lesions only 15/34 lesions showed complete disappearance in dermatoscopy. The authors claim that the disappearance of even one dermatoscopic sign of an AK predicts its clearance (*Lee et al 2014).*

Dermatoscopy has also been used for the detection of LM and delineation of the borders pre-surgically. LM on the face do not show the classical dermatoscopic features found on the other parts of the skin due to atrophic epidermis and pseudonetwork caused by follicular openings and sweat glands. Thus, on the face it is difficult to distinguish between melanocytic lesions from non-melanocytic lesions like seborrheic keratoses or pigmented AKs (*Stolz et al 2002*). The specific dermatoscopic criteria for facial LM are: a variating number of colors, asymmetric hyperpigmented follicular openings, fine grey dots and globules around the follicles (annular granular pattern) and an enhanced vascular network, ***Figure 8***. In invasive forms (LMM) pigmentation might be rhomboidal or obliterate the hair follicles (structureless area), the variation of colors is greater than in LM, in addition rhomboidal vascularity and ulceration might be present, ***Figure 9***. In addition, darkening in the dermatoscopic examination is indicative of the condition (*Stolz et al 2002, Pralong et al 2012*). A sensitivity of 89% and spesificity of 96% have been reported for the combination of 4 dermatoscopic criteria: 1) asymmetrical follicular openings (indicating uneven descent of melanoma cells within hair follicles), 2) dark rhomboidal structures (due to cohesive sheets of melanoma cells in the epidermis and upper dermis), 3) gray globules, 4) gray dots (both indicating melanin-loaded macrophages in the upper dermis) of the LM (*Schiffner et al 2000*). It has been shown that dermatoscopy detects lesion borders more accurately compared to clinical assessment and assessment with Wood's light *(Robinson 2004).* There are also automated analysis methods for the lesion border delineation in digital dermatoscopy images (*Abbas et al 2011*). However, the methods use visible lesion borders as a standard and thus are not useful in the detection of subclinical LM borders.

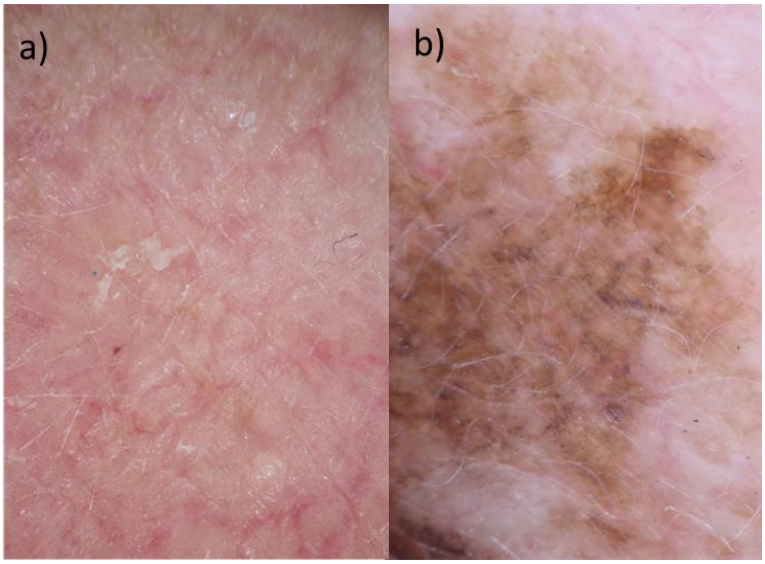

Figure 8.a) Dermatoscopic image of an AK (grade I) showing a red pseudonetwork and discrete white scales, b) Dermatoscopic image of LM showing varieting colors, asymmetric hyperpigmented follicular openings and dark rhomboidal structures. Figures by Noora Neittaanmäki-Perttu with the permission of the patients.

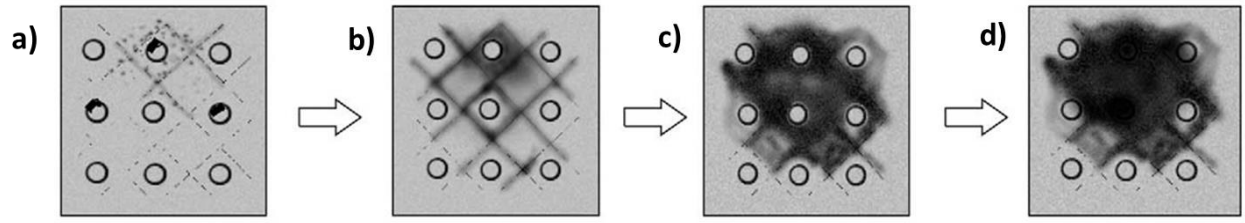

Figure 9. Dermatoscopic criteria, progression model from LM to LMM. a) Dots aggregated around hair follicle, short streaks, asymmetric follicular openings, subtle annular-granular pattern b) annular-granular pattern clearly visible, rhomboidal structures, melanoma cells within the follicle proliferate and invade adjacent dermis, c) homogenous areas, hair follicles spared, d) homogenous areas, hair follicles obliterated, development of milky red areas (invasive melanoma). Edited from *Stolz et al 2002* with the permission of Elsevier.

3.3 Reflectance confocal microscopy

The reflectance confocal microscopy (RCM, VivaScope®, MAVIG GmbH, Lucid Inc.) technique is based on laser scanning microscopy, which unlike conventional microscopes in which thin tissue sections are illuminated from below, illuminates skin surface from above with a focused laser (coherent 700/2500 nm) and collects the reflected and scattered light. Images can be obtained *in vivo* from the skin surface or from excised tissue sections. RCM provides a nearly-histologic resolution (0.5-1μm laterally and 3-5 μm axially) gray-scale (black and white) horizontal (en-face) image of the cellular and subcellular structures in the epidermis and papillary dermis up to a depth of 350 μm (*Horn et al 2008, Ulrich M et al 2010).* In the RCM images the melanocytes' cytoplasm appears intensely white while the keratinocytes reflect less of the laser's light and thus appear darker. Cell nuclei appear dark and collagen very bright *(Carrera et al 2012).*Some

devices combine dermatoscopy to guide RCM imaging (Vivacam®, Mavig). The field of view (FOV) of a single image is small 500 x 500µm, but by using composite images up to 8x8 mm skin areas can be obtained. The small FOV and imaging at several layers leads to a relatively slow imaging process (5 min for 8x8 mm^2 one hour for a whole cheek) and thus the technique is not very suitable for the mapping of wide areas in daily practices. The overall sensitivity and specificity of RCM are high, 90.8% and 77.5%, respectively (*Horn et al 2008).*It's large inter observer variations indicate that the device is strongly user-dependent (*Ulrich M et al 2010).* Furthermore, the device is expensive (approx. 160 000 euros according to the company MAVIG) and costs of RCM are not reimbursed (*Guitera et al 2013*).

In RCM, AK characteristics include parakeratosis/hyperkeratosis, irregular stratum corneum and irregular epidermal architecture ("honeycomb pattern"), atypical keratinocytes (nuclear and cellular pleomorphism). Also spongiosis, solar elastosis, increased vascularity/blood vessel dilatation and superficial inflammatory infiltrate can be present, ***Figure 10*** (*Ulrich M et al 2010*). Grade I AKs present as focal areas of atypical keratinocytes can be seen as irregular honeycomb patterns only at the level of the stratum spinosum, whereas in grade II AKs areas of markedly atypical keratinocytes with varying sizes and shapes, are more diffuse and involve both the stratum spinosum and granulosum. Grade III AK presents itself as markedly atypical honeycomb patterns with partial disruption of the normal epidermal layers *(Zalaudek et al 2014).* The cellular atypia, architectural disruption in stratum spinosum and solar elastosis can be visualized before their clinical appearance, and serve as markers of subclinical AKs. RCM can also be efficiently used for monitoring the treatment response *(Ulrich M et al 2010, Malvehy et al 2014).* The morphologic findings in the skin detected with RCM correlate well with the findings in invasive histopathological examination (*Longo et al 2013, Malvehy et al 2014), **Table 3***.

RMC can be used to differentiate between benign and malignant melanocytic lesions. However, the imaging depth is limited to the epidermis, and thus RCM fails to detect the thicker invasive components of tumors (*Carrera et al 2012)*. The special characteristics of LM ("the LM score") in RCM include major features (2 points): nonedged papillae and round pagetoid large cells; and minor features (one point): nucleated cells in the dermal papilla, three or more atypical cells at the dermoepidermal junction in five 0.5x0.5mm^2 images, follicular localization of pagetoid cells and/or atypical junctional cells; and a single "negative" (benign) feature (-1 point) of broadened honeycomb pattern of the epidermis, ***Figure 11, Table 2***. The sensitivity and specificity of these criteria (≥2 points) for differentiation of LM from benign pigmented facial macules by RCM were 85% and 76%, respectively. Some of the RCM features are present in both LM and benign pigmented lesions e.g. pigmented keratinocytes may have similar reflectance signal as that of melanocytes, which may be confusing (*Guitera et al 2010*). RCM is useful in the detection of LM borders. RCM revealed subclinical continuum, not detected dermatoscopically, in 17 of 29 (59%) LMs and it was suggested that RCM might be more valuable than routine histology (*Guitera et al 2013*). RCM may be used in monitoring the efficacy of non-invasive treatments of LM (*Alarcon et al 2014*).

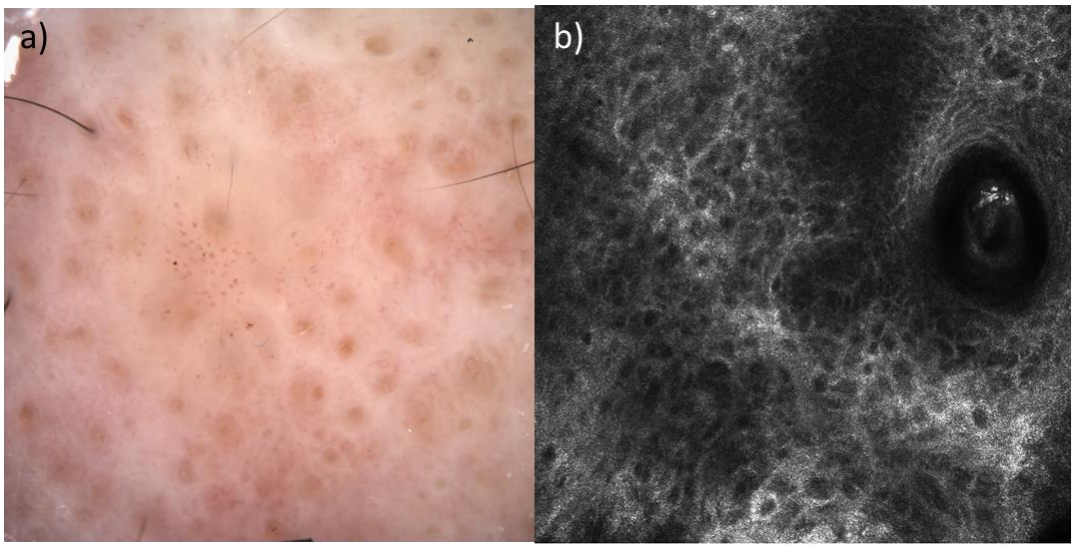

Figure 10 a) Dermastocopic image of an AK (grade II) showing an erythematous background and yellow keratotic enlarged follicular openings, b) Confocal microscopy image of AK (grade II) showing a pleomorphic epidermis. In the granular layer a destroyed honeycomb pattern with atypical keratinocytes is visible. Figure by Dr. Martina Ulrich, with permission of MAVIG.

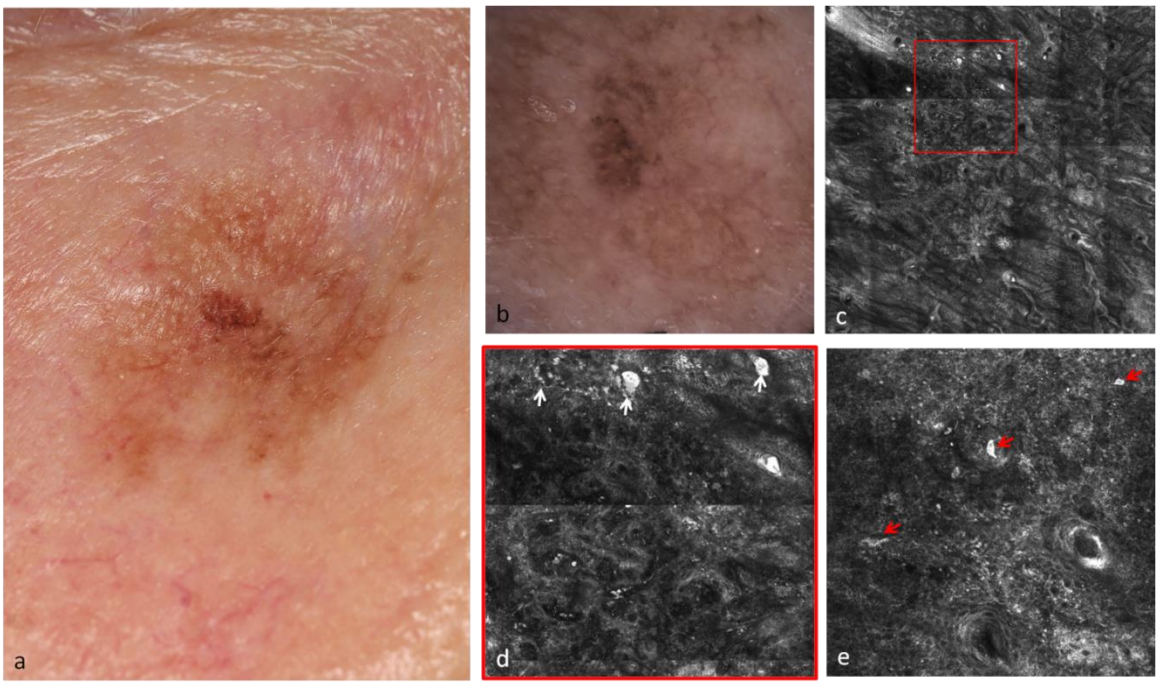

Figure 11.Diagnostisc of lentigo maligna melanoma (LMM) in the face with confocal microscopy. a) a clinical photograph, b) the dermatoscopic examination shows a darker area in the center of the lesion and rhomboidal structures, c-d) the images representing confocal microscopy: c) the composite image allows an overview of the lesion and the total architecture, d) in the single images (1mmx1mm) the cells are visible, e) single malignant pigmented cells can be detected (red arrows) allowing the immediate diagnosis of LMM. Figure by Dr Martina Ulrich with permission.

Histology	Dermatoscopy	RCM
Atypical melanocytes at the dermal-epidermal junction in solitary units and small nests, confluence of melanocytes replacing the basilar layer	Dark rhomboidal structures, varieting color	Nucleated cells in the dermal papilla,atypical cells at the dermoepidermal junction
Periadnexal extension of atypical melanocytes	Asymmetric hyperpigmented follicular openings	Follicular localization of pagetoid cells and/or atypical junctional cells
Effacement of the rete ridges		Nonedged papillae
Pagetoid spread of atypical melanocytes	Pigmented dots	Round pagetoid large cells
Epidermal atrophy, Solar elastosis		
Dermal infiltrate of lymphocytes, melanophages and multinucleated melanocytes	Fine grey dots and globules around the follicles (annular granular pattern)	

Table 2. Correlation of LM characteristics in histology, dermatoscopy and RCM.

3.4 Optical coherence tomography

Optical coherence tomography (OCT) (Vivosight OCT, Michelson Diagnostics Ltd) resembles ultrasound but uses back-scattered infrared-light waves instead of sound waves. OCT provides cross-section images with higher resolution than ultrasound (7μm laterally and 10 μm axially) to depths of 2 mm (deep dermis). FOV is 6x6 mm. In OCT, AKs are seen as disrupted epidermal layering, thickened epidermis, whites strikes/scales are seen in cases of hyperkeratosis (*Banzhaf et al 2014*), ***Figure 12***. OCT can be used to monitor effects of the treatment procedures (*Themstrup et al 2012*), and treatment efficacy (*Banzhaf et al 2014, Themstrup et al 2014*). In conventional OCT image artifacts are common: inflammation, thick hyperkeratosis or ulceration blur the image and lower the image quality (*Mogensen et al 2009, Banzhaf et al 2014*). The OCT procedure is time-consuming and due to its low resolution AK visualization is poor (*Maier et al 2013*). The sensitivity and specificity for distinguishing AK from normal skin is dependent on the observers' skills varying between 58-94% and 43-96% respectively (*Mogensen et al 2009*). When using a computer-assisted analysis to detect the presence of a dark band as a sign of AK in OCT-images, a sensitivity of 86% and specificity of 83% were attained (*Korde et al 2007).* In OCT, different tumor types (AK, BCC, benign lesions) are indistinguishable and the naked eye was more accurate in diagnosing NMSC (*Mogensen et al 2009*).

More advanced high-definition optical coherence tomography (HD-OCT, Skintell®, Afga Healthcare) reaches up to 570 μm depth, i.e. includes thickness of the whole epidermis and superficial dermis, and unlike conventional OCT, provides both horizontal (en face), vertical cross-sectional (slice) images with improved 3-μm resolution. FOV is 1.8 x 1.5 mm. In horizontal imaging AKs are characterized by hyperkeratosis and parakeratosis, disruption of the stratum corneum, cellular/nuclear polymorphism, solar elastosis, perivascular inflammation, and architectural disarray which is seen as atypical honeycomb patterns presenting in the lower 1/3 of the epidermis in grade I AKs, and the lower 2/3 in grade II AKs and throughout the epidermis in

grade II AKs in great correlation with histopathologic evaluation. Signs of AK in vertical imaging are similar than in conventional OCT. Also subclinical AKs are detectable with HD-OCT (*Boone et al 2013, Maier et al 2013*). The characteristics of different grades of AKs in OCT, RCM, dermatoscopy and histology are shown in ***Table 3*.**

OCT is also used in presurgical margin assessment for non-melanoma skin cancers (*Alawi et al 2013*). Due to the poor resolution and visualization of the melanocytes, OCT is rarely used in the detection of pigmented lesions (*de Giorgi et al 2005*) and is not yet used for delineation of LMs. HD-OCT could probably be used in LM delineation, but no data of this apparently exists.

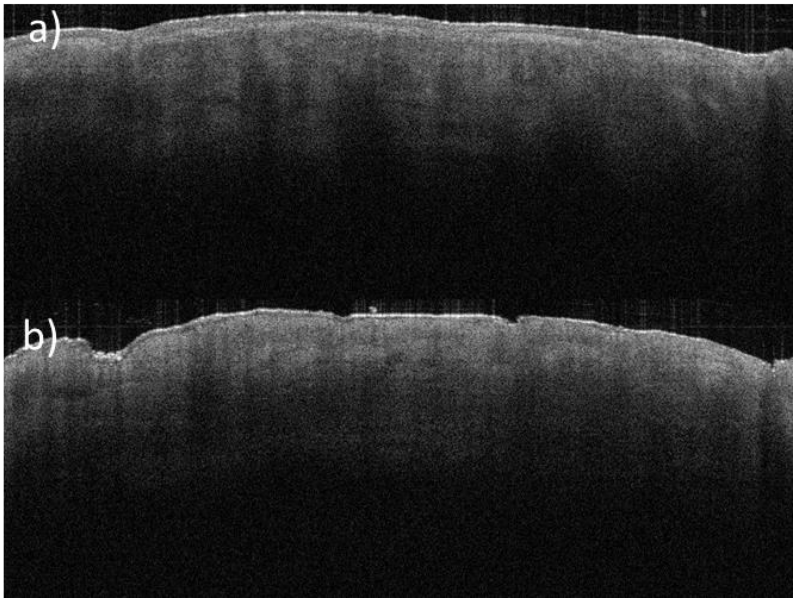

Figure 12.OCT images (Vivosight OCT, Michelson Diagnostics Ltd), a) normal skin on the lower lip: Normal layering, clearly defined dermo-epidermal junction. The hyporeflective streaks in the dermis are vessels. The image depth is 0.98 mm. b) AK on the lower lip: Disrupted layering, thickening of the epidermis, the dermo-epidermal junction is not clearly defined. There are no visible basal cell nests. AK's sometime display white streaks in the epidermis, but they are not evident in this image. The lesion image depth is 1.0 mm and it is 4.8 mm wide. Figure by Lotte Themstrup, MD, with permission.

Actinic keratosis	Histology	Dermatoscopy	RCM	HD-OCT
Typical chacteristics	Irregularly achantotic epidermis, irregular dermo-epidermal junction Atypical keratinocytes including hyperchromatic nuclei, mitoses, disordered maturation. Hyperkeratosis, parakeratosis and orthokeratosis. Elastosis in the dermis, perivascular or lichenoid inflammation.	Pink-to red erytematous pseudonetwork, follicular openings filled with keratotic plugs Light-pink-to-yellowish hue (hyperkeratosis), surface scale Vascular stuctures (linear-wavy or coiled/dotted vessels around the hair follicles)	Irregular stratum corneum and irregular epidermal architecture ("honeycomb pattern") Atypical keratinocytes: nuclear and cellular pleomorphism Parakeratosis/hyperkeratosis Spongiosis, solar elastosis, increased vascularity/blood vessel dilatation and superficial inflammatory infiltrate	Disruption of stratum corneum, architectural disarray (atypical honeycomb pattern) Cellular/nuclear polymorphism Hyperkeratosis and parakeratosis Solar elastosis, perivascular inflammation,
Grade I	Atypia of keratinocytes of lower one third of the epidermis	Red pseudonetwork, discrete white scales	Focal areas of atypical keratinocytes seen as irregular honeycomb pattern only at the level of stratum spinosum	Atypical honeycomb pattern present in lower 1/3 of the epidermis
Grade II	Atypia of keratinocytes of at least the lower two thirds of the epidermis	Erythematous background, white to yellow keratotic enlarged follicular openings (strawberry sign);	Areas of markedly atypical keratinocytes with varying sizes and shapes diffusely in both stratum spinosum and granulosum	Atypical honeycomb pattern in the lower 2/3 of epidermis
Grade III	Diffuse atypical keratinocyte proliferation involving the full epidermal thickness	White-yellow background, enlarged follicular openings filled with keratotic plugs, or white-yellow structuless areas due to marked hyperkeratosis	Markedly atypical honeycomb pattern with partial disruption of the normal epidermal layers. Keratinocytes are characterized with varying cellular size and shape, and irregular intercellular connections	Atypical honeycomb pattern throughout the epidermis in grade II AKs

Table 3. Correlation of the findings of different AK grades in OCT, RCM, dermatoscopy and histology

3.5 Raman spectroscopy

The term spectroscopy means detection of how light uniquely reflects, absorbs, emits and scatters at different wavelengths from different substances based on their molecular composition.

Raman spectroscopy detects the scattered energy of molecular vibrations of tissue biomolecules due to laser light (785nm) excitation. Different vibrational energies, seen in Raman spectral peaks, correspond to different chemical compositions, specific molecular structures (lipids, proteins), and molecular interactions and allows us to distinguish between malignant and benign tissues (*Gniadecka et al 1997, Choo-Smith et al 2002*). Tissues related histogenetically, like AKs and cSCCs, provide similar spectral signals (*Gniadecka et al 1997*). The complexity of the spectra requires automated computer assisted classification algorithms. The technique provides information on whether the detected spot is suspected to be malignant or benign. No

image is provided. In a multicenter study in which the Raman spectra of 518 lesions, including AKs (n=32), LMs (n=20) and LMMs (n=8), the sensitivity of 90%, specificity of 67% was shown for distinguishing malignant from benign skin lesions (*Lui et al 2012*). A limitation in this study was that only 20-42% of the lesions suspected to be premalignant or benign were verified by histopathology, ***Figure 13.*** Due to small FOV (3.5 mm diameter) and that the device fails to provide images the method is not used for delineation of lesion borders. Another disadvantage is the limited detection depth of 200 µm.

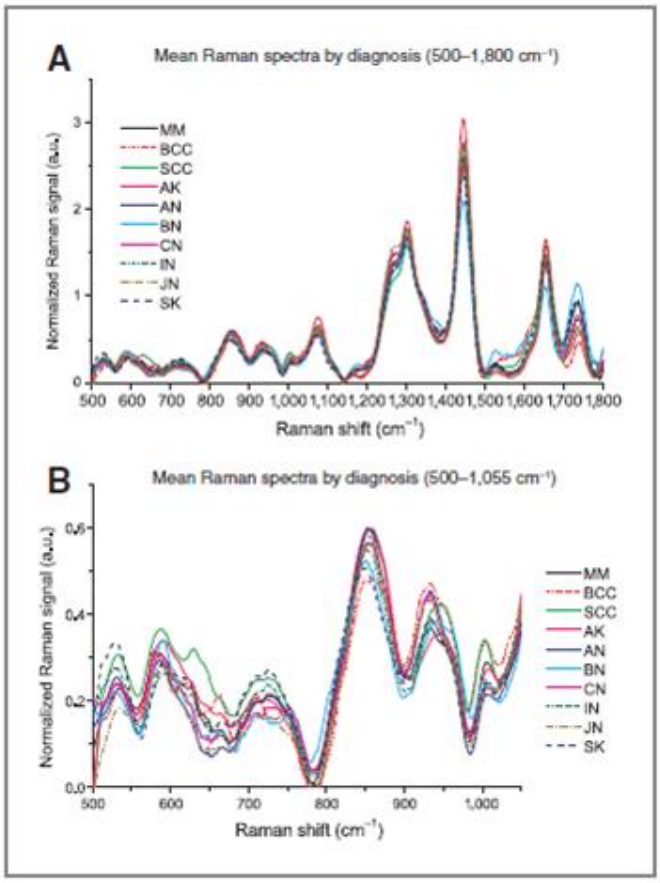

Figure 13. Raman spectral peaks for malignant and benign skin lesions. *Lui et al 2012* with permission from the American Association for Cancer Research.

3.6 Multispectral imaging

In multispectral imaging sequences of images (5-15) are taken at different non-continuous narrow bands of wavelengths (*Marghoob et al 2003*). Two devices are commercially available for multispectral skin detection: spectrophotometric intracutanues analysis, SiaScope (Astron Clinica, Cambridge, UK) and Melafind (Mela Sciences Inc., Irwington, New York, USA). The difference between these two devices is that Melafind provides an automated computer-assisted diagnosis, while Siascope provides graphs and images (SiaGraphs) for the physician to interpret (*Marghoob et al 2003*). FOVs are 12x12mm -24x24 mm and 22x22 mm, imaging depths 2 mm and, and resolutions 50-100 µm and 20µm for SiaScope and MelaFind, respectively. Siascope uses five to eight and Melafind ten different narrow bands of wavelengths ranging

from blue visible light to the near infrared (approx. 400-1000 nm). Both SiaScope and Melafind also provide dermatoscopic images.

Acquired siagraphic images represent the concentration, distribution, and position of skin choromophores (melanin, hemoglobin, and collagen) in different skin layers. Siascopy was initially developed for the diagnosis of melanoma (*Moncrieff et al 2002*), ***Figure 14.*** In addition, Siascope has been used for the detection of different chromophoresin sun-damaged skin and found an increase in the amounts of melanin and a decrease in amounts of collagen due to sun damage and aging (*Stimpfle et al 2014*). In a study assessing the sensitivity and specificity of Siascopy, great inter-observer variability have been observed and dermatoscopy was more specific in aiding diagnosis of NMSC including AKs (*Hacioglu et al 2013*). As far as we know Siascopy has not been used for delineation of LM borders, which clearly could be an indication of the effectiveness of this device even though the FOV is limited to a diameter of 2 cm.

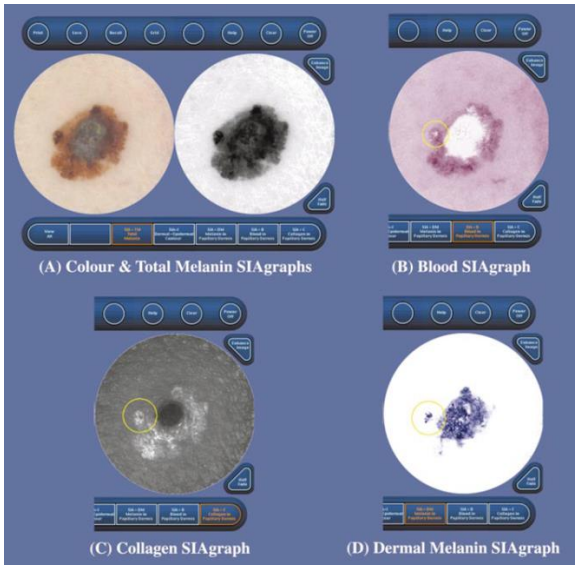

Figure 14. Siagraphs of superficial spreading melanoma Breslow 2.5 mm. From *Moncrieff et al 2002* with permission from John Wiley and Sons.

Melafind provides binary automated analysis of the imaged lesion indicating whether the lesion should be biopsied to rule out melanoma, or not. The sensitivity is high (98.4%) but the specificity is low (9.9%) (*Monheit et al 2011*). To our knowledge Melafind has not been used for delineation of presurgical margins, or in detection of AKs or NMSCs.

3.7 Principle of hyperspectral imaging

Hyperspectral imaging i.e. "imaging spectroscopy" differs from other spectroscopy techniques in that the spectral data can be obtained from an image (*Harris 2006*). The technique combines the advantages of digital imaging and spectroscopy , delivering information that is beyond the level detectable by the human eye including subtle wavelength differences and certain wavelengths (infrared, ultraviolet) which are outside

the range of human vision (*Panasyuk et al 2007, Liu et al 2012*) . A regular camera captures images in three broad wavebands (red, green, blue) while a hyperspectral camera uses tens to hundreds of continuous narrow wave bands of light delivered from a tunable filter. In addition to filters also prisms can be used (*Chang 2007*). In comparison the term multispectral imaging refers to use of multiple (4-15) wider, non-continuous bands of wavelengths resulting in discrete spectral images (*Dicker et al 2006, Jolivot et al 2011*). A hyperspectral image is a composite image consisting of tens to hundreds of overlapping images, of which each image is taken at a different wavelength. Each pixel in the hyperspectral image has its own spectral signature which represents the optical characteristics of each imaged spot at different wavelengths. Thus, in addition to spatial (x, y location) information, hyperspectral image contains a spectral graph (z intensity) for each pixel, ***Figure 15*** (*Martin ME et al 2006*[1]). A hyperspectral imager can either detect diffuse reflectance or fluorescence at different wavelengths of light (*Martin ME et al 2006*[2]). Different biological tissues can rapidly be identified from their unique reflected spectral signatures which provide information on their biochemical characteristics (*Siddiqi et al 2008, Panasyuk et al 2007)*. Diffuse reflectance records both light absorption and scattering and thus provides information on tissue morphology and chromophore content (*Calin et al 2013, Zonios et al 2001).* The tissue choromophores recorded by diffuse reflectance include: oxyhemoglobin, deoxyhemoglobin, bilirubin, methemoglobin, melanin and water (*Zonios et al 2001, Panasyuk et al 2007*). Thus, hyperspectral reflectance imaging of the skin can provide information about the thickness of the skin layers, blood volume, oxygenation, and melanin concentration (*Yudovsky et al 2010*).

Since hyperspectral imaging was first developed for satellite earth investigations (*Harris 2006*), it has been studied for several medical microscopic and in vivo macroscopic applications. Hyperspectral imaging has been used in animal cancer models for detection of residual breast tumors during surgery in rats (*Panasyuk et al 2007*) and the detection of rat oral cancer in sectioned tissue (*Fixler et al 2014*). Human cytological/histopathological studies show that microscopic hyperspectral imaging has some potential in the differentiation of (pre)cancerous cervix cells from healthy cells (*Siddiqi et al 2008*), melanoma detection and classification of spitzoid lesions on histological slides (*Dicker et al 2006, Gaudi et al 2014*). *In vivo* studies in humans show potential in the detection of tongue tumors (*Liu et al 2012*) and gastric cancer (*Akbari et al 2011*). Hyperspectral imaging has also been suggested to have potential in prostate cancer screening in humans (*Manyak et al 2006*). Some pilot studies of hyperspectral imaging of the skin *in vivo* include detection of the microcirculation of the skin surrounding diabetic wounds to predict healing (*Yudovsky et al 2010*) , *in vivo* melanoma detection (*Nagaoka et al 2012*) and *in vivo* assessment of melanoma response to chemotherapy (*Dicker et al 2011*). These studies show that hyperspectral imaging has some potential in the detection of cancer, delineation of tumor margins and assessment of treatment efficacy. As far as we know, no previous hyperspectral data are available for non-melanoma skin cancer or actinic keratoses or the detection of LM borders. The high costs of the hyperspectral sensor and computational complexity are the main reasons why hyperspectral imagers are not yet widely used in medical applications. However, recently

improvements in computers and the development of novel mathematical algorithms have been combined in attempts to overcome this problem (*Pölönen 2013*).

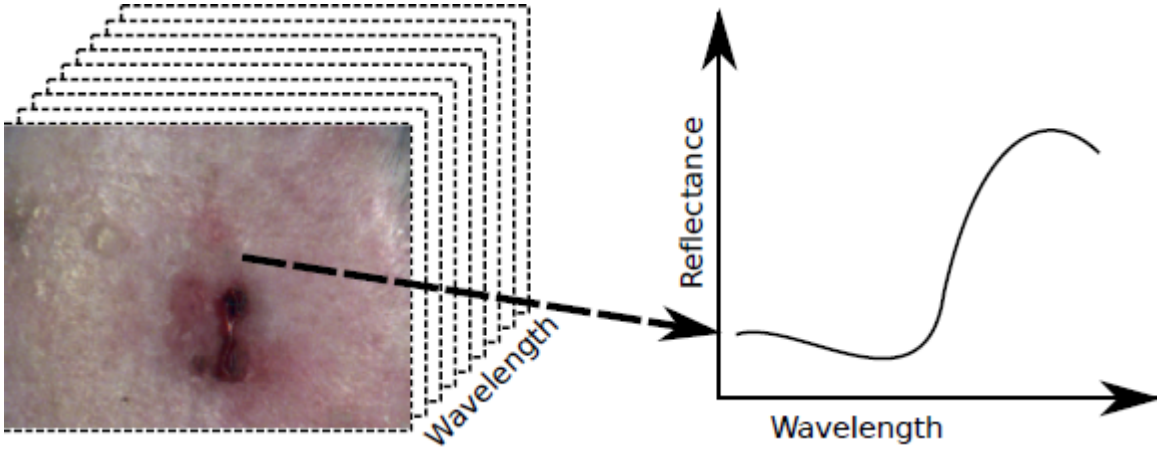

Figure 15. The principle of the hyperspectral image. A hyperspectral image is a composite image consisting of tens to hundreds of overlapping images, with each image taken at a different wavelength. Thus every pixel has its own spectral signature. Figure by Ilkka Pölönen, PhD, with permission.

4. TREATMENT OF ACTINIC KERATOSES AND FIELD CANCERIZATION

4.1 Why treat actinic keratoses?

Even though AKs may spontaneously regress over time, the inability to predict which lesion will regress and which will develop into an invasive cSCC makes it important to treat all AKs. In addition, AKs that regress also commonly recur (*Werner et al 2013*). The risk for a single AK developing into cSCC has been estimated to range between 0.025% and 20% per year (*Quaedvlieg et al 2006*). Based on this it was calculated that for patients with multiple AKs, the annual risk for developing cSCC would range between 0.15% and 80% (*Stockfleth 2012)*. Only a few prospective longitudinal studies that have assessed the true transformation rates and reported the risk to be as low as 0.075% per lesion per year for patients with no previous NMSC and 0.53% per lesion per year for patients with previous NMSC (*Marks et al 1988, Criscione et al 2009*). However, even if the annual risk for a single lesion transfering is low, the risk for a patient with several lesions over a course of several years, increases the possibility for cSCC significantly *(Dodson et al 1991)*. Although, here are some signs for "high risk AKs", invasion can not be predicted clinically (*Quaedvlieg et al 2006)*. Clinically 60-65% of cSCCs progress to the areas of previous diagnosed AKs, and the rest develop in apparently healthy skin (*Marks et al 1988, Criscione et al 2009*). Histologically 72-82% of cSCCs arise contiguously with AKs (*Mittelbronn et al 1998, Czarnecki et al 2002*). The progression from AK to cSCC has been estimated to be 2 years (*Fuchs et al 2007*). Thus, treatment of AKs and surrounding cancerized field can be considered as secondary prevention for cSCCs (*Ceilley et al 2013*).

Reported spontaneous regression rates for single lesions vary greatly from 18% over 7 months, 25.9-74% over one year, and 70% over 5 years (*Marks et al 1986, Thompson et al 1993, Frost et al 2000, Criscione et*

al 2009). A recent review evaluated the lesion regression rate of 15-63% after one year (*Werner et al 2013).* However, of these regressed lesions 15%-53% recurred within a year (*Werner et al 2013).* The regression of the complete field is rare (0-21%) with up to 75% recurrence (*Werner et al 2013).* This is in concordance with the finding that AKs appear as a continual flux and despite the regression, the number of AKs increase over time (*Marks et al 1986*).

There are also other facts that support the treatment of AKs. AKs are the most prevalent cancer precursors in humans (*Quaedvlieg et al 2006).* The treatment of similar precursors in other organs (like the cervix) is widely accepted (*Soergel et al 2012*).In addition patients also suffer from symptoms of AKs on cosmetically sensitive areas. As 25-75% of AK patients require repeated treatments, AKs should be treated as a chronic disease (*Ceilley et al 2013*). Thus, an ideal AK treatment has high clinical clearance rates with low recurrence with minimal side effects, good cosmetic outcome and low costs.

4.2 Primary prevention

Efficient UVR-protection with clothing and broad-spectrum sunscreens, limiting the UVR exposure and avoidance of sunbed use are the key points in primary prevention of NMSC and AKs. Sunscreens inhibit the formation of UV-induced p53 mutations (*Benjamin et al 2007*). In immunosuppressed patients, the regular use of high sun protection factor (SPF 50+UVA) sunscreen for two years, significantly reduced the number of new developing AKs and cSCCs, and also significantly reduced the number of existing AKs (*Ulrich C et al 2009*). The daily use of sunscreen (SPF 16) in immunocompetent patients for 4.5 years reduced the incidence of AKs by 24% (after 2 years but not after 4 years) and cSCCs by 38% (for up to 8 years) compared to discretionary use (including no use) (*Green et al 1999, Darlington et al 2003, Van der Pols et al 2006*). A sunscreen's SPF gives us information about the factor by which the sun exposure can be increased before skin develops perceptibile erythema (minimal erythema dose, MED). To achieve the adequate SPF sunscreens should be applied as a 2 mg/cm^2 layer (*Petersen et al 2014*[2]). Poor compliance and the use of too-low amounts (0.39 to 1.0 mg/cm^2) to achieve the effective SPF of sunscreen reduce the protective effect (*Neale et al 2002, Petersen et al 2014*[2]).

4.3 Photodynamic therapy

4.3.1 Mechanism and indications

Various photosensitizing agents in combination with different wavelengths of light (e.g. psoralens and UVA, porphyrins and visible light) are used in photodermatology for the treatment of various skin diseases (*Hönigsmann 2013*). In photodynamic therapy (PDT), the systemic or topical administration of exogenous tumor-localizing photosensitizing drug, followed by irradiation at an adequate wavelength of non-ionizing radiation corresponding to the absorbance spectrum of the photosensitizer, leads to phototoxic reaction with reactive singlet oxygen causing the death of the target cells (*Calzavara-Pinton et al 1996, Ericson et al 2008*).

PDT was invented at the beginning of the 20th century when Oscar Raab observed a toxic reaction caused by the combination of visible light, photosensitizer (acridine orange) and oxygen to be lethal to paramecia. In 1905 von Tappeiner published the first clinical trial in which daylight-PDT with Eosin and Magdala-red solution was used in the treatment of facial basal cell carcinomas. In the 1970s and 1990s intravenous hematoporphyrin derivate and porfimer sodium causing prolonged photosensitivity, were used. Finally in the 1990s, the use of topical protoporphyrin IX (PpIX) precursor, 5-aminolevulinic acid, with artificial light, was invented by JC Kennedy and colleagues. Soon after this invention photodynamic therapy became a widespread treatment for superficial skin cancers and their precursors (*Calzavara-Pinton et al 1996, Babilas et al 2010, Hönigsmann 2013*).

Currently in dermatology, PDT is widely used in the treatment of AKs and field cancerization, Bowen's disease, superficial (and thin nodular) basal cell carcinomas. It is also used in photorejuvenation, cutaneous T-cell lymphoma, acne, warts and some infective (i.e. leishmaniasis, superficial mycoses), and inflammatory diseases (morphea, lichen sclerosis, perioral dermatitis, scars) (*Ericson et al 2008, Morton et al 2013*[1-2]). Also some attempts for the treatment of lentigo malignas with PDT exist (*Karam et al 2013)*. Besides dermatology, photodynamic therapy with a variety of systemic photosensitizers is widely used in other oncologic indications (head and neck cancers, cervix cancer, lung cancer, uveal melanoma) (*O'Connor et al 2009, Soergel et al 2012, Cai et al 2013, Rundle 2014*).

Heme (iron+protoporphyrin IX) is a crucial component in key biomolecules (hemoglobin, myoglobin, cytochromes etc.) of living cells (*Peng et al 1997*). Normally heme biosynthesis is tightly regulated by a feedback mechanism in which free heme inhibits the syhthesis of 5-ALA, to avoid photosensitization. Abnormalities in heme synthesis, lead to accumulation of porphyrins and extensive photosensitization (porphyria). The first step of the heme biosynthetic pathway is the formation of 5-aminoleavulinic acid (5-ALA) from glycine and succinyl CoA in mitochondria. The next steps take place in the cytosol where 5-ALA is converted into porphobilinogen (PBG), and further into uroporphyrinogen and coproporphyrinogen. Coproporphyrinogen is then converted into protoporphyrogen IX (PpIX) and combined with iron to form heme in the mitochondria (*Peng et al 1997*), ***Figure 16***. Exogenous 5-ALA becomes a substrate in the heme biosynthesis, bypassing the negative feedback control system, and thus leads to intracellular accumulation of PpIX in the tissue. It is unclear whether application of 5-ALA ester such as methyl-5-aminolaevulinate (MAL), requires an extra metabolic step of ester hydrolysis to convert into 5-ALA which then enters the heme pathway, or whether these esters could also act directly as substrates (*Fotinos et al 2006*). The activation of PpIX by visible light leads to the generation of reactive oxygen species (ROS), leading to the destruction of cells via apoptosis or necrosis within 10 hours. Fast proliferating malignant tissues have increased need for heme, and thus an increased activity of the enzymes (e.g. porphobilinogen deaminase, PBGD) involved in the PpIX development. On the other hand the activity of ferrochelatase enzyme, which converts PpIX into heme, is low, which leads to the accumulation of PpIX in malignant tissues (*Peng et al 1997*). Additionally, the abnormal stratum corneum in malignant skin is penetrated by photosensitizer more

easily than normal skin (*Moan et al 2001)*. It has been suggested that these factors lead in the selective uptake of the prodrug and accumulation of PpIX in malignant tissues and further, to their preferred sensitization and destruction compared to healthy skin *(Babilas et al 2010, Fritsch et al 1998)*. The main target of PDT are mitochondria, but after longer incubation times, PpIX also appears in the cytosol (*Peng et al 1997*). Low concentrations of PpIX in the cell lead to ROS formation only in the mitochondria, leading to apoptosis-induced cell death whereas high concentrations lead to ROS generation also in the cytoplasm and lysosomes and induce cell necrosis and thus, more severe adverse effects (*Castano et al 2006*). In addition to the direct destruction of the tumor cells, PDT also has an effect on vascularization and the immune system usually leading to inflammation that can further destroy residual tumor cells (*Castano et al 2006*).

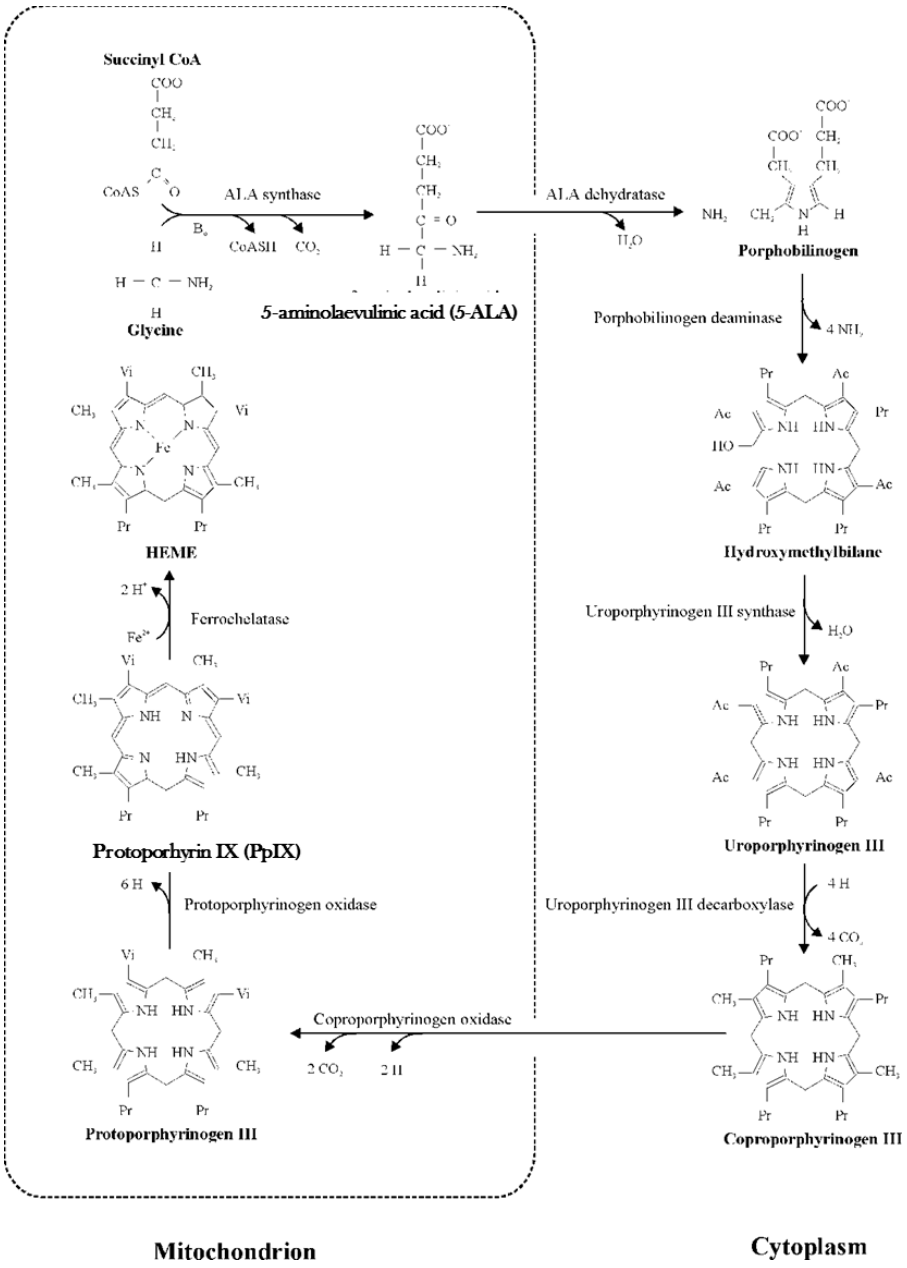

Figure 16. Heme biosynthesis from 5-ALA. Figure by Kaisa Timonen, MD, PhD, edited with permission.

4.3.2 Photosensitizers

The first introduced photosensitizer in dermatology was topical Eosin and Magdala-red dye in 1905 (*Hönigsmann 2013*). Its use was abandoned due to severe side effects and high tumor recurrence rates. In the 1970s and 1990s the first generation intravenous photosensitizers: hematoporphyrin derivate (HpD), tin-protoporphyrin (Sn-Pp) and intravenous porfimer sodium were used for the treatment of NMSC. Due to its large molecular size, topical application was impossible and intravenous application led to prolonged photosensitization of the whole skin for 6-7 weeks (*Calzavara-Pinton et al 1996).* In the 1990s also oral administration of 5-aminolaevulic acid (5-ALA) for cancer treatment was studied, but the treatment caused nausea, vomiting and abnormality in liver function tests (*Calzavara-Pinton et al 1996, Webber et al 1997).* In the 1990s JC Kennedy et al introduced the use of the topical protoporphyrin IX (PpIX) precursor, 5-aminolevulinic acid (5-ALA) (*Hönigsmann 2013)*.

Photosensitizers currently available for topical dermatologic use in Europe are low- molecular-weight second generation protoporphyrin precursors (*Babilas et al 2010*) including methyl-5-aminolaevulinate cream (MAL 160mg/g corresponding 21% MAL hydrochloride, Metvix®, Galderma, Paris France), a patch containing 5-aminolaevulinic acid (5-ALA, Alacare®, 8 mg solid ALA hydrochloride in a 4 cm^2 patch, Galderma-Spirig AG, Egerkingen,Switzerland), and 5-aminolaevulinic acid nanoemulsion gel (BF-200 ALA i.e. "Biofrontera ALA", 78 mg/g corresponding to 10% ALA hydrochloride, Ameluz®, Biofrontera AG Leverkusen, Germany). In the USA, a 5-aminolaevulinic acid stick (5-ALA, Levulan®Kerastick, 20% ALA hydrochloride, DUSA Pharmaceuticals, Wilmington, MA, USA) is available. In addition, non-standardized preparations (e.g. 5-ALA), mixed by hospital pharmacies are commonly used (*Wiegell et al 2003*).

Drawbacks associated with the topical use of 5-ALA are its hydrophility causing limited penetration into the skin and the instability of the active compound (*O'Connor et al 2009*, *Szeimies et al 2010*[2]). It has also been suggested that 5-ALA penetrates more easily to the circulation and has a longer lifetime in tissues as compared to its esters *(Moan et al 2003).* Several efforts have been made to overcome these problems including physical methods (curettage, micro needling and pretreatment CO2-laser) (*Donnelly et al 2008, Haedersdal et al 2014*), derivatization of 5-ALA into liphophilic esters (*Peng et al 1997, O'Connor et al 2009)*, and modifying its formulation into a patch or nano-gel (*Maisch et al 2010, Szeimies et al 2010*[1], *Passos et al 2013)*. Also chemical skin penetration enhancers, like dimethylsulphoxide (DMSO), have been proposed to increase absorption of 5-ALA thus leading to higher PpIX accumulation (*De Rosa et al 2000*).

MAL, a lipophilic short chain 5-ALA ester (ALA-CH_3), has shown superior selectivity for neoplastic cells *(Fritsch et al 1998)* and greater depth of penetration (*O'Connor et al 2009*) compared to 5-ALA. Recently, a novel oil-in-water 5-ALA nanoforrnulation (BF-200 ALA) gel entered the market, ***Figure 17***. BF-200 ALA has increased stability and improved skin and cell penetration, thus leading to higher and deeper accumulation of PpIX in the skin with shorter application times compared to 5-ALA. As a result a low concentration (10%) is efficient (*Maisch et al 2010, Szeimies et al 2010*[2], *Schulten et al 2012*). BF-200 ALA

and MAL showed similar selectivity for dysplastic tumor cell over healthy keratinocytes and PpIX fluorescence was restricted to the application sites in mice implying that neither penetrated to the circulation (*Schulten et al 2012*).

In addition, also long-chained 5-ALA-esters have been developed. Hexyl ester (ALA-C_6H_{13}), transport into the cells more effectively and thus leads to high PpIX amounts with lower concentrations, and shorter application times than needed for 5-ALA, leading to it being proposed as an alternative photosensitizer in topical PDT of skin cancers (*Peng et al 1997, De Rosa et al 2003, Morrow et al 2010).* Despite several preclinical studies with hexylaminolaevulinate (HAL) (*Togsverd-Bo et al 2010, Juzeniene et al 2006, Dögnitz et al 2008*), it has not yet shown its effectiveness in the treatment of human skin cancers. Interestingly, also other novel topical photosensitizers including second generation photosensitizer silicon phthalocyanine, and nonporphyrin-based-photosensitizers like the synthetically produced hypericin and natural extracts from the plant *Hypericum perforatum* are under investigation for use in PDT (*Skalkos et al 2006, O´Connor et al 2009*).

Also systemic photosensitizers are used for non-dermatological-PDT. The systemic first generation photosensitizer, porfimer sodium, (Photofrin®, Axcan Pharma, Birmingham, AL, USA) is currently used for the treatment of lung cancers (*Cai et al 2013*). There are also second generation systemic photosensitizers e.g. temoporfin (Foscan®, Scotia Pharmaceuticals Ltd., UK) ,registered for advanced head and neck cancers, and verteporfin (Visudyne®, Novartis, UK), registered for ophthalmologic use (*Senge et al 2011, Rundle et al 2014*). Temoporfin has also been studied for several other indications including brain, gastrointestinal cancers, breast cancer and urological malignancies including prostate cancer (*Senge et al 2011*).

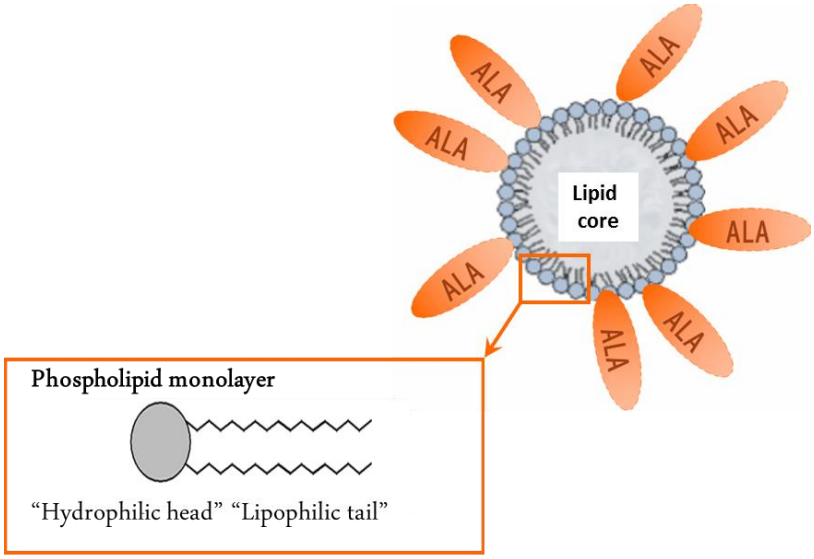

Figure 17. The nanoemulsion (BF-200 ALA) stabilizes 5-ALA and improves penetration through the stratum corneum. The inner part of the nanovesicle consists of lipids. 5-ALA binds to the external hydrophilic part of the vesicles'phospholipid monolayer. Figure by Ben Novak, Biofrontera, edited with permission.

4.3.3 Light sources

Light sources used in PDT match the absorption spectrum of PpIX, which has maximum absorption peak at 410 nm and smaller peaks at 505 nm, 540 nm, 580 nm and 630 nm (*Morton et al 2013[1]*). Unlike ionizing radiation causing carcinogenesis, PDT can be used several times on the same skin area (*Fotinos et al 2006*). Initially, different coherent laser lights were used in PDT (*Moseley 1996*). Nowadays, in conventional PDT, both incoherent red visible light (635 nm) and blue light (417nm Blu®-U, DUSA Pharmaceuticals) are used. Red light penetrates deeper into the skin, but blue light matches the maximal PpIX absorption peak (410 nm, Soret band) and thus may activate PpIX more effectively (*Piacquadio et al 2004)*. Narrow-band light-emitting diode (LED) lamps (Aktilite®Galderma, Paris, France; Omnilux PDT™ Photo Therapeutics, London, UK, and BF-Rhodo LED®, Biofrontera, Leverkusen, Germany; each 630 nm) used with lower light-doses (37 J/cm^2) and shorter illumination times, which are safer (less heating), are preferred over the broad spectrum lamps which are used with higher light doses (100-170 J/cm^2) (Photodyn® 705/505, 580-1400 nm , Hydrosun Medizintechnik GmbH, Germany and Waldman®PDT, 600-750 nm, Waldman-Medizin-Technik, Germany). Narrow-spectrum light sources have been shown to be more effective compared to broad spectrum devices (*Pariser et al 2008, Dirschka et al 2012*). Also green and white light sources, pulsed dye laser, filtered xenon arc, metal halide lamps, and filtered intense pulsed lights (IPLs) have been used in PDT (*Babilas et al 2010, Morton et al 2013[1]*). Recently, also portable LED-light sources (ambulatory-PDT) have emerged (*Moseley et al 2006*). A limitation of these ambulatory devices is that only small areas can be treated simultaneously.

PDT dosimetry has many variables including the photosensitizer dose, drug-light interval, wavelength, irradiance (mW/cm^2), and fluence (J/cm^2) of light (*EDF Guidelines 2014*). Total effective fluence takes into account the spectral irradiance, tissue transmission, and the absorption of the photosensitizer (*Moseley 1996*). Typically red-LED devices are set to give a standard light dose of 37 J/cm^2 in approx.10 minutes (*Moseley 2005)* corresponding to the PplX weighted effective light dose of approx. 1 J_{eff}/cm^2 (*Wiegell et al 2012[2]*).

Daylight is a combination of UVR, visible light and infrared light. The fact that all PpIX absorption peaks are within the visual spectrum of light, allows the use of daylight as a light source in PDT (DL-PDT) (*Wiegell et al 2008, Wiegell et al 2012[2]*), ***Figure 18***. Of the PpIX activation in DL-PDT 87% is caused by blue light (380-495 nm), while 10 % is caused by green-yellow (495-590 nm), and 3% by orange-red light (590-750 nm). The minimum daylight intensity (illuminance i.e. perceived power of light) during a 2-hour exposure should be 100000 lux to match the effective red light dose from traditional LED-PDT, but because also other wavelengths activate PpIX, as low as 2300 lux illumination has been suggested to be efficient (*Wiegell et al 2012[2]*). The threshold of 8 J_{eff}/cm^2 has been set as no association was found between this or greater effective light dose and the response rate (*Wiegell et al 2009*). In addition to the light dose, also outside temperature affects the use of DL-PDT. Meteorological measurements have shown that a >8 J/cm^2 effective light dose in two hours corresponding to an illuminance above 10 000 lux and temperature >10℃

are reached in the northern countries (in Iceland, in Finland, 64˚N) until the middle of September and in southern counties (Israel 31˚N) throughout the year, ***Table 4***, (*Wiegell et al 2013*). However, no correlation between efficacy and effective light dose (range 3-46 J/cm^2) was found in a recent large multicenter study conducted in Australia (*Rubel et al 2014*). Thus, the accurate effective light dose needed for DL-PDT is still unclear.

Recently, indoor simulated daylight sources (Indoorlux® system, Swiss Red AG, Switzerland) giving an illuminance of 15000-25000 lux and irradiance of 21 mW/cm^2 at green-yellow (570-590 nm) and 3mW/cm^2 at orange/red (620-640nm) spectral range corresponding to an effective light dose of 14.3-24.2 J/cm^2 in two hours, have been developed and shown to have successful treatment efficacy for the treatment of AKs (*Kellner et al 2014*).

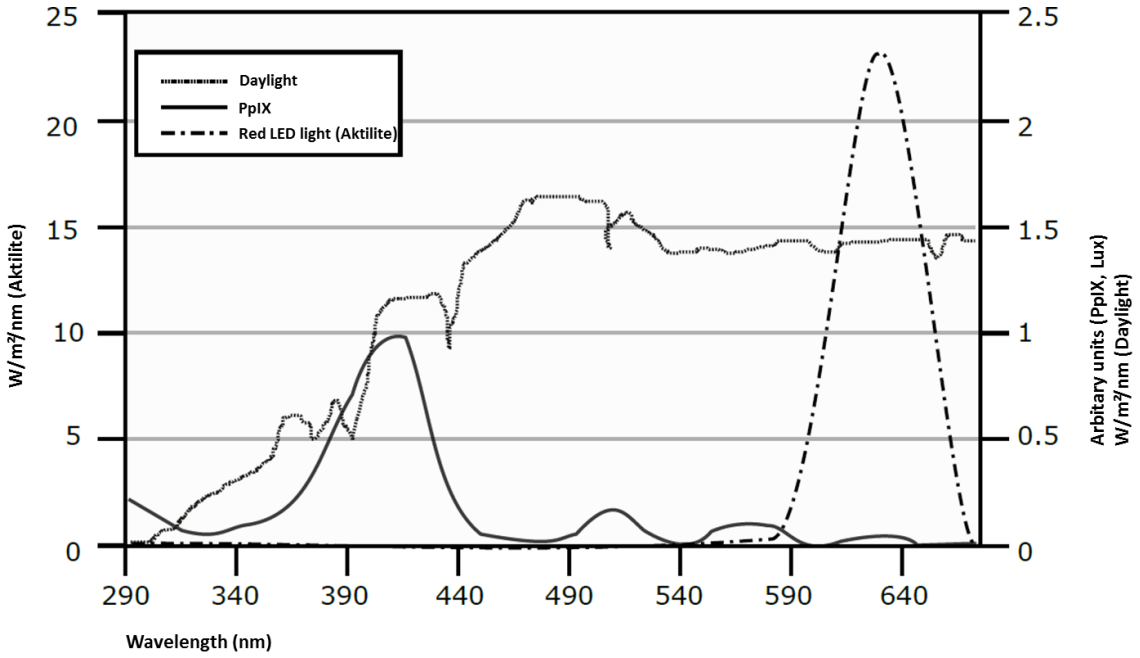

Figure 18. Daylight spectrum and PpIX spectrum. Edited from *Wiegell et al 2012*[2] with permission from John Wiley and Sons.

a)

Latitude	Effective light dose for 2 h of clear sky daylight exposure J/cm²											
	Jan	Feb	Mar	Apr	May	Jun	Jul	Aug	Sep	Oct	Nov	Dec
70 N	0	4	12	23	31	33	31	27	17	7	1	0
60 N	5	12	22	32	39	42	41	35	26	15	7	4
50 N	13	21	31	40	46	48	47	43	35	25	16	11
40 N	23	31	40	47	51	52	51	48	42	34	25	21
30 N	33	39	47	52	54	54	54	52	48	42	34	31
20 N	41	47	52	55	55	55	55	55	53	48	42	39

b)

	Number of days (% of total days that month)					
	Iceland	Norway	Denmark	Germany	Italy	Israel
July		30 (97)	31 (100)			
August	28 (90)	29 (90)	30 (97)	31 (100)		31 (100)
September	21 (67)	24 (80)	29 (97)	27 (90)		30 (100)
October	8 (26)	9 (29)	21 (68)	18 (58)	27 (87)	31 (100)
November	0	0	0	10 (33)	20 (67)	30 (100)
December (28th)	0	0	0	0	19 (68)	17[a] (100)

Days calculated from the first of the month until 28 December. [a]In Israel measurements were only obtained until 17 December.

Table 4, a) Effective light dose for 2-hour daylight exposure at noon at different latitudes. Effective light doses are calculated by weighing the cloud free sky irradiance with the absorption spectrum for PpIX, b) The numbers of days with a effective PpIx light dose above 8J/cm^{2}in two hours between 9 a.m and 4 p.m. From *Wiegell et al 2012*[2] and *Wiegell et al 2013*, with permission from John Wiley and Sons

4.3.4 Treatment protocols

In conventional PDT using artificial light sources, the treatment area is prepared with gentle abrasion (e.g. tape-stripping) or curettage to remove hyperkeratosis and scales to enhance the penetration of the photosensitizers. Then a 1-mm-thick layer of the photosensitizer is applied and covered with light-impermeable dressing for 3 hours (MAL, BF-200 ALA). Afterwards the photosensitizer is wiped off and illumination is performed with an appropriate light matching the PpIX absorption spectrum leading to fast activation of high doses of cumulated PpIX (*Babilas et al 2010, Dirscka et al 2012*). In comparison a 5-ALA patch is used without pre-treatment and incubated for 4 hours prior to illumination and a 5-ALA stick is used without occlusion and illumination is performed 14-18 hours after the application (*EDF Guidelines 2014*). The disadvantage of the conventional treatment is the impractical delay between the drug application and irradiation that burdens the clinics (*Moseley et al 2006*).

In DL-PDT, a chemical sunscreen is applied on sun-exposed skin areas, including the treatment area for 15 minutes before curettage. Afterwards the treatment area is curettaged to remove the crusts and to enhance the penetration of the photosensitizer. The photosensitizer is applied and the area is kept uncovered. After 30 minutes, the illumination with daylight is performed for 2 hours. This process leads to activation of PpIX continuously during its development (*Wiegell et al 2011*). The use of an organic sunscreen does not affect

the efficacy if its absorption spectrum does not overlap the absorption spectrum of PpIX (*Wiegell et al 2011, Wiegell et al 2012*[2]), ***Figure 19***. No difference has been seen in efficacy between 2 and 3 hours daylight exposure (*Wiegell et al 2011*). The use of ablative fractional laser resurfing (AFL) as pretreatment in daylight-PDT, may enhance the efficacy of the treatment (*Togsverd-Bo et al 2014)*.

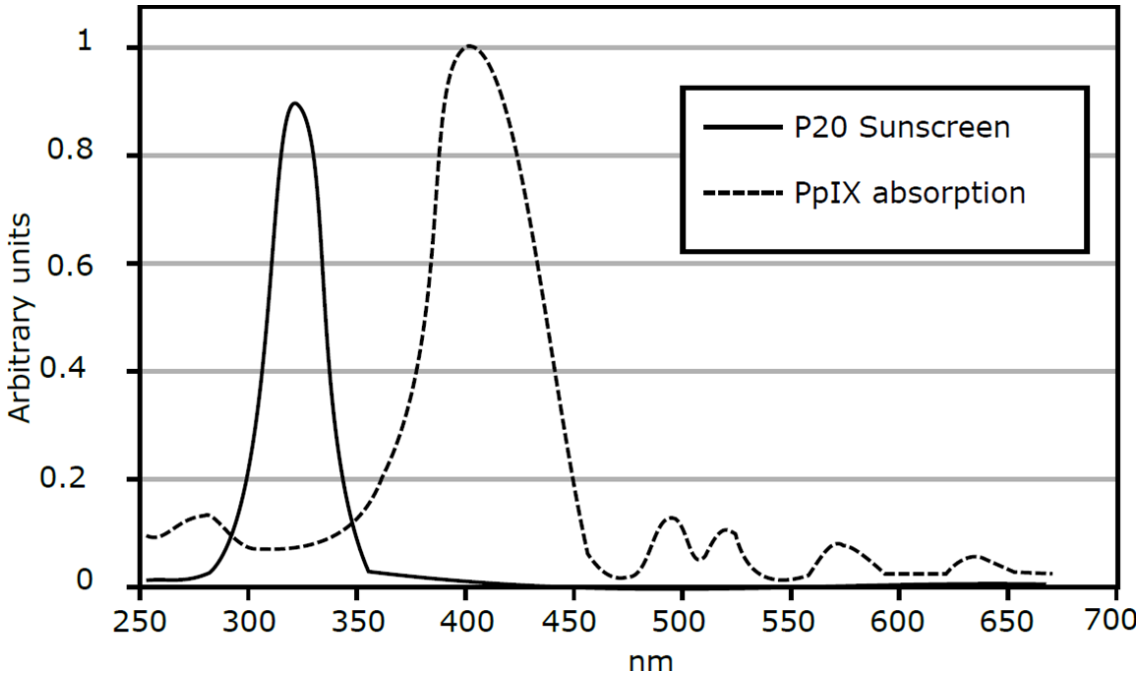

Figure 19. Absorption spectrum PpIX and organic sunscreen (P20®, SPF 20 Riemann & C0. A/S, Hilleroed, Denmark). Edited from *Wiegell et al 2012*[2] with permission from John Wiley and Sons.

4.3.5 Efficacy

Conventional PDT

The placebo-controlled and comparative studies considering different photosensitizers and light sources in PDT are listed in ***Table 5***.

At the 3-month follow-up, MAL-PDT with red LED was superior to vehicle PDT with a lesion complete clearance of 86.2% vs. 52.2% and patient complete response of 59.2% vs. 14.9% respectively (*Pariser et al 2008*). For 5-ALA-PDT with blue light, lesion complete rate was 91% (25% for vehicle), and the patient complete response rate 73% (8% for vehicle) at 3 months (*Piacquadio et al 2004*). A sustained lesion clearance rate of 78% has been reported for ALA-PDT after one year (*Tschen et al 2006*). A comparative intra-individual (split-scalp) study of MAL vs. 5-ALA LED PDT showed photosensitizers as effective with 47% vs. 40% patient complete response and 71% vs. 87% lesion complete clearance, respectively (*Moloney et al 2007*).

PDT with BF-200 ALA showed higher efficacy compared to placebo-PDT with patient complete response of 64% vs. 11% and lesion complete clearance of 81% vs. 22% (*Szeimies et al 2010*[2]). A randomized interpatient trial showed patient complete response of 78% vs. 64% vs. 17.1% and a lesion complete clearance of 90.4% vs.83.2% vs. 37.1% for BF-200 ALA, MAL and placebo respectively at 3-month follow up (*Dirschka et al 2012).* The sustained patient complete response rates rates at 12 months were 46.7% vs. 36% for BF-200 AL and MAL, respectively (*Dirschka et al 2013*).

Conventional-PDT is more effective for thin (gr I) lesions than for thicker (gr II-III) lesions (*Tarstedt et al 2005*). Repeated treatment sessions (two treatments one week apart or a single treatment followed with a repetition at 3-months if needed) are thus recommended for thicker lesions treated with conventional treatment (*Tarstedt et al 2005*).

Daylight-PDT

Lesion complete clearance rates range from 75.9 to 89.2% for DL-PDT, all conducted with MAL with the highest lesion clearance rates seen in a study conducted in Australia (*Wiegell et al 2008, 2009, 2011, 2012*[1], *Rubel et al 2014*). In the initial split-face study, PDT using daylight illumination (DL-PDT) showed as effective (3-month lesion complete clearance 79% vs. 71%) as conventional PDT for AKs on the face and scalp (*Wiegell et al 2008*). In a large multicenter intraindividual study of DL-PDT for thin AKs conducted in Australia, an efficacy of DL PDT was not inferior to conventional-PDT with 3-month lesion complete clearance rates of 89.2% vs. 92.8% respectively, of which 96% and 96.6% were still cleared after 6 months (*Rubel et al 2014*). The lesion clearance rates for thicker AKs (61.2% for grade II and 49.1% for grade III) treated once with DL-PDT were significantly lower than for thin AKs (75.9%) (*Wiegell et al 2012*[1]).

A recent retrospective German study using simulated daylight room and BF-200 ALA showed lesion complete clearance rates of 92.8% and patient complete response of 75% after 3 months (*Kellner et al 2014)*

Study	Treatment protocol	Placebo-control	Study design	Subjects, n	Lesions, n	Follow-up period	Lesion complete clearance	Patient complete response	New AKs	Conclusions
Pariser 2008	16%MAL red LED-PDT, 2 sessions 1 week apart	Vehicle-PDT +curettgae	Randomized double-blinded interpatient	49+47, immunocompetent	363+360, grades I-II	3 months	86.2% vs. 52.2%	59.2% vs. 14.9%	42 vs. 34	MAL -PDT superior to vehichle-PDT
Piacquadio 2004	20% 5-ALA blue light-PDT, re-treatment at week 8 if not cleared	Vehicle-PDT, no curettage	Randomized (3:1)blinded interpatient	181+62 immunocompetent	1403+ 506, grades not specified	3 months	91% vs. 25%	73% vs.8%	-	5-ALA-PDT superior to vehicle-PDT
Moloney 2007	16% MAL vs. 20% 5-ALA LED-PDT	No	Randomized intrapatient	15 immunocompetent	mean 7.3 vs. 8.8 per patient, grade I-III AKs	1 month	71% vs. 87%	46.7% vs. 40%	-	MAL and 5-ALA-PDT as effective
Szeimies 2010	BF-200 ALA red-LED or broad-spectrum lamp, one session, repeated at 3 months for residuals	Vehicle-PDT +curettage	Randomized double-blinded interpatient	81+41 immunocompetent	434+205 grade I-II AKs	3 months after 2. PDT	81% vs. 22%	64% vs.11%,	-	BF-200 ALA superior to vehicle, significant difference in light sources
Dirschka 2012, 2013	BF-200 ALA vs. MAL PDT LED or broadspectrum lamp	Vehicle-PDT +curettage if crusts	Randomized (3:3:1), observed blind interpatient	600 immunocompetent	1504+1557+490 grade I-II AKs 3-8 per patient	3 and 12 months	3 months: 90.4% vs. 83.2% vs . 37.1%	At 3 months 78.2% vs. 64.2% vs. 17.1% At 12 months sustained clearance of 47% vs. 36%	-	BF-200 ALA superior to placebo, non-inferior to MAL
Wiegell 2008	16%MAL DL-PDT vs. LED-PDT	No	Randomized intrapatient split-face	29 immunocompetent	634, majority grade I	3 months	79% vs 71%,	-	-	Daylight non-inferior to LED-light
Wiegell 2009	16% MAL vs. 8%MAL DL-PDT single treatment	No	Double-blinded randomized intrapatient	30 immunocompetent	1107, majority grade I	3 months	76.9% vs 79.5%,	-	-	16% and 8% MAL as effective
Wiegell 2011	16% MAL 1.5 h vs. 2.5 h illumination single treatment	No	Randomized interpatient	120 immunoconpetent	1572, grade I	3 months	77% vs. 75%	-	-	2 h daylight illumination effective
Wiegell 2012	16% MAL 1.5 h vs. 2.5 h illumination single treatment	No	Randomized interpatient	145 immunocompetent	2768 grades I-III	3 months	75.9% (grade I) 62.1 (grade II,) 49.1% (grade III),	-	mean 2.8 per patient	DL-PDT less effective for thin AKs
Rubel 2014	16% MAL LED-PDT vs DL-PDT, one treatment	No	Randomized interpatient	100 immunocompetent	1379 vs 1372 (97% grade I, 3% grade II)	3 and 6 months	3 months: 89.2% vs. 92.8% (grade I), 86.4% vs 89.9% (all grades) 6 months: 96% vs 96.6% of grade I lesions maintained cleared	Not reported	-	DL-PDT non-inferior to LED-PDT for thin AKs
Kellner 2014	BF-200 ALA simulated DL-room, two treatments one week apart	No	Retrospective	32 immunocompetent	Mean 5.3 ± 1.8 per patient, grade I-II	3 months	92.8%	75.0% (all) 82.4% (patients with only AK I lesions) 66.7% (patients with at least one grade II AK)	-	SDL-PDT with BF-ALA effective for grade I-II AKs

Table 5 Efficacy of LED-PDT and DL-PDT

4.3.6 Safety

Both 5-ALA and MAL enter sensory neurons in the free nerve endings in the epidermis via GAT-3 transporter and thus can generate severe pain during their activation (*Novak et al 2011*). This is due to accumulation and sudden activation of high amounts of PpIX during occlusion. To reduce the pain, local anesthesia, cold air analgesia or nerve blocks can be used. The use of topical analgesia is not recommended for two reasons: their high pH might chemically inactivate the photosensitizer, and they might induce local vasoconstriction reducing the oxygen-dependent event. Other common adverse effects of PDT include erythema and edema with erosion, crusting and scaling healing over 2-6 weeks. Localized photosensitivity can be present for up to 48 hours post treatment while PpIX is still formed (*Petersen et al 2014*[1]). The half-life is approx. 24 h for 5-ALA and 48 h for MAL (*Morton et al 2013*[1]). Pruritus, and rarely ulceration,

blistering, scarring, hair loss or post-inflammatory hyper-/hypopigmentation may occur (*Morton et al 2013[1], Babilas et al 2010*). Allergic contact dermatitis to photosensitizing agent has been reported for both 5-ALA and MAL. It seems more likely that sensitization develops to methylester, and 5-ALA may cross-react (*Gniazdowska et al 1998, Wulf et al 2004*). Risks as high as 35% for sensitization after several MAL-PDT sessions have been reported and the question has been put forward whether the persistent inflammatory reactions could actually be caused by contact dermatitis (*Korshøj et al 2009*). Allergic contact dermatitis can occur also from occupational exposure to MAL (*Antonia Pastor-Nieto et al 2011*). In addition, PDT can induce re-activation of herpes simplex (*Ribeiro et al 2012*). There are a few reports of melanomas on post-treatment PDT areas, but they have been considered as incidental events (*Babilas et al 2010*).

The adverse effect profiles in MAL and 5-ALA PDT are similar (*Pariser et al 2008, Piacquadio et al 2004*), but MAL-PDT is less painful than 5-ALA-PDT (*Moloney et al 2007, Wiegell et al 2003*). This might be due to lower PpIX production by MAL (*Novak et al 2011*). BF-200 ALA-PDT showed similar pain values, and skin reactions with MAL (*Dirschka 2012*). Adverse reactions can be reduced by lowering photosensitizer concentration and thus the PpIX dose (*Fabricius et al 2013*). However, 8% and 16 % MAL concentrations provided similar adverse reactions to DL-PDT (*Wiegell et al 2009*). Adverse reaction can also be reduced by post-treatment use of topical corticosteroids (*Wiegell et al 2014*), a cream containing metal ions (e.g. ferrous sulfate) (*Juzenas et al 2010*), or physical sunscreen (*Petersen et al 2014[1]*).

Due to continuous activation of PpIX during its development, DL-PDT is less painful with mean pain scores of 0.8±1.2 (range 0 to 5) vs. 5.7±2.3 (range 0 to10) and maximal pain scores of 2.0 (SD±1.9) 6.7(SD±2.2) (numerical scale 0-10) compared to LED-PDT (*Wiegell et al 2008, Rubel et al 2014*). However, in cases of delay from application of the photosensitizer to daylight exposure or a long pause during exposure, PpIX is accumulated and the treatment might be more painful. Also longer than 3-hour exposure times are associated with higher pain values (*Wiegell et al 2011*). The use of sunscreen during DL-PDT reduces adverse effects. In the initial DL-PDT vs.conventional split-face study, where no sunscreen was used, 42% of the patients had more severe erythema and crusting on the DL-PDT sites compared to 21% on the LED-PDT sites (*Wiegell et al 2008*). When sunscreen was used, fewer adverse reaction were seen in the DL-PDT group (39%) compared to the LED-PDT group (59%) (*Rubel et al 2014*).

In conclusion PDT has several advantages over other AK therapies. It can be performed as an office- or hospital based treatment during one day, has shorter adverse reaction periods compared to most of the home-based topically applied field-therapies (*Braathen et al 2012*). Large areas can be treated during a single session with high clearance rates. In addition, PDT provides an excellent cosmetic outcome (*Rubel et al 2014*). Coampared to LED-PDT, DL-PDT provides further advantages as it is nearly painless and more convenient due to shorter clinic visits (*Wiegell et al 2012[2]*).

4.5 Other therapies

In Europe, over 90% of AKs are treated non-surgically, with liquid nitrogen (LN) cryotherapy being the most frequently used treatment (>60% of the nonsurgical treatments). Newer field-directed treatments, directed for the treatment of multiple lesions, are still waiting to exceed the ablative treatments (i.e. LN cryotherapy) (*Ferrandiz et al 2012*).

4.5.1 Ablative therapies

Ablative therapies physically destroy the target lesion, without any effect on surrounding field-cancerized area and thus leading to "new cancers" (*Ulrich 2009*), they are recommended only for single and thin lesions (*Ceilley et al 2013*). Ablative therapies include surgical procedures (most commonly curettage with electrosurgery) and LN cryotherapy.

LN cryotherapy, being quick and low-cost, is the most commonly used ablative therapy. It is based on quick freezing causing intracellular destruction of the target tissue. Keratinocytes are destroyed at temperatures of -20 - -30℃ (*Suhonen et al 2005*). The overall lesion complete clearance rates were 67.2% after 3 months for gr I-II AKs, while patient complete response was 57% with excellent cosmetic outcome in approx. 50% of the lesions. The freeze duration influenced the clearance rate with a complete lesion clearance rate of 39%, 69% and 83% with freezing times of less than 5s, greater than 5s, and greater than 20s, respectively (*Thai et al 2004*). However, a more aggressive approach may result in hypopigmentation (due to the destruction of melanocytes) and scarring. Other adverse effects include pain, redness, crusting, hair loss at the treatment site, and the potential for infection (*Stockfleth 2012*). LN cryotherapy can be used in combination with field-directed therapies (*Samrao et al 2013*).

Curettage with electrodessication can be used for large/hypertrophic lesions, although histologic verification to rule out cSCC is more recommendable. More commonly curettage is used to debride hyperkeratotic AKs before LN cryotherapy. *Shave biopsies* followed by *electrocautery* can also be used (*Ceilley et al 2013*). Some ablative therapies (*dermabrasion, chemical peels* and *carbon dioxide laser*) are sometimes used to treat larger photodamaged fields, but are mainly focused on skin rejuvenation (*Ceilley et al 2013*).

4.5.2 Field-directed chemotherapies

Topical field-directed therapies cause a localized inflammatory skin reaction leading to the elimination of AKs. These therapies are recommended for areas of multiple AKs. The long treatment times (except for ingenol mebutate) with prolonged local skin reactions, cost of the treatment and cognitive problems (i.e. an inability to understand the treatment plan or to properly use medication) may cause nonadherence (*Ceilley et al 2013*). Evidence for the efficiency of various treatments for AKs vary from the systematic review of randomized trials for 5-fluorouracil and imiquimod, to randomized trials for diclofenac and ingenol

mebutate, to case series for newer topical agents (i.e. resiquimod, piroxicam, betulinic acid and potassium dobesilate) (*Micali et al 2014*).

5-Fluorouracil (5-FU), a fluoropyrimidine antimetabolite that stops the growth of rapidly proliferating (cancerous) cells by disturbing DNA and RNA synthesis, has been used since the 1960s for dermatological (pre)cancerous conditions (*Stockfleth 2012*). 5-FU widely available as a topical cream or solution (Efudex® 5% or 2% FU, Fluoroplex® 1% 5-FU, Carac ® 0.5% 5-FU, Actikerall® 0.5% 5-FU+10% salicylic acid). In Finland 5-FU is approved but not currently marketed. The highest response rates have been reported for daily use of the 5% cream for 2-4 weeks. Also prolonged applications 1-2 times a week for 6-7 weeks have been used. A systematic review evaluated patient complete response rates (overall 80% reduction in lesion count) at 2-12 months to be 49% for the 5% formulation and 34.8% for the 0.5% formulation (*Micali et al 2014*). Lesion clearance rates vary from up to 96% in controlled clinical trials to 50-70% at one year in clinical practice, which has been explained by nonadherence and common side effects (erythema, erosion, desquamation, burning sensation, pruritus, more rarely secondary infections, scarring and discoloration) (*Samrao et al 2013*).

Imiquimod is a toll-like receptor-7 agonist that modifies the immune response and stimulates apoptosis thus disturbing tumor proliferation (*Stockfleth 2012*). Imiquimod is available in Europe in the following concentrations: 5% (Aldara®) and as 3.75% and 2.5% (Zyclara® 2.5% and 3.75%) cream formulations (*Samrao et al 2013*). The duration of the treatment varies from two 2-week cycles of daily application (3.75% and 2.5% cream solutions) to up to 16 week (3 times per week use, 5% cream) resulting in up to 85% lesion complete clearance at one month, 45-48% histologic lesion clearance and 31-84% patient complete response two months after treatment (*Samrao et al 2013, Micali et al 2014*). In a long term follow-up of two years, 20 % of the patients treated with imiquimod had developed new AKs compared with 90% in a placebo group (*Stockfleth et al 2004*). The side effects include erythema, burning, pain, erosion and ulceration. However, imiquimod is better tolerated than 5-FU (*Samrao et al 2013*).

Diclofenac is a nonsteroidal anti-inflammatory drug used in combination with hyaluronic acid which supports transport into the epidermis (Solaraze®;3% diclofenac+2.5% hyaluronic acid). Diclofenac acts through anti-inflammation by inhibiting cyclooxygenase (COX-2) production, and it also has anti-angiogenetic and apoptose-inducing effects (*Maltusch et al 2011*). The duration of treatment with this drug is long, being 60-90 days .The side effects (mild erythema, pruritus) are milder than with FU or imiquimod (*Samrao et al 2013*). Patient complete response rates of 33-50% have been reported after 60-90 days treatment and thus its efficacy appears to be lower than that of other topical treatments (*Micali et al 2014*).

Ingenol mebutate, a macrocyclic diterpene ester extracted from the plant Euphorbia peplus, induces a rapid necrosis of primary tumors and stimulates a neutrophil-mediated immune response cytotoxic to residual tumor cells (*Stockfleth 2012*). Treatment with ingenol mebutate significantly reduces mutant p53 keratinocyte patches (*Cozzi et al 2012*). This relative new treatment is available in 0.05% and 0.015% gels

(Picato®). The milder formulation is applied once a day for three days to AK on the face or scalp, and stronger formulation once a day for two days on the body. Lesion complete clearance rates of 87% at two months, sustained at one year, and patient response rates of 37-47% at two months of which 44-46% were sustained at one year have been reported (*Lebwohl et al 2013*). Adverse effects include erythema, scaling and scabbing. The advantage is its short application time enhancing patient adherence but a limitation is that the treatment should be limited to 25 cm^2 areas (*Micali et al 2014*).

New topical agents including 5-FU combined with salicylic acid, resiquimod, piroxicam, betulinic acid and potassium dobesilate are under investigation for the treatment of AKs (*Samrao et al 2013, Micali et al 2014*). Topical difluoromethylornithine (DFMO) inhibits the enzyme ornithine decarboxylase (ODC), which when induced by UV-radiation initiates tumor growth.DFMO is currently studied for chemoprevention and treatment of AKs (*Pommergaard et al 2013*).

4.5.3 Efficacy of PDT compared with other therapies

Most of the AK treatment trials are placebo-controlled but comparative studies of different treatments are rare and thus information on treatments relative efficacy is limited. In addition, due to the continuum of sun-damaged skin and AKs, counting AKs appear to be unreliable and variation exists even among experienced dermatologists, which interferes with the accuracy of the results (*Weinstock et al 2001*). Varying end points (lesion vs. patient clearance rates (75%, 100%), preventive effect i.e. counting new lesions) and follow up periods (1-24 months) complicates comparisons between studies. AK counts can also change spontaneously with high regression and recurrence rates (*Werner et al 2013).*

A multicenter study comparing LN cryotherapy and conventional MAL-PDT (1-2 sessions 12 week apart) showed significantly higher lesion complete clearance rates for LN cryotherapy (88%) than for MAL-PDT (78%) (*Kaufmann et al 2008*). In a randomized intra-individual split-face study, MAL-PDT (one treatment session, repeated at 3 months if needed) and LN cryotherapy (double freeze-thaw, repeated if needed at 3 months) showed higher clearance rates for PDT (86.9% vs. 76.2%) at 3 months before retreatments and equal clearance rates: 89.1% vs. 86.1% respectively for MAL-PDT and LN cryotherapy at 6 months. Fewer side effects were reported with MAL-PDT than with LN cryotherapy (*Morton et al 2006*). MAL-PDT as a single session was proven to be as effective (69% vs. 75% clearance), and two treatment sessions of MAL-PDT more effective (91% vs. 68% clearance) than LN cryotherapy (*Babilas et al 2010*). All the studies reported significantly better cosmetic outcome and patient-preference for PDT´ than for LN cryotherapy.

A network meta-analysis based on Cochrane review ranked FU at 0.5-5% concentrations to be the most effective treatment followed by ALA-PDT (all photosensitizers, narrow and broad spectrum red and blue lamps) ≈ imiquimod ≈ ingenol mebutatate ≈MAL-PDT> LN cryotherapy> diclofenac+hyaluronic acid> placebo (*Gupta et al 2013*). The analysis ranked the complete patient clearance and did not value tolerability, costs or cosmetic outcome.

Another recent network meta-analysis based on the same Cochrane review valued the effect of different ALA-agents and different concentrations of imiquimod, and showed the highest probability for complete patient clearance (75.8%) for LED-PDT with BF-200 ALA, followed by imiquimod (63.3% for 5% cream 16-week-treatment , 56.3% for 5% cream 4-week-treatment, 39.9% for 3.75% cream 4-week treatment), 5-FU 0.5% (59.9%), ALA-patch LED-PDT (56.8%), MAL LED-PDT (54.8%), ingenol mebutate (54.5%), LN cryotherapy (38.2%), diclofenac 3%+hyaluronic acid (24.7%) and placebo (6.9%) . However, this study excluded 5% FU cream and was funded by Biofrontera (*Vegter et al 2014*).

4.5.4 Secondary prevention

Despite several treatment options for AKs, only a few of them have been shown to be effective for secondary prevention of new AKs and cSCCs. Photodynamic therapy (PDT) is widely studied for secondary prevention of AKs and cSCCs (*Bissonnette 2007*). In UV-radiated mice, topical MAL-PDT significantly delayed and reduced the number of developed AKs and cSCCs (*Sharfaei et al 2002*). A single treatment with conventional PDT has been shown to delay the development of new lesions (mostly AKs, also warts and keratoacantomas, no cSCC developed) in renal transplant recipients (*Wulf et al 2006*). In immunocompetent patients, with previous NMSC, conventional 5-ALA-PDT significantly reduced the number of newly developed AKs compared to placebo-PDT (*Apalla et al 2010*). In organ transplant patients, repeated conventional MAL-PDT reduced the number of new AKs (*Wennberg et al 2008*) .When ALA-PDT was used without curettage as a single session no preventive effect was seen in the development of cSCCs although a trend for decreased "keratotic lesions" was seen in OTR patients (*de Graaf et al 2006*). MAL-PDT and imiquimod 5% effectively prevented the appearance of the new AKs, however, the study was not placebo-controlled (*Sotiriou et al 2014*). In a recent placebo-controlled trial topical retinoid (0.1% tretinoin) was shown to be ineffective in the prevention of AKs and NMSC (*Weinstock et al 2012*). Topical diclofenac (NSAID), calcipotriol (vitamin D-3 analog), and difluoromethylornithine (DFMO) as monotherapy failed to prevent NMSC but a combination of diclonefac+DFMO and diclonefac+calsipotriol reduced tumor incidence and size of the tumors compared to placebo in UV-radiated mice (*Pommergaard et al 2013*). Currently no evidence exists for a chemopreventive effect of topical FU or ingenol mebutate.

4.6 Principles of the cost-effectiveness analysis

Taking into account the high AK prevalence rates, AK treatments cause also a significant economical burden to society. As a high percentage of patients with field cancerized skin require repeated treatments (*Ceilley et al 2013*), an ideal AK treatment should not only be effective and well tolerated, but also provide economically good value for money i.e. have a good balance between the costs and benefits. Here I will briefly review the terminology regarding the economic evaluation, which could be used to assist decision making between different treatment options.

Efficacy means the outcome of a treatment in an ideal situation like in a controlled trial (i.e. does the treatment work?). *Effectiveness* means the outcome of a treatment in everyday practice (i.e. does the treatment work in real life?). *Efficiency* is the net ratio between a treatment's effectiveness and the required resources (i.e. is it worth it?*). Cost-utility analysis* takes into account the effectiveness of the intervention, and patients' morbidity and mortality. Cost-utility can be expressed in terms of cost per a quality adjusted life year (QALY) gained (*Robinson R 1993[1]). Cost-minimization analysis* can be used to identify the least costly treatment option if it can be assumed that two options provide similar treatment outcomes (*Robinson R 1993[1]). Cost-effectiveness analysis* (CEA) includes a systematic comparison of the relative health care costs and benefits and thus provides information on whether the intervention provides good value for money (i.e. what is the most effective way to use the resources?) (*Gordon et al 2014*). This approach can be used when the outcomes of the interventions may vary between the interventions (*Robinson R 1993[1]).* The results of CEA are expressed in terms of cost per unit of outcome (*Robinson R 1993[1]). The incremental cost-effectiveness ratio* (ICER) is the ratio between the net costs and the net effects of two interventions (A and B). ICER can be calculated using the formula:

ICER= (cost of intervention B – A) - (savings of intervention B-A)/effects of intervention B-A

If this ratio is low, the intervention B is said to be cost-effective (*Caekelbergh et al 2006*). To reduce uncertainty of the results of the CEA, the results can be tested with a sensitivity analysis (*Robinson R 1993[2]).* There are different types of sensitivity analyses including a simple sensitivity analysis, an extreme scenario analysis and a probabilistic sensitivity analysis; all of these investigate the extent to which results are sensitive to alternative assumptions. An ideal economic evaluation should be conducted along prospective clinical trials, which rarely is the case (*Robinson R 1993[2]).* Most of the cost-effectiveness studies of AK treatments are funded by drug companies and use estimated and modeled values instead of prospective study designs. In addition, they commonly fail to use proper sensitivity analyses. The studies considering cost-effectiveness of different AK treatments are detailed in the *Discussion* section.

5. TREATMENT OF LENTIGO MALIGNA (MELANOMA)

5.1 Prevention

LMs are treated in order to prevent the development of invasive LMMs. Sunscreens can be used in the prevention of melanomas (*Hirst et al 2012*). To our knowledge, no specific studies that consider the prevention of LMs exist.

5.2 Surgical treatment of LM

The standard treatment for LM and invasive LMM is wide surgical excision. The current recommendations for clinical excision margins are the following: 0.5-1 cm for in situ melanoma (LM), 1 cm for melanomas equal or under 1 mm in Breslow thickness, 1-2 cm for melanomas 1,01-2.0 mm in Breslow thickness and 2 cm for melanomas over 2.0 mm in Breslow thickness (*Bichakjian et al 2011*). Lentigo maligna subtype melanomas often represent wide (several mm to several cm) superficial subclinical extension and thus wider margins are suggested for their adequate removal (*Bichakjian et al 2011*). Another challenge in LM excision is their frequent location on the facial area where wide excision can cause serious morbidity and thus surgeons may attempt to limit any deformity by using less safety margins than recommended (*Debloom et al 2010*).

LM/LMMs are typically located on sun-damaged dispigmented skin areas; this complicates the assessment of the lesion borders and thus achievement of adequate margins. After standard surgical wide excision of LM with 5 mm margins, recurrence rates vary between 6-20% *(Erickson et al 2010).* The width of the required surgical margin is significantly related to the lesion thickness (*Bricca et al 2005*). The average margins required to clear LM and LMM were 7.1 mm and 10.3 mm, respectively (*Hazan et al 2008*). Sixty percent of patients with the majority of *in situ* lesions required a 10-mm margin and two or more stages of excisions (*Bosbous et al 2009*). Nine-mm margins have shown their superiority over 6-mm margins with adequate removal of 99% of LMs (*Kunishige et al 2012*). In addition, larger LMs require wider margins than do smaller lesions due to their greater subclinical components (*Bub et al 2004, Hazan et al 2008*). Up to the present the question: "How wide is wide enough?" remains controversial.

Considering the high recurrence rates, it has been argued that residual LMs are unlikely to be detected in routine cross-sectioning "bread-loafing" histology which enables the detection of 1% of the true specimen margins (*Osborne et al 2002, Bosbous et al 2010*). The accuracy of cross-sectioning for finding positive margins is directly dependent on the interval between the cross-sectional cuts with a sensitivity of 50% for cross-sectioning performed every 1 mm and as low as 7% when sectioning is performed every 4 mms (*Kimyai-Asadi et al 2007)*. Consequently, cross-sectioning must be performed every 0.1 mm to meet the 100% specimen margin requirement. Mohs micrographic surgery (MMS), using horizontal sectioning of frozen excised tissue, has been developed to solve this problem. MMS potentially allows the excision of the smallest amount of tissue by confirming histologic clearance of 100% of the peripheral margins (*Clark et al 2008*). Nevertheless, in frozen sections malignant melanocytes are poorly visualized due to processing artifacts, melanocyte-mimicking vacuolated keratinocytes mimicking, and obscuring dermal inflammatory cells, and thus MMS is not a very suitable technique for LM or LMM excisions. Variations of the MMS technique, called staged surgical excisions (SSE), using permanent formalin-fixed sectioning and/or immunostainings (e.g. Mel-A/MART-1, Mel-5, S-100, HMB-45), are used for more accurate detection of the melanocytes. Traditional Mohs surgery reports from nil to up to 33% and its variants 0-9.7% recurrence rates

for LM, respectively (*Erickson et al 2010, McLeod et al 2011)*. The center of the tumor should always be sent for permanent vertical sectioning in order to rule out an invasive component *(Iorizzo et al 2013).*

5.3 Non-surgical treatment of LM

There are also non-invasive treatment options for LM but their efficacy has not been established and they should only be considered when surgical excision is not realistic. Non-surgical treatments options include topical imiquimod, radiation therapy, LN cryotherapy (*Bichakjian et al 2011*). In addition lasers, PDT and tazarotene gel have been studied for this use (*Cotter et al 2008, Bosbous et al 2010, Karam et al 2013)*. A disadvantage of non-invasive treatments is the lack of the histological examination of the whole lesion for hidden invasive components (*Erickson et al 2010*). In addition, clinical follow-up of LMs may be challenging due to treatment-induced pigmentation (*Cotter et al 2008*) and amelanotic recurrences (*Fleming et al 2004*).

Imiquimod shows 66-100% clinical and 53-75% histologically confirmed clearance rates for LM (*Micali et al 2014*). The effect is claimed to be caused by activation of the immune response, especially interferon-α which also has effect in systemic treatment of metastatic melanoma (*Erickson et al 2010*). However, reported follow-up periods are limited (12-18 months) and in most studies histologic verification was only available from partial biopsies and thus there are inadequate data to prove the efficacy. Progression to invasive melanoma may occur under treatment with imiquimod (*Cotter et al 2008*). The level of evidence of topical pharmacotherapy for LM treatment is IV (case series) (*Micali et al 2014*). Imiquimod treatment may remove the visible pigment while no clearance is seen histologically (*Fleming et al 2004*) and also produce post-treatment pigmentation which may be misdiagnosed as a recurrence (*Cotter et al 2008*).

Radiation therapy has been reported to be effective in LM treatment with clinical cure rates of 86-95%. However, histological clearance reports are not available and the studies include relatively low numbers of patients with short (2-5 years) follow-up periods (*Erickson et al 2010, Bichakjian et al 2011).*The high voltage schedules (100-280 kV up to 5-6 mm depth) are effective but induce a risk for adverse effects while low voltage (10-50kV) reach only up to 1mm which may be insufficient to destroy the malignant melanocytes deeper down the follicular structures (*Bosbous et al 2010*).Thus, radiation therapy should be considered as a second-line treatment option only if surgery is contra-indicated. In addition, also ultra-soft x-ray i.e. grenz-ray (GR) treatment is used for the treatment of LM (*Hedblad MA et al 2012*).

Melanocytes are more sensitive to cold injury than keratinocytes. *Cryotherapy* for LM shows varying clinical clearance rates (65.7-93.4). Studies done with this technique to date fail to report the histological clearance and long-term follow-up, and are not controlled and thus cryotherapy is not recommended for LM (*Bosbous et al 2010, Bichakjian et al 2011).*

Several *lasers (*argon, carbon dioxide, Q-switched Nd: YAG, Q-switched ruby*)* have been studied for the treatment of LM. However, the recurrence rates are high (40-50%) and thus laser treatment is not recommendable for LM *(Bosbous et al 2010).*

One study experimentally used *PDT* (light doses 40-90 J/cm^2 and 3-9 sessions*)* for treatment of LM. It has been suggested that the effect is probably due to PpIX binding to benzodiazepine receptors and thus affecting the proliferation of and differentiation of melanoma cells. Complete clinical and histological clearance was found in 12 of 15 (80%) cases (*Karam et al 2013).*However, the follow-up period was short (10-29 months) and histology was only performed from partial treatment areas and thus the results are rather unreliable.

In addition retinoids (tazaroten gel 0.1%) have been suggested to enhance the effect of topical imiquimod (*Cotter et al 2008).*

AIMS OF THE PRESENT STUDY

1. To study the feasibility of a novel hypespectral imaging system (HIS) in preoperative lesion margin assessment of subclinical borders of LM and LMM

2. To study HIS in the detection of inpicient subclinical AKs and field cancerization

3. To study the effectiveness and safety of a novel photosensitizer formulation, 5-ALA nanoemulsion (BF-200 ALA), in DL-PDT for AKs and field cancerization

4. To study the effect of repeated treatment sessions for grade II-III AKs in DL-PDT

5. To study the histological and immunohistochemical effects of DL- PDT

6. To assess the cost-effectiveness of DL-PDT compared to LED-PDT in the treatment of AKs

METHODS

1. PATIENTS

The study was performed in accordance with the Declaration of Helsinki, and the study protocols were approved by the Ethics Committee of Tampere university District. Patients were recruited from the Department of Dermatology in Päijät-Häme central hospital. All patients gave their written informed consent for their participation.

Study **I** was conducted between 2012 and 2014, study **II** between 2011 and 2012, study **III** in 2013, and study **IV** between 2011 and 2014. The patient characteristics are shown in ***Table 6***. Altogether 121 patients were included in the studies.

In study **I** we included patients with suspected LM or LMM on their faces or scalps. In addition to 19 patients described in article **I**, four additional patients who were recruited after submitting the paper will be presented. Study **II** was implemented in two phases. The inclusion criteria for phase one was at least three clinical AKs located on the same area on the face or scalp. For phase two we included less photodamaged patients with at least one AK on their faces, scalps or necks. Inclusion criteria in study **III** was at least two symmetrically located clinically similarly graded AKs ≥6 mm in diameter on face or scalp. For study **IV** we included patients with at least three clearly detectable AKs on the face or scalp. In studies **II-IV** AKs were clinically graded into three grades according to Olsen et al: I, mild (slightly palpable AK, more easily felt than seen); II, moderate (moderately thick AK, easily seen and felt); III, thick (very thick or obvious AK) (*Olsen et al 1991*). All AK grades were included. Exclusion criteria for all studies were lactation, pregnancy and likelihood of non-compliance. In addition exclusion criteria for studies **II-IV** were immunosuppression, known history of porphyria or photosensitivity, allergic reaction to ingredients of the photosensitizers or treatment of the studied skin areas 3 months earlier.

													Previous treatments			
Study	Period	Patients recruited	Patients completed	AKs All	Mean (range)	LM(M)s	Female	Male	Mean age (range)	Phototype I-VI	Outdoor workers	AK	Bowens disease	SCC	BCC	Melanoma
I	2012-2014	23	23	-	-	23	10	13	78.7 (67-97)	I=3 II=11 III=9	-	7	1	-	7	-
II	2011-2012	12	12	52	4.3 (1-13)	-	5	7	77.3 (65-94)	I=10 II=2	-	8	-	2	3	-
III	2013	14	13	177	13.6 (4-24)	-	6	7	79.8 (66-88)	I=4, II=3 III=6	4	9	1	2	6	1
IV	2011-2014	73	70	210	3 (3)	-	31	39	76 (59-73)	I=8 II=25 III=34 IV=3	11	46	3	6	18	1
All		122*(121)	118* (117)	439		23										

Table 6. Patient characteristics studies **I-IV** * one patient participated in studies **II** and **IV**

2. PHOTOGRAPHING AND FLUORESCENCE IMAGING

All studied lesions were photographed (Canon Ixus 130 or Olympus Pen Lite E-pl5). Fluorescence detection with Wood's light was used in studies **I** and **II**.

In study **I** we used Wood's light (320-400 nm, peak 365 nm, Philips Burton®, Somerset, USA) to help in defining the borders of LM and LMM preoperatively. In this UV light lesion were photographed and their borders were marked with a black pen, photographed, and compared with those assessed with a hyperspectral camera.

In study **II** and phase one we used PpIX fluorescence detection to find the subclinical AKs. After marking and photographing the clinical lesions a standard 1 mm-layer of MAL, evaluated by the researcher, was applied on 12–70 cm^2 areas surrounding them and kept occluded for three to four hours under a light-impermeable cover (Tegaderm matrix wrap and aluminum foil). Afterwards the MAL was wiped off with sodium chloride liquid and the area was illuminated with Wood's light (Philips Burton®, Somerset, USA). The fluorescence was documented with a digital camera (Canon Ixus 130) and the most brightly fluorescent areas were marked with a blue pen and photographed again. All the marked areas were kept covered by a cloth and aluminum foil for 2–3 days to avoid activation of the MAL-induced pIX. Two to three days later when the MAL had vanished, we took the hyperspectral images and punch biopsies. In phase two of the same study we took hyperspectral images of the naive AKs followed by a biopsy, ***Figure 20***.

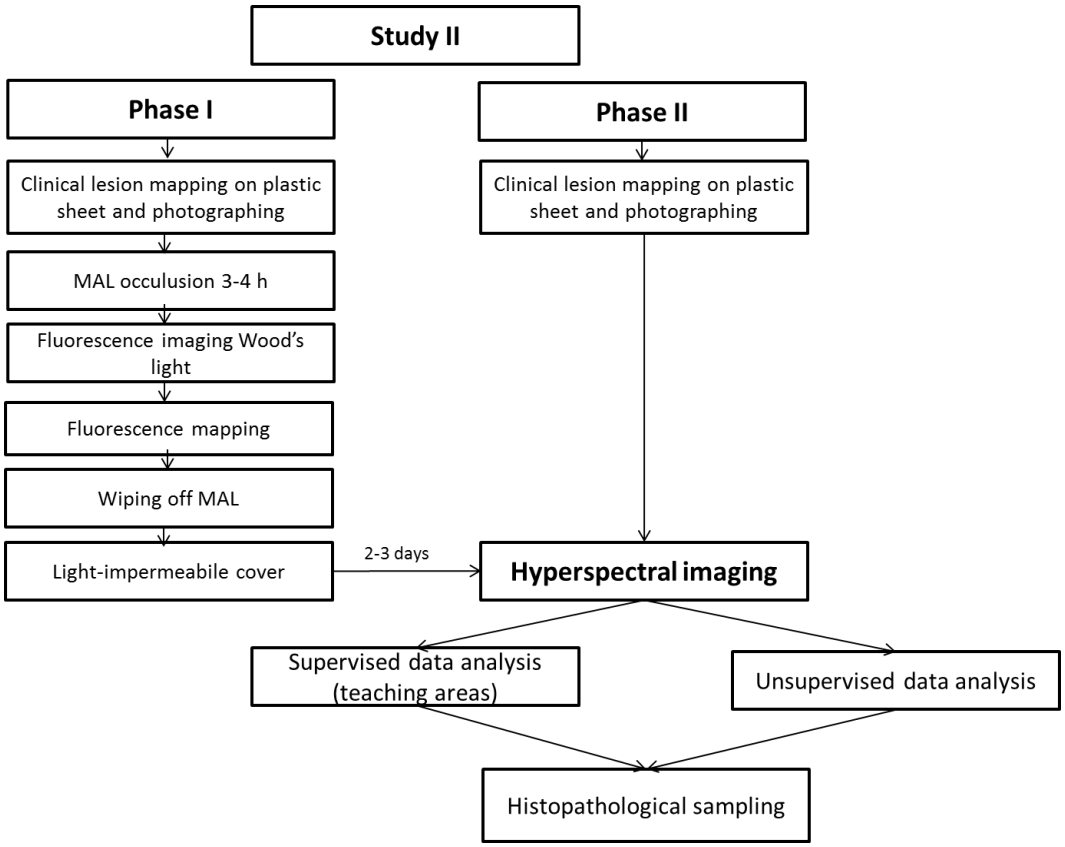

Figure 20. Flow chart for study **II**

3. HYPERSPECTRAL IMAGING

Hyperspectral imaging was used in study **I** to assess the subclinical borders of LM and in study **II** to detect the areas of incipient subclinical AKs.

3.1 Device

The handheld hyperspectral imaging system (HIS) was developed for the study at the VTT Technical Research Centre of Finland and the data processing was developed by the University of Jyväskylä, Finland, ***Figure 21***. The technical characteristics are detailed in the appendix of the original article **I** and in *Pölönen et al 2013*. The prototype imaging system consisted of a novel small sized hyperspectral imager (VTT FPI VIS-VNIR Spectral Camera, 500-850 nm) (*Saari et al 2010 and 2013*), an external light source of visible and infrared light (500-850 nm), a fiber optic ring light, and a holder for the imager and the ring light.The used hyperspectral imager is based on a Fabry-Perot interferometer (FPI) which enables the use of tuneable wavebands and thus detection of the whole waveband range rapidly compared to scanning prism techniques. The imager's spectral bands widths are 5–10 nm. We used 70 wavebands between 500 and 850 nm. FPI allows changes to be made to the wavelengths in milliseconds. The imaged data was transferred from the camera to a laptop via a USB cable. Images with 320x240 pixel spatial resolutions were taken with a five-megapixel image sensor using 8x8 binning. Binning enables one pixel on the image to contain information from 8x8 pixels on the image sensor, which improves the signal-to-noise ratio and makes the sensor more sensitive to light. With the 12 cm^2 field of view (FOV) the spatial resolution was 6400 pixels/cm^2. The size of one pixel was approx. 125µm. The imaging depth was approx. 2 mm. The weight of the handheld system was approx. 1.2 kg.

In study **I** all 23 lesions were imaged at their naive state prior to any surgical procedure. In study **II** phase one, hyperspectral images were taken 2-3 days after the fluorescence imaging process when we assumed there was no MAL fluorescence left. In phase two of study **II** no fluorescence imaging was used and the images were taken directly before the biopsies. HIS acquired the diffuse reflectance of the detected skin areas rapidly in a few seconds.

Figure 21. The handheld hyperspectral imager (VTT FPI VIS-VNIR Spectral Camera).

3.2 Hyperspectral data analysis

There are different approaches to analyze hyperspectral data including supervised classification algorithms and unsupervised linear spectral unmixing (*Harris 2006*). In our study, two different methods were used in analyzing the data from the acquired hyperspectral data cube, ***Figure 22***. In study **I** the data was analyzed using the linear signal unmixing method. In study **II** we used both supervised neural network analysis, and unsupervised linear signal unmixing analysis.

In the unsupervised linear signal unmixing we assumed that the obtained spectra were a linear mixture of the pure spectra. In this method the acquired hyperspectral data was analyzed using the assumption that it complied with the linear mixture model (vertex component analysis, VCA and filter vector algorithm FVA) (*Nascimento et al 2005, Bowles et al 1995, Bro et al 1997*) to achieve pure spectra (endmembers) of the lesional and healthy skin and to produce abundance maps of their diffuse reflectance.These abundance maps each represented different pure pixels and their appearance in the image and were used for detection of field cancerized skin areas and for delineation of the LM borders. The analysis methods are detailed in another thesis (*Pölönen et al 2013*).

The supervised method was a classical feed forward neural network method with multi-layer perceptron (*Ripley 1996*). This method had to be trained with "healthy" and "sick" data sets. We used training areas from 1) clinical AKs, 2) subclinical AKs detected earlier by their PpIX fluorescence, and 3) from healthy-looking non-fluorescent skin. The neural network method provided map-like diffuse reflectance images with binary results ("sick/not sick") of the whole obtained area.

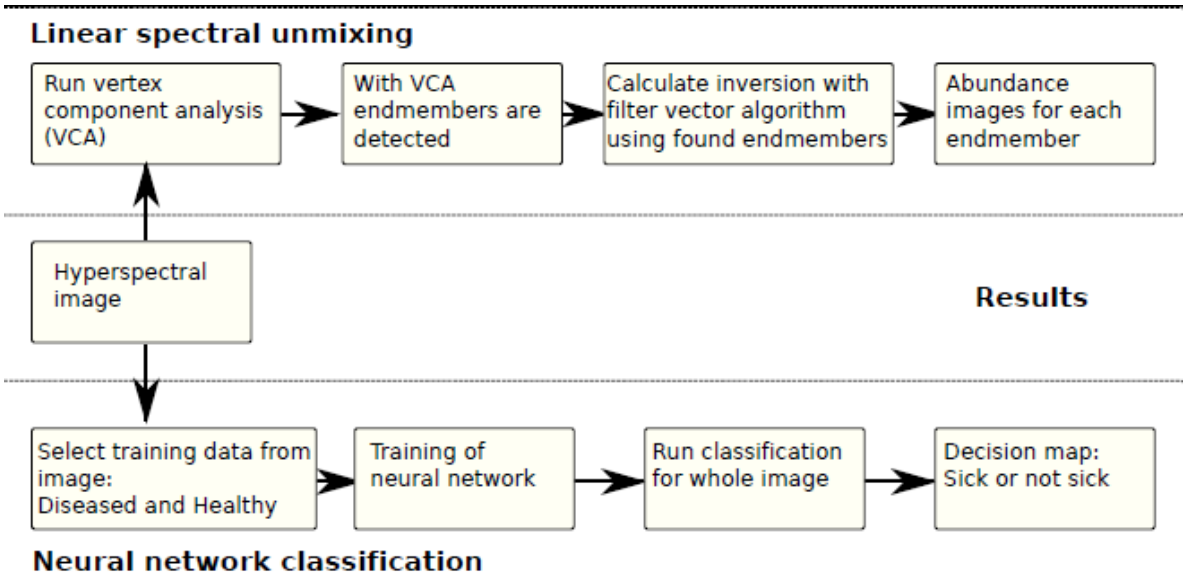

Figure 22. Hyperspectral data analysis process. Figure by Ilkka Pölönen, PhD, with permission.

4. HISTOPATHOLOGICAL AND IMMUNOHISTOCHEMICAL METHODS

4.1 Sampling techniques

In study **I** six of the 23 LM/LMM lesions were biopsied before recruiting to the study and immediately excised with wide margins after the imaging processes. To help map the findings for 17/23 patients, we took targeted 3 mm punch biopsies (1-3 per patient) from the middle and from the lesions' borders, defined using the HIS, and afterwards the lesions were completely excised with wide excision margins. In addition to better evaluate the subclinical extension of the lesion borders 10 of 23 lesions were excised directly at the clinical border shown by Wood's light and the 5-mm margin border was excised as a separate 5 mm circumferential strip. The biopsy sites and excision margins were marked and photographed. The edges of the specimens were marked with orienting sutures, inked and oriented on a map. In the four additional patients all lesions were excised using a separate circumferential strip.

In study **II** phase one, we took 4-5 punch biopsies (3 mm diameter) per patient after all the imaging procedures. The sampling sites were (1) clinical AK, (2) subclinical AK detected by its strong fluorescence and/or HIS, (3) healthy looking skin showing no or weak fluorescence. For ethical reasons, we could not biopsy all the clinical and subclinical AK on the wide cosmetically sensitive areas, and thus the sampling sites had to be limited. In phase two of the same study we limited the biopsies to one per patient to verify the diagnosis of the clinical AKs.

In study **III** we took 3-mm-punch biopsies from symmetrically located equally graded AKs $\geq$ 6 mm in diameter prior to treatment and again at the 3-month follow-up visit. The control biopsies were taken from the same lesion, but avoiding the previous biopsy site to eliminate the changes from scar formation. No biopsies were taken in study **IV**.

All the biopsy samples were fixed (10% formalin), embedded in paraffin, sectioned (3 μm thickness), and stained with hematoxylin and eosin (HE) using standard methods. We used vertical permanent sectioning for all the lesions.

4.2 Histopathology and immunohistochemistry

A specialist in dermatopathology (Leila Jeskanen) interpreted all the samples for the LM study (**I**).Immunohistochemical stainings for MART-1/Melan A was used in 7/23 cases and S-100 staining in one case.

In studies **II-III** a specialist in pathology (Taneli Tani) interpreted the specimens in a randomized order, being unaware of the site and the identification of the volunteer being tested and whether the sample was taken prior to or after the treatment (in studies **II-III**). The dysplasia in AKs was graded using a three-step grading system, where grade I was mild, grade II intermediate and grade III severe dysplasia (*Cockerell 2000*).

In addition to HE-stainings, in study **III**, paraffin-embedded material was used for p53 immunohistochemistry. The used method detected the overall p53 expression without distinguishing between mutant and wild-type p53. The protocol was optimized for diagnostic purposes. The tissue was made into 2 µm sections. After rehydration, the slides were pretreated by heat-induced epitope retrieval with an alkaline buffer. Primary antibody (clone DO-7, Dako M7001, Dako Co., Carpinteria, CA, USA) was diluted 1:200. The slides were stained in a Labvision Autostainer with a Dako EnVision detection kit with copper sulfate enhancement. The slides were counterstained with hematoxylin. Negative control slides were prepared by omitting the primary antibody. The p53 reactivity was quantified by counting the percentage of positive nuclei in three consecutive high power fields from the region of highest reactivity, and expressed as the average of the three high power fields. We set the threshold of a p53 score >10% to be considered pathological.

5. PHOTODYNAMIC THERAPY

5.1 Photosensitizers

Two different photosensitizer precursors were used including methyl-5-aminoleavulinate (MAL 160mg/g, Metvix®, Galderma, Paris, France) and 5-aminolaevulinate nanoemulsion (BF-200 ALA, 78 mg/g Ameluz®, Biofrontera, Leverkusen, Germany).

DL-PDT was used in studies **III-IV** and conventional LED-PDT in study **IV**; ***Figure 23*** shows the treatment protocols. In study **III** MAL was compared with BF-200 ALA in DL-PDT. In study **V** MAL was used in DL-PDT and for conventional LED-PDT for AKs to assess the cost-effectiveness of these two treatment modalities.

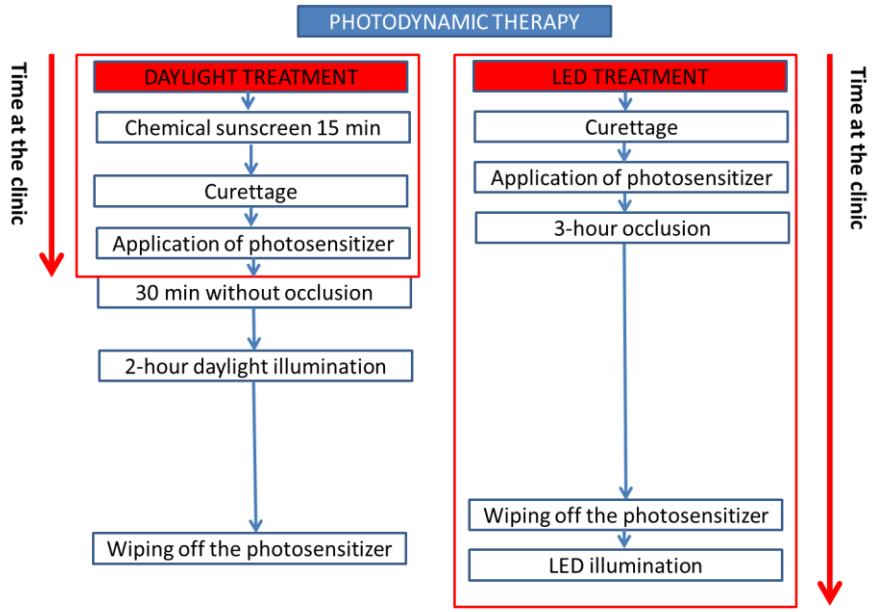

Figure 23. Treatment protocols for DL-PDT and LED-PDT.

5.2 Daylight treatment

In study **III** we used a randomized split-face design so that one side of the face was treated with MAL and the other with BF-ALA with DL-PDT. Before the treatment, identical treatment areas were measured symmetrically on the face or scalp and lesions were counted, graded, photographed and drawn on a plastic sheet, ***Figure 24***. AKs, ≥6 mm in diameter and equally graded clinically, were bilaterally biopsied prior to treatment and at 3 months. Studies were double-blinded i.e. neither the patient nor the investigator assessing the outcome measurements were aware of which photosensitizer was used on which side.

An organic sunscreen (SPF 20, P20®, Riemann & C0. A/S, Hilleroed, Denmark described in detail in *Wiegell et al 2009, **Figure 19***) was applied to all the sun-exposed skin areas for 15 minutes prior to superficial curettage of the treatment area. The skin was wiped with alcohol (A12T Dilutus 80%,Berner Oy, Helsinki, Finland) prior to application of the sunscreen. No anesthetic was used. The amount of the photosensitizers was weighed to achieve a 0.25 mm thick layer on the whole treatment field (mm^2 * 0.25 mg/mm^2) on both sides and the area was left uncovered. Daylight illumination was performed 30 min later for 2 hours on the hospital balcony and the illumination time was controlled by a nurse.

At the end of the 2-hour daylight exposure, residual photosensitizer precursors were wiped off, and the patients were instructed to spend the rest of the day indoors. In all DL studies, treatments were postponed on very dark or rainy days, or if the temperature was below10℃.

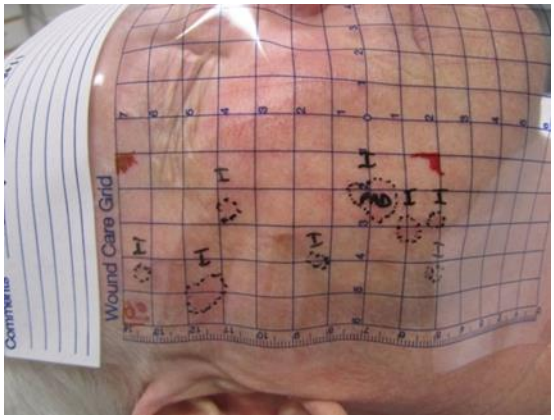

Figure 24. AK treatment fields, individual lesions and biopsy sites marked on a plastic sheet to help mapping later during the follow-up visit. With permission of the patient.

In the treatment protocol in study **IV** comparing DL-PDT and LED-PDT in randomized intervidual study design differed from that in study **III**. Three clearly detectable target lesions per patient were chosen for the study follow-up. Grade I lesions were given one treatment session and grade II-III lesions two treatment sessions 1-3 weeks apart. Before curettage, for DL-group sunscreen (ACO Sun Kids High Protection Sun Spray® SPF 30, ACO; octocrylene, ethylhexyl salicylate, diethylamino hydroxybenzoyl hexyl benzoate, bis-ethylhexyloxyphenol methoxyphenyl triazine, methylene bis-benzotriazolyl tetramethylbutylphenol) was

applied for 15 minutes to all the sun-exposed skin areas also including the treatment area. The absorption spectrum of the sunscreen had two peaks in the UV-region and only minimally overlapped with the visible blue light region, ***Figure 25***. After 15 minutes, the lesions were curettaged under local anesthesia (50:50 Lidocain c. adrenalin® 10 mg/ml + 10 µg/ml Orion Pharma and Naropin® 7.5 mg/ml AstraZeneca) (gr II-III lesions) or without anesthesia (gr I lesions). After curettage, a thin visible layer (approx. 0.25 mm) of MAL was applied to the lesional area but not on the surrounding field. The amount photosensitizer of used was separately weighed for each patient. No occlusion was used. The patients were instructed to start the daylight illumination 30 minutes after leaving the clinic and continue the exposure continuously for a total of 2 hours. The treatment time was controlled only by the patients.

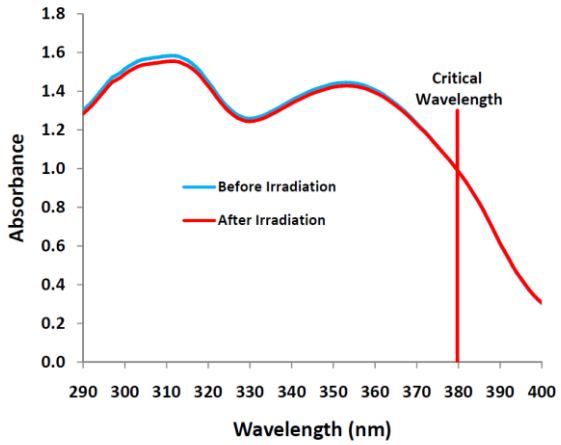

Figure 25. The absorbance spectrum of an ACO Kids sunscreen. As PpIX absorption peaks are in the visible region of light at wavelengths of 410, 505, 540, 580 and 630 nm, this sunscreen is usable in DL-PDT. With permission of Ulf Åkerström, ACO.

5.3 Conventional treatment

Conventional LED-PDT was used for the comparison with DL-treatment in study **IV**. Local anesthesia (50:50 Lidocain c. adrenalin® 10 mg/ml + 10 µg/ml Orion Pharma and Naropin® 7.5 mg/ml AstraZeneca) was used for grade II-III lesions to reduce pain during illumination. All lesions were superficially curettaged to remove crusts prior to application of the photosensitizer. For LED-treatment an approximately 1-mm-thick-layer MAL was applied to lesional target areas and kept occluded (Tegaderm™+aluminum foil) for 3 hours. The consumption of photosensitizer was weighed. Afterwards the excess MAL was wiped off. For illumination we used a red-LED lamp (Aktilite® CL16 or CL128, Galderma; peak irradiance at 632 nm, Galderma, Paris, France) (*Moseley 2005*). The lamps were set to give a total light dose of 37 J/cm^2 achieved in approx. 9 minutes (CL128, average irradiance 65 mW/cm^2) or in 7 minutes (CL16, average irradiance 86 mW/cm^2). Primarily, one lamp with a larger 90x190 mm field (CL128) was used but if the lesions were far

apart, another lamp (CL16, field 40x50 mm) was used at the same time. If the three target lesions were all far apart from each other, the nurse used several illuminations.

5.4 Efficacy assessment

In study **III** treatment efficacy was assessed clinically and histologically by blinded observers at 3 months. The responses were evaluated separately for the lesions (lesion complete clearance) and whole treated area including assessment of the new lesions (area complete response).In study **IV** the efficacy was assessed at 6 months separately for the patients (patient complete response) and for the lesions (lesion complete clearance) by a non-blinded observer.

5.5 Safety assessment

In both PDT studies (**III-IV)** the patients were instructed to record pain during and after the treatment using theVisual Analog Scale (VAS 0-10). In study **III** pain was recorded separately for both treatment sites every 30 minutes during and every 2 hours after the treatment until 9 p.m., ***Figure 26***. In study **III** we also assessed the adverse reaction at one week by a blinded observer, and patient preference.

In study **IV**, the LED-PDT group assessed pain at the beginning, middle, and at the end of each 8-minute irradiation session and the DL-PDT group assessed pain every 15 minutes during the 2-hour daylight exposure. After the treatments both groups assessed pain once every 30 minutes for 2 hours, and then every 60 minutes until no pain was experienced. No evaluation for adverse reactions was done.

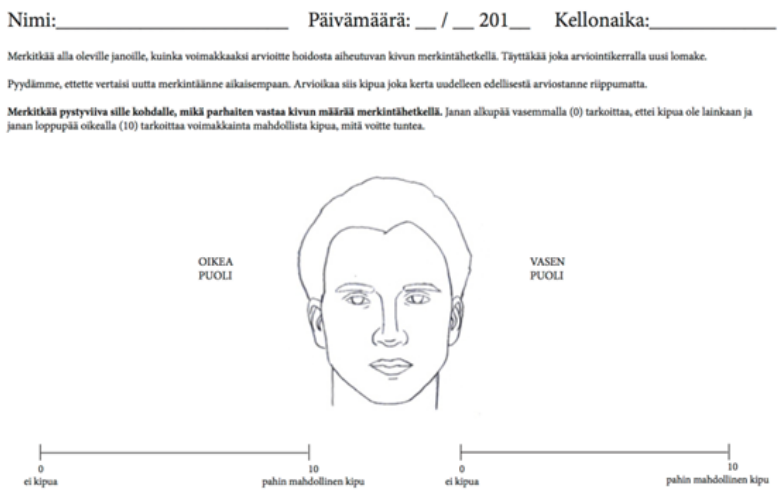

Figure 26. The Visual Analog Scale for split-face assessment of pain in study **III**

6. COST-EFFECTIVENESS ANALYSIS

In study **IV** we assessed the cost-effectiveness of DL-PDT (intervention) compared to LED-PDT (control). For the cost-effectiveness analysis (CEA) we calculated the incremental cost-effectiveness ratio (ICER). We tested the uncertainty around the point estimate of the ICER with a bootstrapping simulation and presented the results using the cost effectiveness plane (CE-plane).

The probability of a patient's complete response was estimated by using logistic regression estimation, where complete response was defined in cases where 3/3 lesions were completely cleared (value =1) and respectively no response if only 0-2/3 lesions were cleared (value=0). Patients' age and gender, as well as treatment group were used as regressors in the logistic models.

For cost calculations we included the societal costs: monetary valued time-consumption of the nurse (***Figure 27***), and the doctor, costs of the photosensitizer, anesthetics and equipment and treatment room rent. We also assessed the patients' cost perspective by valuing patients' time used for the treatment and patients' travel costs, *Table 1* in original article **IV**. For valuing the time costs we used the mean monthly salaries of nurses (€3089.16) and doctors (resident €4616.1), and for the patients' the average monthly retirement pension in Finland (€1408 in 2012, source: Official Statistics in Finland).

Costs were assessed for the first 42 patients and the values for each cost item were imputed item by item into a multivariate regression model using the following regressors: patients' age, gender, occupation (outdoors vs. indoors work), number of treatment sessions (1-2) and treatment group (daylight vs. LED light) to acquire estimated costs for all 70 patients included in the study.

Costs per complete responder were assessed by dividing the average total cost per patient by the estimated probability for a patient's complete response.

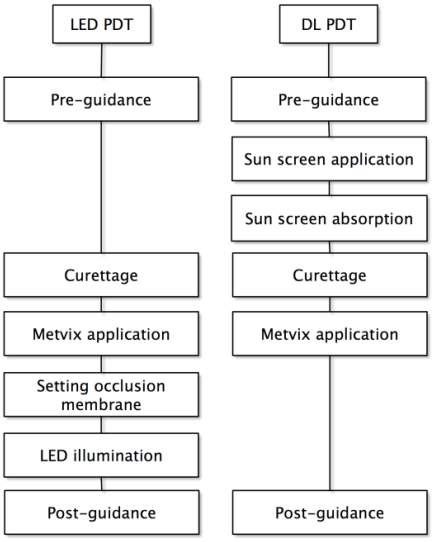

Figure 27. Nurses' time measurements in study **IV**

7. OTHER STATISTICAL ANALYSES

Randomizations

In studies **III-IV** the randomizations were generated using a web-based validated program (Research Randomizer©, http://www.randomizer.org/) that created a random assignment of the treatment sides (study **III**) or treatment protocols (study **IV**) to randomization numbers. In double-blinded study **III** the randomization result was kept blinded from the investigator who conducted the follow-up visits, from the pathologist, and the patients. In study **IV** we used unblinded protocol. At recruitment neither the patient nor the recruiting doctor knew which treatment the patient would receive. The randomization list was printed and concealed in an envelope. The envelope was only opened during the treatment visits.

Sample size evaluation

No sample size calculations were done for pilot studies **I** and **II**.

In study **III** we calculated the sample size by assuming 30% difference in histological lesion clearance between the two studied photosensitizers. Based on *Szeimies et al 2012* we used an alpha error of 0.05 power of 0.80 and sigma value of 0.26 and this resulted in a sample size of 12 subjects.

In study **IV** the sample size was calculated based on costs of the treatments. Based on previous publications (*Wiegell et al 2008, Rubel et al 2014*), we assumed DL-PDT to be as effective as LED-PDT but to be less costly due to less time spend at the clinic (*Wiegell et al 2008)*. As no previous data on the costs of DL-PDT was available, we used the smallest acceptable difference of 20% between the costs of DL-PDT and LED-PDT. For the sample size calculator we used an alpha error of 0.05, power of 0.80 and sigma value of 0.3 giving a sample size of 36 subjects per group.

The statistical tests used in the studies are listed below. P-values <0.05 were regarded as statistically significant.

Wilcoxon's test

Study **III**: per patient half face baseline and clearance, histological baseline and lesion clearance, reduction in histological grading, p53 reduction in immunochemical stains, VAS pain scores (split-face intrapatient setting).

Fisher's exact test

Study **III**: per lesion baseline characteristics and complete clinical response rates, differences in clinical and histological clearance between thin and thick lesions, and decrease in clinical grading.

Study **IV:** baseline characteristics, lesion complete clearance rates.

McNemar's test

Study **III:** the complete histological clearance.

Pearson's chi-squared test (χ2)

Study **IV** patient response.

Mann-Whitney test

Study **IV**: time use, total cost, cost per complete responder and VAS pain scores (interpatient setting).

Agresti-Coull interval

Study **III**: the 95% confidence intervals (95% CI) for clearance rates

RESULTS

Study I

In this study we used HIS for the detection of subclinical borders of LM and LMM. In addition to the 19 patients described in article **I**, we recruited four additional patients who are only described in this thesis. Altogether we included 23 patients with 23 lesions of which 17 were LMs and six invasive LMMs (Breslow thickness range 0.5 and 1.25 mm). The mean clinical lesion size was 2.3 cm^2 (range 1.6 cm^2 -7.6 cm2).

The results are shown in ***Figure 28*** (all 23 patients) and in *Table 1* original article **I** (original 19 patients). The HIS results were in concordance with the histopathology in 20/23 (87%) cases while in 3/23(13%) cases HIS result differed from those assessed histologically. HIS was valuable in 11/23 (48%) cases for detecting the lesion borders more accurately than assessed clinically with Wood's light, of these in eight cases the lesions were wider (***Figure 29***) and in three cases smaller than detected clinically. In 10/23(43.5%) cases HIS gave no additional information as the lesion borders were similarly delineated clinically, histologically and by HIS. In 2/23 cases HIS showed lesion extensions that could not be confirmed by histopathology (false positives). In 1/23 case (4.3 %) HIS missed the subtle lesion extension revealed histologically. This study was not used to differentiate in situ and invasive LM.

In the two false positive cases LMs were surrounded by benign lentigines (melanosis dermidis) and in one case also actinic keratosis which may have complicated not only the HIS interpretation but also the histological evaluation.

After the histopathological evaluation, 6/23 lesions needed re-excision because of the subclinical extension of the lesion borders. With the more accurate lesions demarcation with HIS these re-excisions could have been avoided.

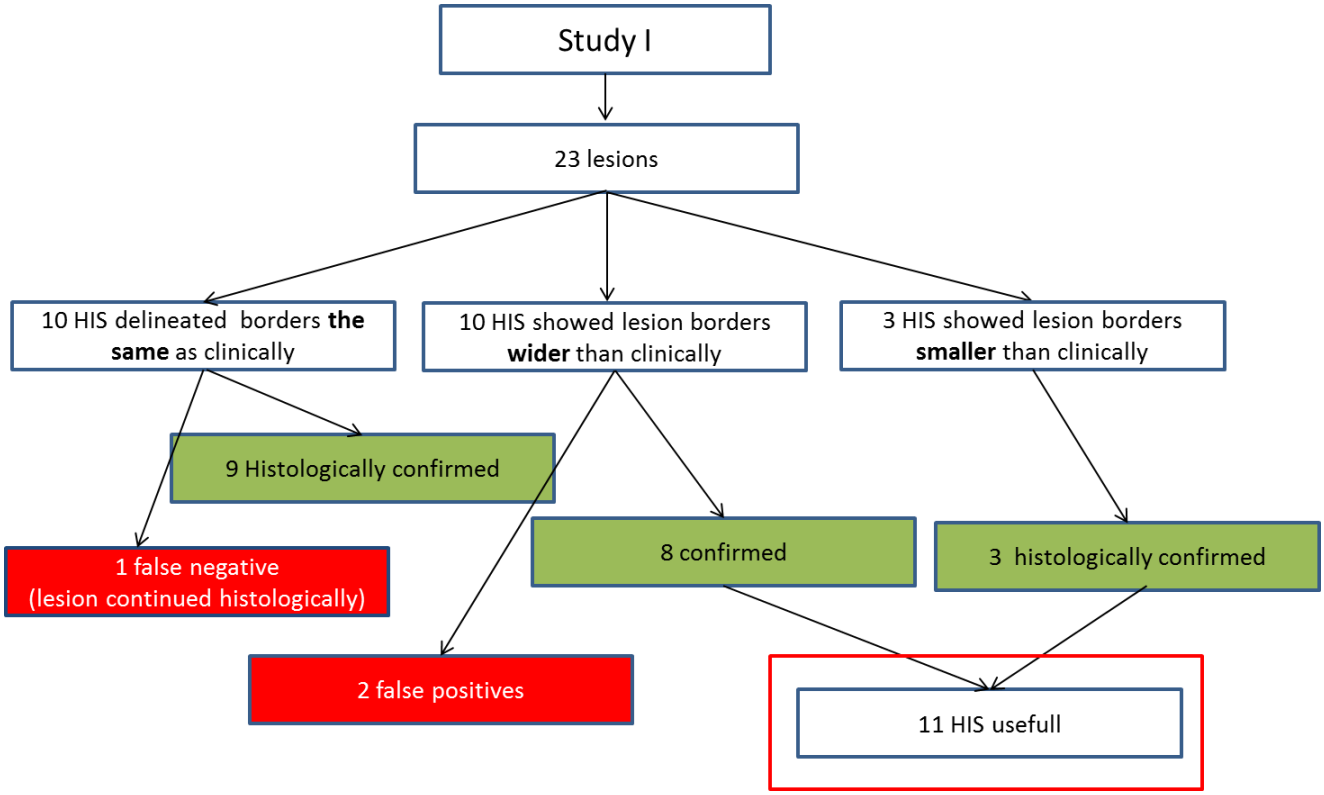

Figure 28. Flow chart results study **I**. HIS was found useful in 11/23 cases 48% giving more accurate information than assessed clinically. In3/23 (13%) of the cases HIS assessed the margins less accurately than a clinician with Wood's light.

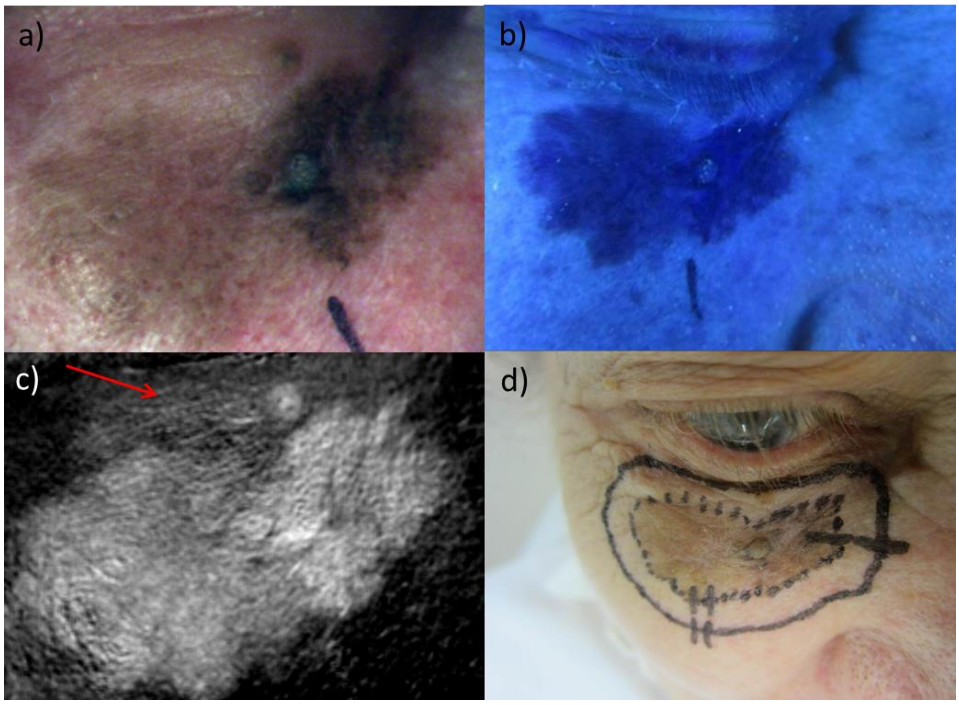

Figure 29. LM on the lower eyelid, a) a clinical photograph, b) lesion in Wood's light, c)HIS showing subclinical lesion extension (arrow), d) 5-mm clinical excision margins, the lesion continued histologically up to the periphery of the superior margin and patient needed re-excision.

Study II

Altogether 12 patients with 52 clinical AKs were included in study **II**. HIS detected all the clinical AKs, and the numerous areas that represented the subclinical lesions. In phase one (6 patients, 41 clinical AKs) we detected subclinical AKs using PpIX-fluorescence and used this data as teaching areas for HIS, ***Figure 30***. In addition teaching areas for "healthy skin" were taken from clinically healthy-looking, non-fluorescent skin. Altogether 27 biopsies were taken from: 1) AKs detected clinically, by fluorescence and HIS (n=6), from subclinical AKs detected by fluorescence and/or HIS (both n=6; HIS only, n=9; fluorescence only, n=1), and from healthy appearing skin (n=5), ***Figure 30*** and *Table 1* in the original article **II**. From the 27 biopsies 22 fulfilled the criteria of an AK, and 5 represented healthy skin.

Of the 22 AKs 6 were clinically detected, and 16 were subclinical. HIS data analyzed by the neural network revealed all the clinically detected AKs and all the histologically confirmed 16 subclinical AKs. In comparison, fluorescence detection missed 9 of the HIS detected subclinical areas and misdiagnosed one area representing healthy skin as an AK, ***Figure 31***.

As the neural network needed pre-defined teaching areas we had to run the data again in two cases after receiving the histopathological reports. In one case it was noticed that one area assumed to be healthy histologically represented an AK and this area had incorrectly been used as a teaching area for HIS. The data was reanalyzed by using another healthy looking skin area but the diagnosis was not confirmed by histology

(group 1, patient 1). In another patient the fluorescent skin area revealed histologically not to fulfill criteria of an AK and the data was re-analyzed using this area as a teaching area for healthy skin (group 1, patient 3).

In phase two (6 patients, 11 clinical AKs) no PpIX fluorescence was used and we took the hyperspectral images from naive skin without marking the lesions and again after marking lesion borders. As we wanted to conduct the analyses without teaching areas, we used the unsupervised linear signal unmixing method for analyzing the data. We calculated the abundance images by searching the spectra derived from a typical biopsy confirmed AK (*Fig 4* in the original article **II**), and calculated the abundance images based on this spectra, *Fig 5* in original article **II**. Afterwards we took 6 biopsies, one from each patient to confirm the diagnosis. We then rerun the data using a white background reference and identified the mean pure AK spectra (end-member) of an AK and healthy skin, ***Figure 32***. After completing the study eight of 12 patients received daylight-PDT and twoLED-PDT. Two patients received LN cryotherapy for milder skin damage (both in phase two).

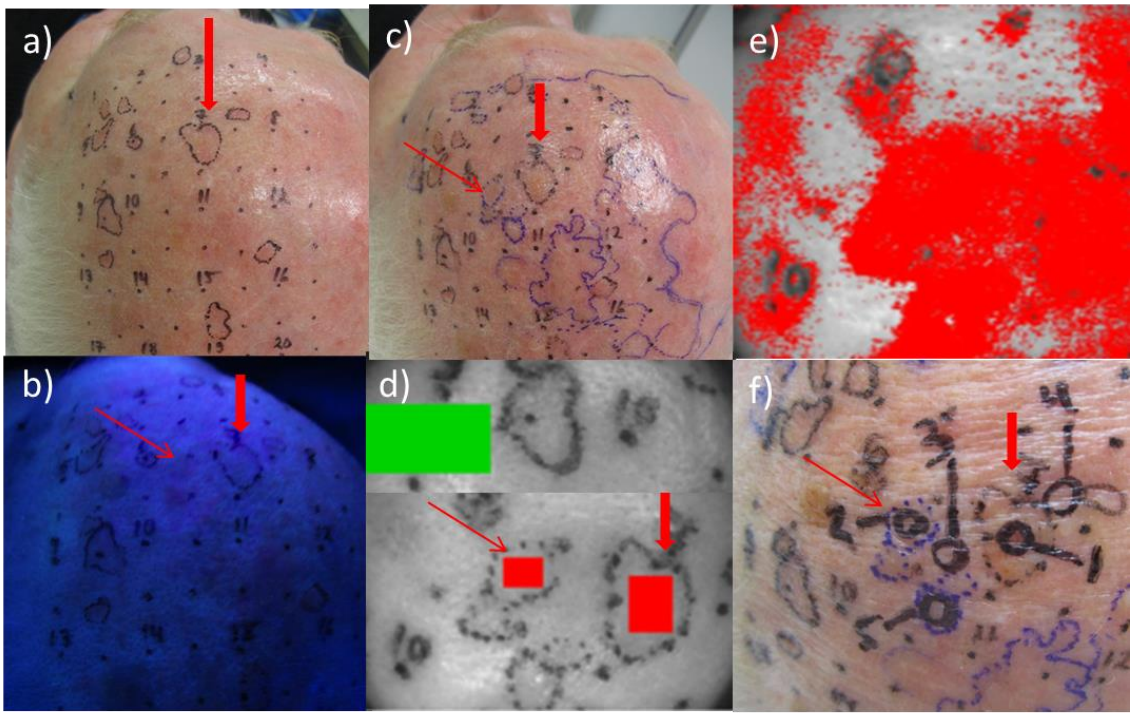

Figure 30. Neural network teaching with PpIX fluorescence. a) Clinically clearly detected AKs marked with a black pen, b) fluorescence in Wood's light (clinical lesion thick arrow, subclinical thin arrow), c) fluorescent areas marked with a blue pen, d) teaching areas for HIS: healthy appearing skin (green), sick areas (red; clinical and subclinical AK) e) Neural network analysis showing field cancerized areas red, f) site of the punch biopsies to confirm the results. Results presented with the permission of the patient.

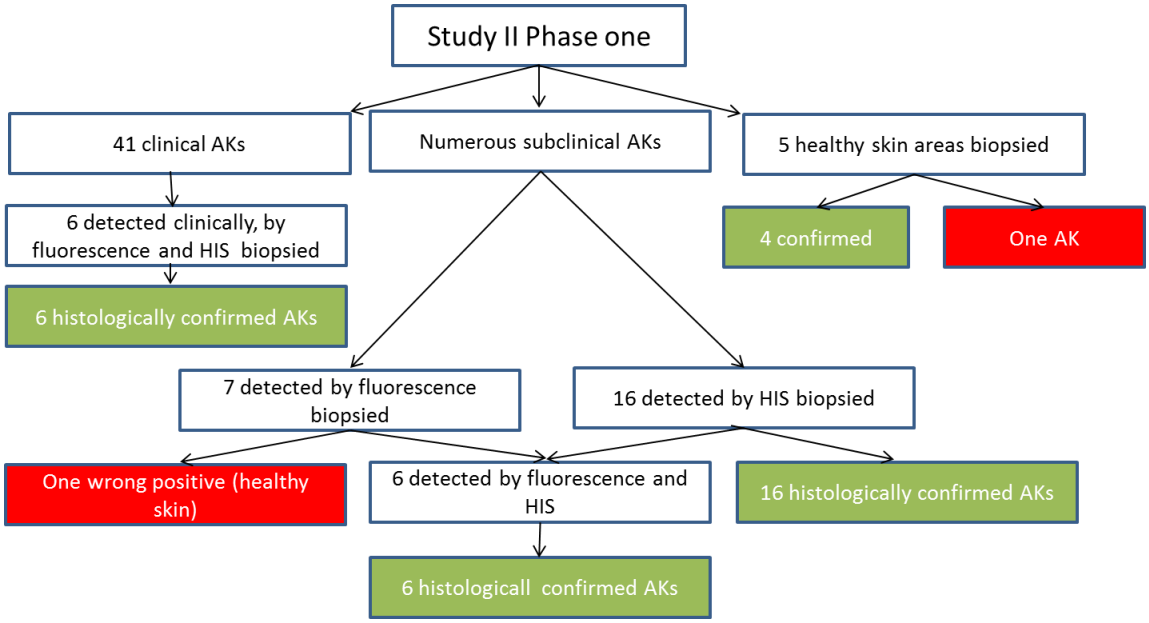

Figure 31. Results Study **II**, phase two.

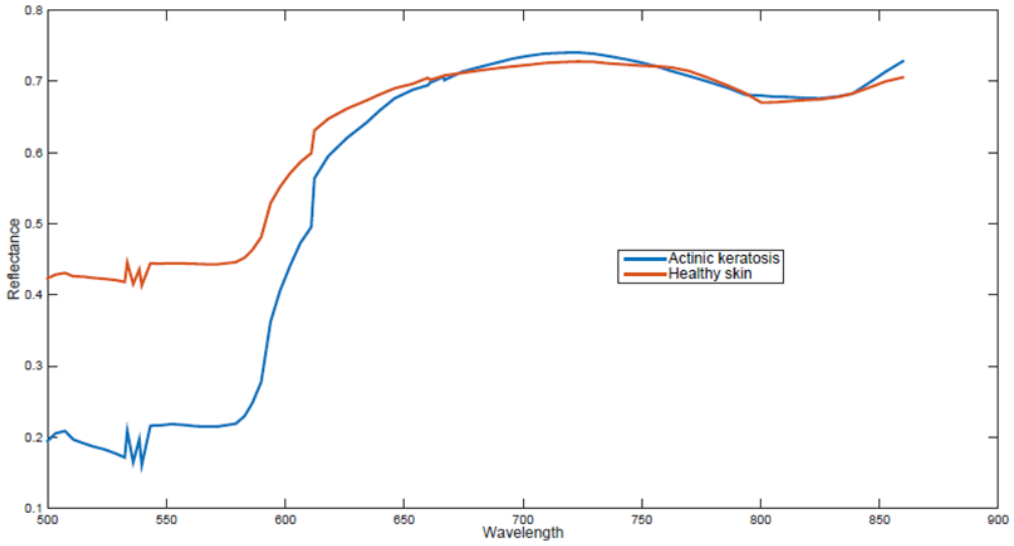

Figure 32.End members of AK and healthy skin, mean reflectance (converted with white reference) patients 1-6 (phase 2). Wavelength (nm), reflectance (relative).

Study III

Of the 14 patients included 13 completed the study. One patient was withdrawn from the study due to health problems not related to the study. The patient characteristics are shown in ***Table 6***. The patients were treated in a split-face randomized design so that 84 AKs (grade I, n=61, grade II-III, n=23) were treated with BF-200 ALA and 93 AKs (grade I n=73, grade II-III, n=20) were treated with MAL. Altogether 26 biopsies were

taken, one from each site, prior to treatment and at three months. No difference was found in the baseline between BF-200 ALA and MAL groups in lesion count or clinical grading (p= 0.524), or in histological grading (p=0.157), *Tables 1*and *2* in the original article **III**.

When assessed clinically at 3 months, in a per patient half-face analysis BF-200 cleared more thin lesions than MAL (p=0.027) but no difference was found for thicker lesions (p=0.564) or in lesion total clearance (p=0.110), *Table 2* in original article **III**. In per lesion analysis, BF-200 ALA had completely cleared 71 of 84 AKs (84.5 %; 95% CI 75.2-90.9%) and MAL 69 of 93 (74.2 %; 95% CI 64.4-82.1%) AKs, p=0.099, ***Table 7***. Of the residual lesions 17.4% in BF-200 ALA group and 25% in MAL group were in partial response i.e. the grade had diminished by one or two grades compared to the baseline. No difference was found between BF-200 ALA and MAL in reduction of the lesion grading (p=0.065). Thicker lesions (gr II-III) responded equally with thin lesions (gr I) in both groups when treated twice (p=0.330 and p=1.00 for BF-200 ALA and MAL), ***Table 8***, ***Figure 33***.

Altogether four new lesions appeared during the follow up in three areas treated with BF-200 ALA and eight in three areas treated with MAL (p=0.379). One patient developed new lesions on both treatment sites. We conducted an experimental outcome analysis of area complete response including both the clearance of the baseline lesions and appearance of the new lesions clearly separate from these. The area complete response was 79.8% for BF-200 ALA and 65.6% for MAL, p=0.044, ***Table 7***.

Histologically, the complete clearance rates were 61.5% (8 of 13) for BF-200 ALA and 38.5% (5 of 13) for MAL (p=0.375) with all grades responding equally (p=1.000 in BF-200 ALA and p=0.103 in MAL group), *Table 3*and *Fig 3* in original article **III**. Reduction in histological grading was significant in both groups (p=0.005 in BF-200 ALA and p= 0.017 in the MAL group, p=0.187 between BF-200 ALA and MAL).

Positive p53 expression (>10%) was obtained in 13/13 samples in BF-200 ALA group and in 10/13 samples in MAL group before treatment, *Fig 4*, original article **III**. Of the positive samples in the baseline, p53 was completely cleared to <10% in 3/13 in the BF-200 ALA group and in 5/10 in the MAL group after the treatment. In one case in the BF-200 ALA group and in two cases in MAL group the p53 expression was increased compared to the baseline and in one case in BF-200 ALA group and in two cases in MAL group p53expression stayed at the baseline level. The mean reduction in p53 expression was 54.4% (p=0.003) in the BF-200 ALA group and 33.7% (p=0.019) in the MAL group, p=0.552, ***Figure 34***.

Both BF-200 ALA and MAL treatments were overall painless with a mean maximal pain score of 2.1 (range 0.2-8.6) and 2.0 (range 0.2-8.6) with no significant difference between the groups. One patient had high pain scores on both sites 4 hours after the first treatment but not the second treatment. This patient had not received any previous AK treatments and had severe photo damage with a total of 16 AKs (7 on BF-200 ALA site and 9 on MAL site). When assessed by a blinded observer one week after the first treatment, seven patients had more severe reactions (erythema, crusting) at the site treated with ALA, five patients had more

severe reactions at the MAL site and one patient showed no difference between sites. Six patients expressed no preference for further treatment while four favored MAL and three, BF-200 ALA.

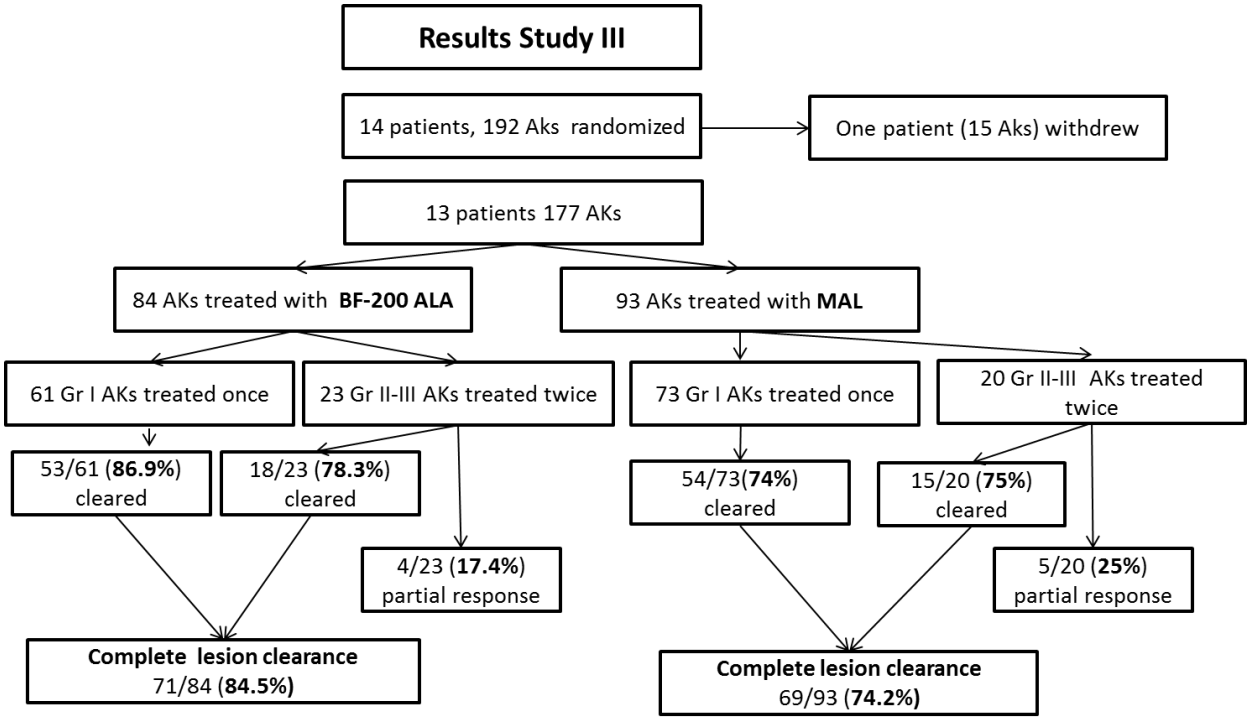

Figure 33. Results Study **III**

Study	Treatment protocol	Study design	Subjects, n	Lesions, n	Follow-up period	Lesion complete clearance	Patient complete response	New lesions	Area complete response	Histological clearance	p53 expression, men decrease	Conclusions
III	BF-ALA +daylight	Randomized Intravidual Slipt-face	13	84 Aks gr I n=61, gr II-III n=23	3 months	84.5%	-	4	79.8%	61.5%	54.4%	DL-PDT with BF-ALA showed a trend towards higher efficacy compared to DL-PDT with MAL
	MAL +daylight			93 Aks gr I n=73, gr II-III n=20		74.2%, p=ns	-	8	65.6%, p= 0.044	38.5%, p=ns	33.7%, p=ns	
IV	MAL +daylight	Randomized intervidual	35	105 AKs gr I n=92, gr II-III n=13		72.4%,	42.9%,	-	-	-	-	DL-PDT with MAL is less effective compared with LED-PDT with MAL
	MAL + LED-PDT		35	105 AKs gr I, n=93, gr II-III n=12	6 months	89.2% p=0.0025	68.6% p=0.030	-	-	-	-	

Table 7. Results studies **III-IV**

Study	Treatment protocol	Subjects, n	Grade I AKs	Grade II-III AKs	Follow-up period	Lesion complete clearance grade I	Lesion complete clearance grade II-III	p-values thin vs thick	Conclusions
III	BF-ALA +daylight	13	134 (76%)	43(24%)	3 months	53/61 (87%)	18/23(78%)	p=ns	In both groups Gr I and Gr II-III lesions responded equally.
	MAL +daylight					54/73(74%) p= ns	15/17 (88%) p= ns	p=ns	
IV	MAL +LED-PDT	70	185 (88%)	25 (12%)	6 months	82/93(88%)	12/12(100%)	p=ns	In both groups Gr II-III lesions responded equally with Gr I AKs. LED-PDT was more effective for AKs of all grades
	MAL +daylight					68/92(73.4%) p=0.015	8/13(61.5%) p=0.039	p=ns	

Table 8. Lesion clearance thin vs. thick lesions, studies **III-IV.**

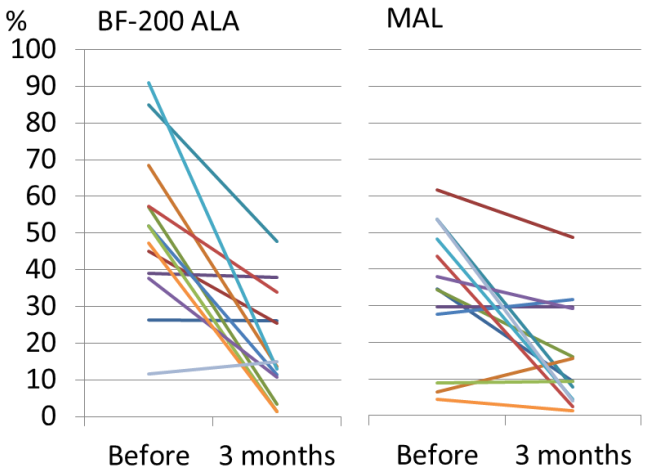

Figure 34. p53 expression level prior to treatment and at 3 months study **III**.

Study IV

Of the 73 randomized patients 70 completed the study, *Fig 2* in original article **IV**. Patient characteristics are shown in ***Table 6***. Altogether 210 lesions were treated 105 (gr I, n=93, gr II-III n=12) in 35 patients with LED-PDT and 105 (gr I, n=92, gr II-III, n=13) in 35 patients with DL-PDT, p=0.46, ***Table 7***. Seven patients in both groups received two treatments for grade II-III lesions and 28 one treatment for grade I lesions.

When assessed at the patient level the complete response rates (3/3 lesions cleared) were 24 of 35 for LED-PDT and 15 of 35 for DL-PDT, p= 0.030. Lesion complete clearance rates were 94 of 105 (89.2%, 95% CI 82.1%-94.2%) for LED-PDT and 76 of 105 (72.4%, CI 95% 63.1%-80.1%) for DL-PDT with LED PDT being significantly more effective, p=0.0025. When assessed separately for grade I lesions clearance rates were 82/93(88%) and 68/92(73.4%) and for grade II-III lesions12/12(100%) and 8/13(61.5%) for LED-PDT and DL PDT, respectively (p=0.015 and p=0.039), ***Table 8***.

We estimated the probability for a patient's complete response to be 0.429 (95% CI 0.4140 – 0.4432) for DL-PDT and 0.686 (95% CI 0.6736 – 0.6978) for LED-PDT. Thus, the incremental efficacy value was -0.257. The imputed mean total costs per patient were €132 (95% CI 111.3-152.6) for DL-PDT and €170 (95% CI 126.0-213.5) for LED-PDT, p=0.022. The costs per item are specified in the attached original article **IV**, *Table 1*. The incremental costs (savings) were -38 euros. The results suggest that DL-PDT is

associated with an incremental cost saving of €147 with a decremental probability to get healed of -0.257, *Table 2* in original article **IV.** The CE-plane showed ICER results reliable i.e. the use of DL-PDT would lead to costs savings but also lower the probability for a patient's complete response, *Fig 2* in original article **IV**.

The costs per complete responders were €248 for LED-PDT and €308 for DL-PDT (p=0.004).

DL-PDT was less time consuming for the nurse (median 51 minutes vs. 78 minutes per treatment, p=0.003) and for patients (median 194.5 min vs. 271 min, p<0.0001) compared to LED-PDT. DL-PDT was significantly less painful (mean maximal pain value 1.53, range from 0.1 to 6.0) compared to LED-PDT (mean maximal pain value 4.36, range from 0.3 to 8.4) despite the use of local anesthetic for grade II-III lesions, p<0.001, ***Figure 35***.

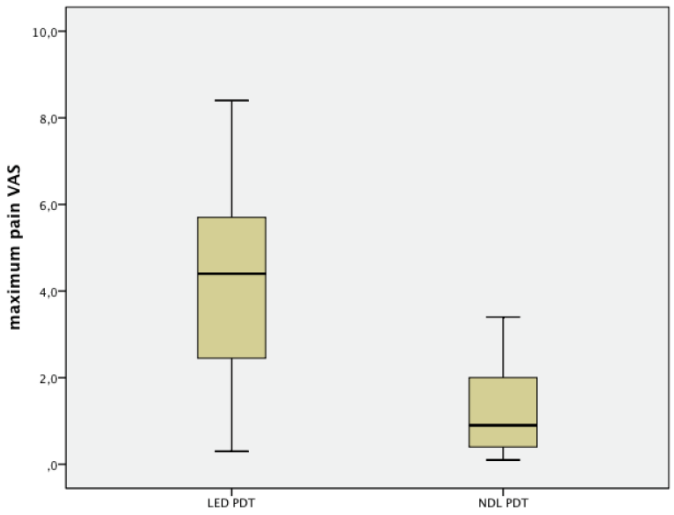

Figure 35. Pain values LED-PDT vs. DL-PDT. DL-PDT was significantly less painful (mean maximal pain 1.53 vs. 4.36, VAS 1-10, p<0.001) despite the use of local anesthetic for thicker lesions.

DISCUSSION

The novel hyperspectral imaging system (HIS) was found to be useful in the delineation of ill defined LM and LMM borders. It did so more accurately than could be clinically detected by Wood's light for both tasks, and in the detection of subclinical AKs (studies **I** and **II**) .Compared to currently available techniques, HIS offers a large FOV (12 cm^2), which is suitable for investigations of large skin areas rapidly (seconds) followed by quick data processing and classification of the spectra. The results are obtained from abundance maps representing end-members i.e. pure spectra of affected areas and healthy skin. As these pilot studies have produced promising preliminary results, further studies are warranted to qualify the optimal mathematical algorithms and to assess the sensitivity and specificity of the method for diagnostic use.

The hyperspectral system used detected diffuse reflectance and thus provided information about light's scattering and absorption properties in the skin. While light scattering is mainly caused by cells in the epidermis and collagen in the dermis, absorption is mainly dominated by light absorption from hemoglobin and melanin. Changes in the skin morphology during carcinogenesis leads to changes in the skin's optical properties (*Rajaram et al 2010*). As far as we know, no current studies use diffuse reflectance hyperspectral imaging for the detection of AKs or LMs.

In study **I** HIS was used for differentiating subclinical LM borders from surrounding skin. We found HIS useful in 11/23 cases where lesions were either wider (n=8= or smaller n=3) than could be clinically detected. In six cases HIS revealed subclinical extensions which could have led to avoidance of the re-excision. In three cases where the LMs were smaller than clinically detected HIS could have been helpful in saving tissue in cosmetically sensitive facial areas.

As the experimental study proceeded, the protocol was improved. Six lesions were directly operated on with wide excisions after the HIS imaging. As the study proceeded, we changed the protocol so that the HIS findings were more easily mapped with the histological findings. We found targeted biopsies of the lesion borders useful for this purpose. Another useful approach was to excise the lesion directly from its clinical border and then excise the margin as a separate circumferential strip. We used vertical sectioning of the samples. The use of horizontal sectioning and/or MMS would have led to an even more accurate comparison of the HIS finding and histology. In the cases of suspected subclinical extension, extra cuts were prepared for the specific HIS detected areas if subclinical extensions were not seen in the initial samples. The presence of benign melanosis or an AK in the vicinity of the LM border complicated the delineation of the LM borders in the two false positive cases but they also might have complicated the interpretation of the histologic samples. However, we will have to further develop our analysis process to differentiate spectral data from LMs and other skin lesions like pigmented AKs and lentigines more accurately. We are currently working on finding the specific spectra for the common lesions of photo-damaged skin for their accurate separation (*Neittaanmäki-Perttu et al 2014*, unpublished data).

The current methods for surgical margin control (SSE, MMS) require resources (technicians, pathologists, and surgeons) and the high degree of expertise required makes the process time-consuming and often requires multiple office visits. Based on these facts here is an urgent need for a noninvasive tool for pre-surgical margin control and for follow-up examinations. One of the currently used techniques for aiding detection of LM borders is fluorescence detection with Wood's light (*Paraskevas et al 2005,, Kimyai-Asadi et al 2007, Hazan et al 2008)*. In our study, we used Wood's light for the detection of lesion borders as we routinely use it in our daily practice. We did not compare the margins seen by the unaided eye and those seen under Wood's light. Our result showed that in 11/23 cases HIS was more useful than a clinician using Wood's light for detection of the lesion borders. Other techniques for this purpose include dermatoscopy and reflectance confocal microscopy. In addition, multispectral analyses like Siascopy (*Moncrieff et al 2002)* or HD-OCT (*Boone et al 2013)* could potentially be used for LM border detection but as far as we know no studies of this currently exist. A limitation in our study is that we used dermatoscopy only as a diagnostic aid and not for lesion border detection. This would have been interesting as dermatoscopy can accurately be used for detection of LM borders (*Robinson JK 2004*). RCM is a promising tool for mapping the LM borders (*Guitera et al 2013*). However, the small FOV makes the mapping of the wide areas slow and currently the costs of the device limit its availability. Both dermatoscopy and RCM are strongly user-dependent and thus not comparable with HIS.

In study **II** we used MAL fluorescence detection to find subclinical incipient lesions for teaching areas in order to find areas that could be use to assess HIS. 10/16 of the subclinical lesions detected by HIS were not detected by fluorescence. In addition one fluorescent lesion was found to be sun damaged skin and not AK. A limitation in our study is that we used fluorescence detection by Wood's light with visual inspection instead of using a more sensitive CCD camera that corrects the images for the skin's auto fluorescence (*van der Beek et al 2012*). Fluorescence detection is a common method for subclinical AK detection even though it lacks specificity as inflammatory skin diseases also accumulate PpIX (*Smits et al 2005*). In addition it is time-consuming, due to the hours of photosensitizer occlusion needed prior to imaging (*van der Beek et al 2012*). In our study 6 of the 7 fluorescence detected biopsied lesions were confirmed as AKs, which shows the method has a high specificity. However 10 of the 16 histologically confirmed lesions were not brightly fluorescent but were seen in HIS analysis which shows HIS may be more sensitive in the detection of these lesions from sun-damaged skin. In our study the HIS detected subclinical lesions were histologically verified as fully developed AKs. The histologic diagnostic criteria for early subclinical AK are not clear. Sun-damaged skin often represents many histological characteristics of an AK and it has been suggested this presents the very early stages of AKs (*Einspahr et al 1997*). A limitation of study **I** is that in phase two where linear signal unmixing was used we took only one biopsy per patient to verify the diagnosis and did not take biopsies from the surrounding skin as we did in phase one where we used the supervised neural network method.

We found that HIS accurately detected yet invisible premalignant changes in the skin. However, it should be noted, that the specificity of the method was not studied. Instead of differentiating AKs from different skin conditions, this pilot study concentrated on the detection of AKs from surrounding healthy skin for early detection of the premalignant changes. As AKs are characterized in the superficial part of the skin and diffuse reflectance also detects the dermal part, diffuse reflectance may not be specific enough for detecting optical differences derived only from the superficial part of the skin. From the mean spectrum of AK and healthy skin (***Figure 31***) it can be concluded that the difference is mainly seen at 500-600 nm where hemoglobin dominates the spectra. Thus the difference between AK and normal skin might likely be due to different amounts of blood volume, which can also be a feature of many skin conditions other than AK. Thus, we also experimentally tested imaging facial eczema with HIS and found that the spectrum differed from that of an AK (*Neittaanmäki-Perttu et al 2015*, unpublished data). Currently we are working on a new mathematical modeling based approach to differentiate chromophore-specific parameters from the HIS images. These parameters are retrieved from a mathematical reflectance model of the skin. When experimentally testing this new approach to eczema we found clearly more blood volume in the skin for eczema areas than in areas containing an AK and also detected differences in other skin chromophores (*Neittaanmäki-Perttu et al 2015*, unpublished data). The specificity of the HIS findings should be given more attention in future studies.

A device, which to our knowledge is not yet commercially available, which combines the measurement of diffuse reflectance (350-700 nm) and laser-induced fluorescence *in vivo* (FOV 6.5 mm in diameter), and provides automated classification was able to separate AK from cSCC with 100% sensitivity and 50% specificity and detected significant spectral differences between lesional and normal skin (*Rajaram et al 2010*). This device, unlike HIS, fails to produce images and was not used for the detection of subclinical lesions. Dermatoscopy can be used for the detection of clinical AKs and might help but no current criteria for subclinical AKs exist. RCM accurately detects clinical and subclinical AKs but it is time consuming due to small FOV, it is also expensive and highly-user dependent and thus not widely used for this indication (*Ulrich M et al 2010, Guitera et al 2013*). HD-OCT is another promising tool for the detection of AKs in their early phases and also for monitoring treatment efficacy (*Maier et al 2013).* It also offers the advantage of both horizontal and vertical imaging, but like RCM it has a small FOV (1.8 x 1.5 mm) and is user-dependent which makes observations of large areas time-consuming. Conventional OCT with larger FOV (6x6mm) has too poor a resolution for the visualization of AKs (*Maier et al 2013).* Raman spectroscopy provides point based spectral information of small areas (diameter 3.5 mm) and does not provide images and thus can not be compared with HIS. In comparison with the other methods Raman spectroscopy uses automated classification of the acquired spectral signals. It was only recently that multispectral Siascopy has been used for the detection of different chromophores in sun-damaged skin but the study was not used to detect AKs (*Stimpfle et al 2014).* The imaging depth and resolution of our HIS are comparable with that of

multispectral devices but the analyzing technique detects characteristics that are beyond the single pixel resolution. In addition, the FOV is larger.

In studies **I-II** we used two different analyzing processes: supervised neural network analysis and the unsupervised linear spectral unmixing method. These methods are detailed elsewhere (*Pölönen et al 2013*). As neural network analysis needs pre-defined teaching data and is thus user-dependent, we have found spectral unmixing to be more useful. As we noted in study **II**, defining incorrect teaching areas could lead to misclassification of the data. A limitation is that in study **II** we did not initially use a white reference for data normalization and thus the AK spectra in original article **II**, *Fig 4* differs from that shown in this thesis (***Figure 31***). Further studies should concentrate on the diagnostic accuracy of these methods and combining spectra of different lesions apparent in sun damaged skin as well as inflammatory processes. Multicenter studies are warranted to validate the method. A future aspect should also include a cost-effectiveness analysis for HIS.

Our studies **III-IV** are the first DL-PDT studies conducted in Finland and the first studies to use photosensitizers other than MAL in this manner. Our results of DL-PDT for grade I-III AKs show lesion clearance rates of 84.5% for BF-200 ALA, 72.4-74.5% for MAL. However, the clearance rates for LED-PDT were higher resulting in 89.2% complete lesion clearance. Interestingly the lesion clearance rate for BF-200 ALA DL-PDT approached the clearance rate of MAL LED-PDT. As the nanoformulation enables the use of low concentrations of 5-ALA, the costs of BF-200 ALA are significantly lower than those of 16% MAL (199 vs. 398 e per 2g according to Biofrontera, Germany). Currently BF-200 ALA is approved but not on market in Finland, but it can be purchased for special purposes.

When compared to previous DL-PDT studies, all conducted with MAL, our lesion clearance rates are comparable with the earlier studies conducted in Denmark, Norway and Sweden showing lesion clearance from 75.9 to 79.5% (mostly thin AKs) (*Wiegell et al 2008, 2009, 2011, 2012*[1]). A recent Australian multicenter DL-PDT study reached higher clearance rates of 89.2% but included only thin lesions in the analysis (*Rubel et al 2014*). Our slightly lower efficacy rates compared to previous studies conducted in Europe for DL-PDT could be explained by the fact that we treated lesions of all grades and used a longer 6 month follow-up period in study **IV** compared to most of the DL-PDT previous studies, which reported only the 3-month clearance. In addition, in study **IV** the behavior of the patients (e.g. the illumination time) was not controlled reflecting the situation in real life practice.

In a recent study using BF-200 ALA in a controlled simulation of daylight treatments the clearance rates were higher (93% lesion clearance and 75% patient response) than seen in previous DL-studies (*Kellner et al 2014*). In a simulated DL- room the irradiance can be controlled and treatment can be implemented all year round. However the retrospective studydesign questions the counting and mapping of the lesions during the study and there is a need for further prospective controlled trials. DL-PDT can not be implemented during

the dark winters in northern countries (*Wiegell et al 2012*[2]) but simulated DL-rooms could eliminate this limitation.

The clearance rates for thicker lesions in DL-PDT have previously been reported to be 61.2% for grade II and 49.1% for grade III AKs (*Wiegell et al 2012*[1]). We used repeated treatment (two sessions 1-3 weeks apart) for thicker grade II-III AKs and achieved higher clearance rates, 76-5-88% for MAL and 78% for BF-200 ALA after 3 months. We found no significant differences in the lesion clearance rates for MAL or BF-ALA PDT as a function of lesion thickness. However, LED-PDT significantly cleared more thin and thick lesions than DL-PDT.

The patient complete response rate was reported in our study **IV** for MAL-DL-PDT (42.9%) and for MAL-LED-PDT (68.6%) at 6 months. No previous DL-PDT studies had reported the clearance rates at the patient level. Previously, the complete patient clearance rates for MAL-LED PDT varied from 46% after one month (*Moloney et al 2007*) to 59.2%-68.4% after 3 months (*Pariser et al 2008, Zane et al 2014*) and to 55.2% after one year (*Zane et al 2014).* Our results for LED-PDT support these findings. Due to the intra-individual split-face design in study **III** using DL-PDT it was not possible to assess patient complete response rates. However, we evaluated the data in per-patient half-face analysis. In addition, we reported an experimental value for area complete response including cleared lesions and also the newly appeared lesions on the whole treated field during the 3-month follow-up. Complete area clearance rates were 79.8% for BF-200 ALA and 65.6% for MAL. The area complete response rates had not been reported in previous studies. The appearance of new lesions i.e., the preventive effect is rarely reported. Wiegell et al reported a mean of 2.8 new lesions per patient during a 3-month follow-up after DL-PDT (*Wiegell et al 2012*[1]). We found altogether 8 new lesions in MAL treated sites and 4 in BF-200 ALA treated sites in 13 patients after 3 months in study **III**. In the future, more attention should be paid to the preventive effect of field directed treatments and also more attention should be paid to clearance reports at the patient level.

The spontaneous regression rates for AKs vary between 15-63% after one year, but remission rates are also high (15%-53%) (*Werner et al 2013*). No placebo-controlled DL-PDT trials currently exist. In LED-PDT studies placebo treatment with curettage leads to significantly lower clearance rates (***Table 5***). It is obvious that there is a need for a placebo-controlled DL-PDT trial.

To our knowledge, our study **III** is the first to report the histological clearance rates for DL-PDT. BF-200 ALA showed a trend towards higher histological efficacy than did MAL with 61.5% vs. 38.5% complete histological clearance rates. We also assessed the p53 expression from the biosy samples. Sun-exposed skin expresses higher level of p53 (approx. 1% for skin not adjacent to AKs and up 10% for AK-adjacent skin) than non-sun-damaged skin (approx.0.1%), but at a rate lower than that seen for AKs (approx.30%) even though there is a great heterogeneity between individuals (*Einspahr et al 1997*). Different treatments and radiotherapy can cause reactive atypia and elevated p53 expression levels (*Aron M et al 2013*). Thus, we set the 10% threshold for "normal" p53 expression. At the baseline, we found positive (>10%) p53 expression in

23/26 (88.5%) of the pre-treatment skin biopsies. Compared to the baseline, p53 expression reduced by 54% with BF-200 ALA and by 34% with MAL. Previously, a single conventional MAL-PDT session cleared AK dysplasia completely in 55%, and showed significant, but not complete reduction in p53 expression in 50% of the samples, indicating that a single treatment session is not effective enough to completely clear the actinic damage (*Bagazgoitia et al 2011*). Another group took biopsies from healthy-appearing skin field cancerized areas before and three months after three separate sessions of MAL-PDT. Histological findings of keratinocyte atypia and extent decreased significantly but p53 expression showed only a non-significant trend towards reduction. This was thought to result from the biopsy sites being on normal appearing-skin and thus having lower baseline expression of p53. Also a significant increase in collagen deposition, and reduction of solar elastosis were seen indicating that PDT also reduces signs of photoaging and offers excellent cosmetic outcome (*Szeimies et al 2012*). Our results show a significant reduction in histological signs of carcinogenesis after DL-PDT. Also, the reduction in p53 expression indicates a reversal in the carcinogenic process, and thus that DL-PDT can be used as well in a preventive manner. The fact that p53 expression did not decrease in all the studied samples might be due to further cumulative UV exposure, as we cannot confirm that the patients followed the instructions for photoprotection after the treatment. We have continued the follow-up for up to 12 months in order also to assess the long-term effects histologically (*Neittaanmäki-Perttu et al 2015*, unpublished data). A limitation of study **IV** was that we did not confirm the AK diagnosis by biopsies or assess the histological clearance. However, in the other studies (**II-III**), we biopsied clinically detected AKs in each patient and the accuracy of the clinical diagnosis was 100% as all the lesions biopsied as AKs under clinical diagnosis showed signs of AKs also histologically.

We used a thinner 0.025mm-thick layer of the photosensitizers in our DL-PDT studies than previously reported (1 mm) (*Wiegell et al 2012*[2]).It is possible that in DL-PDT where PpIX is activated during its development, lower amounts of PpIX are needed, and thus lower concentrations and thinner layers of the photosensitizers can be used than in conventional treatments. Both could significantly reduce the costs of the treatment. Only one study used lower MAL concentrations for DL-PDT in humans and found that MAL8% is as effective as MAL16% in DL-PDT of AKs (*Wiegell et al 2009*). The effect of the layer thickness had not been reported earlier. Further studies are warranted to assess the optimal layer thickness and photosensitizer concentration in order to lower the costs without affecting the efficacy.

In both studies considering DL-PDT (**III-IV**) the mean maximal pain values were low and in study **IV** patients treated with LED-PDT reported significantly higher pain scores. This is in accordance with the previous studies, which had reported lower pain values for DL-PDT compared to LED-PDT due to continuous activation of PpIX (*Wiegell et al 2008, Rubel et al 2014)*. Our pain values are not directly comparable as the other DL-studies report pain values using a numerical 1-10 scale while we used VAS. The mean maximal pain scores during DL-treatment were slightly higher in study **III** than in study **IV**. This might be due to the local anesthetic used for the thicker lesions in study **IV**. In study **III**, one patient reported severe pain (VAS>8) on both sites 4 hours after the treatment. It is possible that the patient did not

follow the instructions to stay indoors after the treatment or stayed outside for longer than instructed. During the second treatment, the same patient reported the pain scores <1 on both sides during the whole treatment day. A similar effect of increased pain was reported earlier when the illumination time was not controlled (*Wiegell et al 2009*). Also another patient in study **III** reported high (approx. VAS 9) pain scores on both sites during the second treatment (at 1.5 hours) even though the patient experienced almost no pain during the first treatment. This might be due to direct sunlight during the second treatment as during the first treatment it was partly cloudy and the temperature was two degrees lower. However, in both cases no difference between the treatment sides was reported. In study **IV** we used local anesthetic in both groups mainly to reduce pain during the LED-illumination. Due to this, the mean maximal pain values in our LED-group were lower than reported previously (*Wiegell et al 2008*). However, again the numbers are not directly comparable due to different scaling (numerical 1-10 vs. VAS). One patient in the LED-group had to spend the night in the hospital because of the pain in the LED-treated areas after the second treatment. This patient received three illuminations due to the location of the lesions on different sides of the face. The need for more than a single illumination is not unusual in patients with severe wide spread photodamage. In these patients, DL-PDT should be considered to increase the tolerability of the treatment.

A limitation in our study **III** is the limited follow-up period of 3 months and a relatively small sample size. We have assessed the efficacy of study **III** again at 12 months (*Neittaanmäki-Perttu et al 2015*, unpublished data). In study **IV** the follow-up period was longer, i.e., 6 months, which might have caused the slightly lower clearance rate for DL-PDT in this study. A further limitation is that the sample size in study **III** was calculated based on histological lesion clearance, which was assumed to be a continuous variable based on a previous study (*Szeimies et al 2012)*. In our study the histological clearance was assessed using a three step grading system. Another limitation in all of our DL-PDT studies (**III-IV)** is that we did not record the light dose during the daylight illuminations. This would have been interesting because the strength of the irradiance may change with weather conditions. However, it has been suggested that the minimum effective light dose of 8 J/cm^2 can be reached in northern countries like Finland (latitude 64˚N) until mid-September (*Wiegell et al 2012*[2]). The study treatments implemented during summers 2011-2013 (studies **III-IV**) showed very similar efficacy for MAL, a photosensitizer used in both DL-PDT studies, which reflects the repeatability of our results. In study (**IV**) we used home-based setting and thus did not monitor the time patients spend outside for illumination. In this study the clearance for MAL was slightly lower (72.4%) than in study **III** (74.2%) where the 2-hour-illumination was monitored by a nurse. This difference may also be due to the longer follow-up period (6 months) than in other two studies (3 months). Patient compliance is important when using DL-PDT. However, this is not such a problem as with most of the topical AK treatments with long application times at home and prolonged adverse reactions. Another limitation is that in study **IV** we did not use blinded assessment of the efficacy as we did in study **III**.

DL-PDT is well tolerated. Adverse reactions were recorded by a blinded observer in study **III**. We found no difference in adverse reactions after DL-treatment between MAL (more severe reactions on the 5 MAL

sides) and BF-200 ALA (more severe reactions on 7 BF-200 ALA sides) (study **III**). A limitation is that we did not assess the adverse reactions in study **IV** comparing LED-PDT and DL-PDT. However, it has been shown that DL-PDT is better tolerated than LED-PDT (*Rubel et al 2014*). When we assessed patient preferences in study **III** six patients expressed no preference for further treatment while four favored MAL and three, BF-200 ALA. A further limitation is that we did not include evaluation of the cosmetic outcome. However, it is known that both LED-PDT and DL-PDT result in excellent cosmetic outcomes (*Rubel et al 2014).*

As showed in study **IV**, DL-PDT required less of the nurse's and patient's time and was less costly compared to LED-PDT. However, DL-PDT with MAL was less effective compared to LED-PDT with MAL. In CEA, DL-PDT with MAL showed to provide less value for money compared to LED-PDT with MAL.

In our own experience it is much more convenient and practical to use DL-PDT. In conventional-PDT, the size of the treatment area is limited due to the size of the lamp (*Moseley 2005*), and due to pain. With DL-PDT the treatment is painless which enables treatment of large areas simultaneously. A limitation is that we did not include the assessment of pain and QALYs in our CEA analysis. As DL-PDT requires less time at the clinic, more patients can be treated and the illuminations are not limited by the number of available lamps or nurses. DL-PDT is also suitable for private practices with short visiting times.

The strengths of our cost-effectiveness study (**IV**) were that we used a prospective study design and included accurate costs of the treatments. Most of the cost-effectiveness studies of AK treatments are funded by drug companies and use estimated and modeled values. Conventional PDT has been considered a "cost-effective" therapy for AKs, with total cost of care of €381 per patient and €58 per lesions including pretreatment visit, treatment costs and follow-up visits (*Annemans et al 2008*). To our knowledge this conclusion can not be drawn as the study failed to compare two interventions, which is the principle of any cost-efficacy evaluation. The study was funded by Galderma. In comparison, the estimated costs for destructive treatments were 131 USD per one AK and 258 USD for ≥15 AKs (*Warino et al 2006*). In a non-sponsored study, the costs per complete responder were €363 for MAL-PDT and €379 for LN cryotherapy including the cost of yearly re-treatments, and also valuing the cosmetic-outcome in a decision tree model (*Caekelbergh et al 2006*). When compared in a decision tree model estimating quality –adjusted life years (QALY) vs. the cost of the treatments over one year, imiquimod was implied to be more cost-effective than MAL-PDT. The authors had connections with MEDA (*Wilson 2010*). On evaluating patient complete response and cosmetic outcome in a decision-tree model, MAL-PDT was found to be more cost-effective compared to imiquimod and 5-FU (*Muston et al 2009*). The limitations were that the model only included the price of the topical drugs and authors had connections to Galderma. Even though more expensive, MAL-PDT showed equal cost-effectiveness compared with imiquimod and 5-FU when evaluated in a decision tree model (*Neidecker et al 2009*). As far as we know, in addition to our study, there is only one prospective non-sponsored head-to head cost-effectiveness study comparing AK treatments. In this Italian study MAL-PDT was more cost-

effective compared with diclofenac+hyaluronic acid gel (DHA) with the costs per complete patient response of €566.7 and €1026.2 for MAL-PDT and €595.2 and €2295.2 for DHA at 3 and 12 months (*Zane et al 2014*). The Italian researchers failed to use appropriate sensitivity analysis for verification of their results. Our results can not be directly compared with the previous studies as we included the accurate costs in a head-to-head design but did not include the costs of further treatments or quality of life (QALY) aspects.

A limitation of our study **IV** is that we used a treatment method targeted to lesions and did not record the size of the lesions. If we had instead targeted the whole field, the consumption of the photosensitizer and thus cost in both treatments would have been higher. In addition this might have affected the time used by the nurse, and thus the cost of the LED-treatment. This protocol would have enabled us to record the appearance of new lesions and thus also to record the preventive effect. Further studies comparing the cost-effectiveness of lesion targeted vs. field targeted PDT are warranted. In our DL-studies we used thinner layers of photosensitizers than instructed for conventional treatment. This showed comparable efficacy values with previous treatments. However the results should be confirmed in larger trials comparing different thicknesses of the photosensitizers. The use of lower amounts of the drug could lead to a more cost-effective treatment protocol. In addition the use of novel and possibly more effective formulations of photosensitizers could further increase the cost-effectiveness of PDT. These subjects require further studies.

CONCLUSIONS

- The hyperspectral imaging system (HIS) can be used for the detection of subclinical lentigo maligna (LM) and lentigo maligna melanoma (LMM) borders and thus could reduce the number of re-excisions
- HIS offers a practical non-invasive tool for the detection of incipious actinic keratoses (AK) on field cancerized skin
- Further studies are warranted to validate the mathematical method for HIS analysis
- As HIS was used to separate lesions from surrounding sun-damaged skin, further studies are warranted to separate the spectra of different skin tumors for diagnostic use
- Daylight photodynamic therapy (DL-PDT) is a well tolerated and effective treatment for actinic keratoses (AK)
- Also thicker grade II-III AKs can be treated with DL-PDT with repeated treatment sessions
- Compared to conventional LED-PDT, DL-PDT is less painful and more convenient to use as it requires significantly less patients' and nurses' time
- Although DL-PDT using methylaminoleavulinate (MAL) can be implemented with lower costs, conventional LED-PDT with MAL resulted in higher patient complete response rates. In an incremental cost-effectiveness analysis, MAL-DL-PDT provided less value for money compared to MAL-LED-PDT.
- The novel photosensitizer formulation 5-aminolaevulinic acid nanoemulsion (BF-200 ALA) can be used with daylight activation
- In the treatment of AKs, DL-PDT with BF-200 ALA showed a trend towards improved efficacy compared to MAL-DL-PDT
- At three months after DL-PDT, the complete histological clearance was seen in 61.5% of the BF-200 ALA-treated AKs, in 38.5% MAL-treated AKs
- Reduction in p53 was seen with both photosensitizers implying the reversal of the carcinogenesis process with DL-PDT
- In DL-PDT, a thin 0.25-mm -thick layer of the photosensitizer (compared to the recommended 1-mm-thick layer used in conventional PDT) seems enough with both MAL and BF-200 ALA, which could lower the treatment costs
- The novel nanoformulation, BF-200 ALA, enables the use of lower photosensitizer concentrations, which could further reduce the costs of the treatment
- This thesis reported relatively short term clearance rates (3-6 months) and thus long-term efficacy needs more attention in the future
- Further studies are also warranted to assess the cost-effectiveness of lesion vs. field targeted treatment, and the cost-effectiveness of the novel treatment protocol with BF-200 ALA in DL-PDT

ACKNOWLEDGEMENTS

First of all I want to express my gratitude to my supervisors Professors **Erna Snellman** and **Olli Saksela** for guiding me into the exiting world of clinical research and for their patience, support and guidance during this thesis project. I have been endlessly inspired by Erna's admirable attitude towards scientific work, and her knowledge of the field of photodermatology. The HIS project partly introduced in this thesis, would not exist without Olli's invaluable ideas and endless knowledge of skin cancers and their treatment.

My warmest thanks to the supervisory group for their enthustiastic and supportive participation in this project. Professor **Annamari Ranki**, the head of the department at the Skin and Allergy Hospital, has offered her valuable comments when planning the projects, applying for the funding and preparing the manuscripts. She has also greatly helped me in arranging the defence. A special thanks to **Mari Grönroos,** MD, PhD the Chief of Dermatology and Allergology at Päijät-Häme Central hospital for her never ending enthusiasm towards clinical skin cancer research. Furthermore, a special thanks to Mari for her assistance in recruiting the patients, and for performing the challenging surgical operations for the LM patients.

I am greatful to Professors **Veli-Matti Kähäri** and **Raimo Suhonen** for reviewing the thesis. Their valuable comments greatly helped me to improve the thesis.

My special thanks to Professor **Martti Talja**, the director of the Päijät-Häme Central Hospital for enabling to conduct the prospective clinical studies included in this thesis. I also thank the research nurse **Ulla Oesch-Lääveri** for her commitment to the studies and for the long summer evenings we spent at the clinic when conducting the DL-PDT studies. I would also like to thank research organizer **Marjo Soini** for her assistance during the project. My warmest thanks to the whole Department of Dermatology and allergology at Päijät-Häme central hospital. Im indebted to the patients for their participation in the studies included in this thesis.

My warmest gratitude to my fellow reserachers: **Ilkka Pölönen** PhD for the development of the mathematical modeling for HIS, to **Toni Karppinen** MD for his enthusiastic assistance in the PDT-studies and to **Mari Salmivuori** MD for her help during the HIS project. A special thank to the dermatopathologist **Leila Jeskanen** MD and pathologist **Taneli Tani** MD, PhD for interpreting the histopathological samples. My warmest thank to all collegues who helped recruiting the patients for the studies.

I am greatful to Prof **Pekka Rissanen** for his expertise and help for preparing the cost-effectiveness study. I would also like to thank **Mika Helminen** and **Hannu Kautianen** for their statistical assistance.

Im also greatful to to VTT technical research center of Finland and especially **Heikki Saari** for developing the first prototype of HIS used in this thesis.

I have received financial support for this project from the following foundations, which are all warmly acknowledged: The Finnish Dermatological Society, The Irja Karvonen Cancer Foundation, Orion-Pharmos

Research Foundation, The Novo Nordisk Foundation, the Foundation for Clinical Chemistry Research and Instrumentarium Foundation.

I am greatful to all the patients included in the studies. They showed dedication and motivation in helping to enhance the treatment of skin cancer precursors.

Finally, I would like to express my gratitude to my family: my father for giving me inspiration, my mother for her care, my brother Petri for his support, my sister Eerika for her enthusiasm towards PDT and endless pharmaceutical consultations, and to my little sister Henriikka for her company during those evenings when I was too overwhelmed with all the research. Thanks to my lovely friends, I stayed sane and didn't miss too many social events during this 4-year project. Last, but not least, thanks to my beloved husband Ilkka, who coped with all the moodiness.

Helsinki, May 2015

Noora Neittaanmäki-Perttu

REFERENCES

Abbas Q, Celebi ME, Fondón García I, Rashid M. Lesion border detection in dermoscopy images using dynamic programming. *Skin Res Technol* 2011;17(1):91-100.

Acker SM, Nicholson JH, Rust PF, Maize JC. Morphometric discrimination of melanoma in situ of sun-damaged skin from chronically sun-damaged skin. *J Am Acad Dermatol* 1998;39:239-45.

Akbari H, Uto K, Kosugi Y, Kojima K, Tanaka N. Cancer detection using infrared hyperspectral imaging. *Cancer Sci* 2011;102(4):852-7.

Alarcon I, Carrera C, Alos L, Palou J, Malvehy J, Puig S. In vivo reflectance confocal microscopy to monitor the response of lentigo maligna to imiquimod. *J Am Acad Dermatol* 2014;71(1):49-55.

Alawi SA, Kuck M, Wahrlich C, Batz S, McKenzie G, Fluhr JW, Lademann J, Ulrich M. Optical coherence tomography for presurgical margin assessment of non-melanoma skin cancer - a practical approach. *Exp Dermatol* 2013;22(8):547-51.

Alexandrescu DT. Melanoma costs: a dynamic model comparing estimated overall costs of various clinical stages. *Dermatol Online J* 2009;15(11):1.

Andersson-Engels S, Johansson J, Svanberg K, Svanberg S. Fluorescence imaging and point measurements of tissue: applications to the demarcation of malignant tumors and atherosclerotic lesions from normal tissue. *Photochem Photobiol* 1991;53(6):807-14.

Annemans L, Caekelbergh K, Roelandts R, Boonen H, Leys C, Nikkels AF, van Den Haute V, van Quickenborne L, Verhaeghe E, Leroy B. Real-life practice study of the clinical outcome and cost-effectiveness of photodynamic therapy using methyl aminolevulinate (MAL-PDT) in the management of actinic keratosis and basal cell carcinoma. *Eur J Dermatol* 2008;18(5):539-46.

Antonia Pastor-Nieto M, Olivares M, Sánchez-Herreros C, Belmar P, De Eusebio E. Occupational allergic contact dermatitis from methyl aminolevulinate. *Dermatitis* 2011;22(4):216-9.

Apalla Z, Sotiriou E, Chovarda E, Lefaki I, Devliotou-Panagiotidou D, Ioannides D. Skin cancer: preventive photodynamic therapy in patients with face and scalp cancerization. A randomized placebo-controlled study. *Br J Dermatol* 2010;162(1):171-5.

Aron M, Luthringer DJ, McKenney JK, Hansel DE, Westfall DE, Parakh R, Mohanty SK, Balzer B, Amin MB. Utility of a triple antibody cocktail intraurothelial neoplasm-3 (IUN-3-CK20/CD44s/p53) and

α-methylacyl-CoA racemase (AMACR) in the distinction of urothelial carcinoma in situ (CIS) and reactive urothelial atypia. *Am J Surg Pathol* 2013;37(12):1815-23.

Babilas P, Schreml S, Landthaler M, Szeimies RM. Photodynamic therapy in dermatology: state-of-the-art. *Photodermatol Photoimmunol Photomed* 2010;26(3):118-32.

Bagazgoitia L, Cuevas Santos J, Juarranz A, Jaén P. Photodynamic therapy reduces the histological features of actinic damage and the expression of early oncogenic markers. *Br J Dermatol* 2011;165(1):144-51.

Banzhaf CA, Themstrup L, Ring HC, Mogensen M, Jemec GB. Optical coherence tomography imaging of non-melanoma skin cancer undergoing imiquimod therapy. *Skin Res Technol* 2014;20(2):170-6.

Benjamin CL, Ananthaswamy HN. p53 and the pathogenesis of skin cancer. *Toxicol Appl Pharmacol* 2007;224(3):241-8.

Bentzen J, Kjellberg J, Thorgaard C, Engholm G, Phillip A, Storm HH. Costs of illness for melanoma and nonmelanoma skin cancer in Denmark. *Eur J Cancer Prev* 2013;22(6):569-76.

Bichakjian CK, Halpern AC, Johnson TM, Foote Hood A, Grichnik JM, Swetter SM, Tsao H, Barbosa VH, Chuang TY, Duvic M, Ho VC, Sober AJ, Beutner KR, Bhushan R, Smith Begolka W; American Academy of Dermatology. Guidelines of care for the management of primary cutaneous melanoma. American Academy of Dermatology. *J Am Acad Dermatol* 2011;65(5):1032-47.

Bissonnette R. Chemopreventative thoughts for photodynamic therapy. *Dermatol Clin* 2007;25(1):95-100.

Boone MA, Norrenberg S, Jemec GB, Del Marmol V. Imaging actinic keratosis by high-definition optical coherence tomography. Histomorphologic correlation: a pilot study. *Exp Dermatol* 2013;22(2):93-7.

Bosbous MW, Dzwierzynski WW, Neuburg M. Staged excision of lentigo maligna and lentigo maligna melanoma: a 10-year experience. *Plast Reconstr Surg* 2009;124(6):1947-55.

Bosbous MW, Dzwierzynski WW, Neuburg M. Lentigo maligna: diagnosis and treatment. *Clin Plast Surg* 2010;37(1):35-46.

Bowles J, Palmadesso P, Antoniades J, BaumbackM, Rickard LJ. Uses of filter vectors in hyperspectral data analysis. *Proc SPIE* 1995; 2553:148–157.

Braakhuis BJ, Tabor MP, Kummer JA, Leemans CR, Brakenhoff RH. A genetic explanation of Slaughter's concept of field cancerization: evidence and clinical implications. *Cancer Res* 2003;15;63(8):1727-30.

Braathen LR, Morton CA, Basset-Seguin N, Bissonnette R, Gerritsen MJ, Gilaberte Y, Calzavara-Pinton P, Sidoroff A, Wulf HC, Szeimies RM. Photodynamic therapy for skin field cancerization: an international consensus. International Society for Photodynamic Therapy in Dermatology. *J Eur Acad Dermatol Venereol* 2012;26(9):1063-6.

Brancaleon L, Durkin AJ, Tu JH, Menaker G, Fallon JD, Kollias N. In vivo fluorescence spectroscopy of nonmelanoma skin cancer. *Photochem Photobiol* 2001;73(2):178-83.

Breuninger H, Schlagenhauff B, Stroebel W, Schaumburg-Lever G, Rassner G. Patterns of local horizontal spread of melanomas: consequences for surgery and histopathologic investigation. A*m J Surg Pathol* 1999;23(12):1493-8.

Bricca GM, Brodland DG, Ren D, Zitelli JA. Cutaneous head and neck melanoma treated with Mohs micrographic surgery. *J Am Acad Dermatol* 2005;52(1):92-100.

Bro R, De Jong S. A fast non-negativity-constrained least squares algorithm. *J Chemom* 1997; 11 393–401.

Bub JL, Berg D, Slee A, Odland PB. Management of lentigo maligna and lentigo maligna melanoma with staged excision: a 5-year follow-up. *Arch Dermatol* 2004;140(5):552-8.

Caekelbergh K, Annemans L, Lambert J, Roelandts R. Economic evaluation of methyl aminolaevulinate-based photodynamic therapy in the management of actinic keratosis and basal cell carcinoma. *Br J Dermatol* 2006;155(4):784-90.

Cai XJ, Li WM, Zhang LY, Wang XW, Luo RC, Li LB. Photodynamic therapy for intractable bronchial lung cancer. *Photodiagnosis Photodyn Ther* 2013;10(4):672-6.

Calin MA, Parasca SV, Savastru R, Calin MR, Dontu S. Optical techniques for the noninvasive diagnosis of skin cancer. *J Cancer Res Clin Oncol* 2013;139(7):1083-104.

Callen JP, Bickers DR, Moy RL. Actinic keratoses. *J Am Acad Dermatol* 1997;36(4):650-3.

Calzavara-Pinton PG, Szeimies RM, Ortel B, Zane C. Photodynamic therapy with systemic administration of photosensitizers in dermatology. *J Photochem Photobiol B* 1996;36(2):225-31.

Carpenter PM, Linden KG, McLaren CE, Li KT, Arain S, Barr RJ, Hite P, Sun JD, Meyskens FL Jr. Nuclear morphometry and molecular biomarkers of actinic keratosis, sun-damaged, and nonexposed skin. *Cancer Epidemiol Biomarkers Prev* 2004;13(12):1996-2002.

Carrera C, Puig S, Malvehy J. In vivo confocal reflectance microscopy in melanoma. *Dermatol Ther* 2012;25(5):410-22.

Castano AP, Mroz P, Hamblin MR. Photodynamic therapy and anti-tumour immunity. *Nat Rev Cancer* 2006;6(7):535-45.

Ceilley RI, Jorizzo JL. Current issues in the management of actinic keratosis. *J Am Acad Dermatol* 2013;68(1):28-38.

Chang C., Hyperspectral Data Exploitation: Theory and Applications. *Wiley* 2007. URL: http://books.google.fi/books?id=JznyW9csyRoC.

Chen AC, Halliday GM, Damian DL. Non-melanoma skin cancer: carcinogenesis and chemoprevention. *Pathology* 2013;45(3):331-41.

Choo-Smith LP, Edwards HG, Endtz HP, Kros JM, Heule F, Barr H, Robinson JS Jr, Bruining HA, Puppels GJ. Medical applications of Raman spectroscopy: from proof of principle to clinical implementation. *Biopolymers* 2002;67(1):1-9.

Clark GS, Pappas-Politis EC, Cherpelis BS, Messina JL, Möller MG, Cruse CW, Glass LF. Surgical management of melanoma in situ on chronically sun-damaged skin. *Cancer Control* 2008;15(3):216-24.

Cockerell CJ. Histopathology of incipient intraepidermal squamous cell carcinoma ("actinic keratosis"). *J Am Acad Dermatol* 2000;42:11-7.

Cotter MA, McKenna JK, Bowen GM. Treatment of lentigo maligna with imiquimod before staged excision. *Dermatol Surg* 2008;34(2):147-51.

Cox NH, Aitchison TC, Sirel JM, MacKie RM. Comparison between lentigo maligna melanoma and other histogenetic types of malignant melanoma of the head and neck. Scottish Melanoma Group. *Br J Cancer* 1996;73(7):940-4.

Cozzi SJ, Ogbourne SM, James C, Rebel HG, de Gruijl FR, Ferguson B, Gardner J, Lee TT, Larcher T, Suhrbier A. Ingenol mebutate field-directed treatment of UVB-damaged skin reduces lesion formation and removes mutant p53 patches. *J Invest Dermatol* 2012;132(4):1263-71.

Criscione VD, Weinstock MA, Naylor MF, Luque C, Eide MJ, Bingham SF; Department of Veteran Affairs Topical Tretinoin Chemoprevention Trial Group. Actinic keratoses: Natural history and risk of

malignant transformation in the Veterans Affairs Topical Tretinoin Chemoprevention Trial. *Cancer* 2009;115(11):2523-30.

Czarnecki D, Meehan CJ, Bruce F, Culjak G. The majority of cutaneous squamous cell carcinomas arise in actinic keratoses. *J Cutan Med Surg* 2002;6(3):207-9.

Dalton SR, Gardner TL, Libow LF, Elston DM. Contiguous lesions in lentigo maligna. *J Am Acad Dermatol* 2005;52(5):859-62.

Darlington S, Williams G, Neale R, Frost C, Green A. A randomized controlled trial to assess sunscreen application and beta carotene supplementation in the prevention of solar keratoses. *Arch Dermatol* 2003;139(4):451-5.

DeBloom JR 2nd, Zitelli JA, Brodland DG. The invasive growth potential of residual melanoma and melanoma in situ. *Dermatol Surg* 2010;36(8):1251-7.

de Giorgi V, Stante M, Massi D, Mavilia L, Cappugi P, Carli P. Possible histopathologic correlates of dermoscopic features in pigmented melanocytic lesions identified by means of optical coherence tomography. *Exp Dermatol* 2005;14(1):56-9.

de Graaf YG, Kennedy C, Wolterbeek R, Collen AF, Willemze R, Bouwes Bavinck JN. Photodynamic therapy does not prevent cutaneous squamous-cell carcinoma in organ-transplant recipients: results of a randomized-controlled trial. *J Invest Dermatol* 2006;126(3):569-74.

de Oliveira Poswar F, de Carvalho Fraga CA, Gomes ES, Farias LC, Souza LW, Santos SH, Gomez RS, de-Paula AM, Guimarães AL. Protein Expression of MMP-2 and MT1-MMP in Actinic Keratosis, Squamous Cell Carcinoma of the Skin, and Basal Cell Carcinoma. *Int J Surg Pathol* 2015;23(1):20-5.

De Rosa FS, Marchetti JM, Thomazini JA, Tedesco AC, Bentley MV. A vehicle for photodynamic therapy of skin cancer: influence of dimethylsulphoxide on 5-aminolevulinic acid in vitro cutaneous permeation and in vivo protoporphyrin IX accumulation determined by confocal microscopy. *J Control Release* 2000;65(3):359-66.

De Rosa FS, Tedesco AC, Lopez RF, Pierre MB, Lange N, Marchetti JM, Rotta JC, Bentley MV. In vitro skin permeation and retention of 5-aminolevulinic acid ester derivatives for photodynamic therapy. *J Control Release* 2003;89(2):261-9.

Dicker DT, Lerner J, Van Belle P, Barth SF, Guerry D 4th, Herlyn M, Elder DE, El-Deiry WS. Differentiation of normal skin and melanoma using high resolution hyperspectral imaging. *Cancer Biol Ther* 2006;5(8):1033-8.

Dicker DT, Kahn N, Flaherty KT, Lerner J, El-Deiry WS. Hyperspectral imaging: a non-invasive method of imaging melanoma lesions in a patient with stage IV melanoma, being treated with a RAF inhibitor. *Cancer Biol Ther* 2011;12(4):326-34.

Dirschka T, Radny P, Dominicus R, Mensing H, Brüning H, Jenne L, Karl L, Sebastian M, Oster-Schmidt C, Klövekorn W, Reinhold U, Tanner M, Gröne D, Deichmann M, Simon M, Hübinger F, Hofbauer G, Krähn-Senftleben G, Borrosch F, Reich K, Berking C, Wolf P, Lehmann P, Moers-Carpi M, Hönigsmann H, Wernicke-Panten K, Helwig C, Foguet M, Schmitz B, Lübbert H, Szeimies RM; AK-CT002 Study Group. Photodynamic therapy with BF-200 ALA for the treatment of actinic keratosis: results of a multicentre, randomized, observer-blind phase III study in comparison with a registered methyl-5-aminolaevulinate cream and placebo. *Br J Dermatol* 2012;166(1):137-46.

Dirschka T, Radny P, Dominicus R, Mensing H, Brüning H, Jenne L, Karl L, Sebastian M, Oster-Schmidt C, Klövekorn W, Reinhold U, Tanner M, Gröne D, Deichmann M, Simon M, Hübinger F, Hofbauer G, Krähn-Senftleben G, Borrosch F, Reich K, Berking C, Wolf P, Lehmann P, Moers-Carpi M, Hönigsmann H, Wernicke-Panten K, Hahn S, Pabst G, Voss D, Foguet M, Schmitz B, Lübbert H, Szeimies RM; AK-CT002 Study Group; AK-CT003 Study Group. Long-term (6 and 12 months) follow-up of two prospective, randomized, controlled phase III trials of photodynamic therapy with BF-200 ALA and methyl aminolaevulinate for the treatment of actinic keratosis. *Br J Dermatol* 2013;168(4):825-36.

Dodson JM, DeSpain J, Hewett JE, Clark DP. Malignant potential of actinic keratoses and the controversy over treatment. A patient-oriented perspective. *Arch Dermatol* 1991;127(7):1029-31.

Donnelly RF, Morrow DI, McCarron PA, Woolfson AD, Morrissey A, Juzenas P, Juzeniene A, Iani V, McCarthy HO, Moan J. Microneedle-mediated intradermal delivery of 5-aminolevulinic acid: potential for enhanced topical photodynamic therapy. *J Control Release* 2008;129(3):154-62.

D'Orazio J, Jarrett S, Amaro-Ortiz A, Scott T. UV Radiation and the Skin. *Int J Mol Sci* 2013 7;14(6):12222-48.

Dögnitz N, Salomon D, Zellweger M, Ballini JP, Gabrecht T, Lange N, van den Bergh H, Wagnières G. Comparison of ALA- and ALA hexyl-ester-induced PpIX depth distribution in human skin carcinoma. *J Photochem Photobiol B* 2008;93(3):140-8.

Eder J, Prillinger K, Korn A, Geroldinger A, Trautinger F. Prevalence of actinic keratosis among dermatology outpatients in Austria. *Br J Dermatol* 2014;171(6):1415-21.

Einspahr J, Alberts DS, Aickin M, Welch K, Bozzo P, Grogan T, Nelson M. Expression of p53 protein in actinic keratosis, adjacent, normal-appearing, and non-sun-exposed human skin. *Cancer Epidemiol Biomarkers Prev* 1997;6(8):583-7.

Elder D, Elenitsas R, Rubin AI, Ioffreda M, Miller J, Miller OF. Atlas and synopsis of Lever's histopathology of the skin. Lippincott Williams&Wilkins, Wolters Kluwer 2013 3rd Edition.

Elmets CA, Ledet J, Athar M. Cyclooxygenases: Mediators of UV-Induced Skin Cancer and Potential Targets for Prevention. *J Invest Dermatol* 2014;134(10):2497-2502.

El Shabrawi-Caelen L, Kerl H, Cerroni L. Melan-A: not a helpful marker in distinction between melanoma in situ on sun-damaged skin and pigmented actinic keratosis. *Am J Dermatopathol* 2004;26(5):364-6.

Ericson MB, Sandberg C, Stenquist B, Gudmundson F, Karlsson M, Ros AM, Rosén A, Larkö O, Wennberg AM, Rosdahl I. Photodynamic therapy of actinic keratosis at varying fluence rates: assessment of photobleaching, pain and primary clinical outcome. *Br J Dermatol* 2004;151(6):1204-12.

Ericson MB, Wennberg AM, Larkö O. Review of photodynamic therapy in actinic keratosis and basal cell carcinoma. *Ther Clin Risk Manag* 2008;4(1):1-9.

Erickson C, Miller SJ. Treatment options in melanoma in situ: topical and radiation therapy, excision and Mohs surgery. *Int J Dermatol* 2010;49(5):482-91.

Eriksson T, Tinghög G. Societal Cost of Skin Cancer in Sweden in 2011. *Acta Derm Venereol* 2014. Electronic publication ahead of a print.

European Dermatology Forum (EDF). Guideline on photodynamic therapy 2014. http://www.euroderm.org/index.php/edf-guidelines

Fabricius S, Lerche CM, Philipsen PA, Wulf HC. The relation between methyl aminolevulinate concentration and inflammation after photodynamic therapy in healthy volunteers. *Photochem Photobiol Sci* 2013;12(1):117-23.

Fargnoli MC, Kostaki D, Piccioni A, Micantonio T, Peris K. Dermoscopy in the diagnosis and management of non-melanoma skin cancers. *Eur J Dermatol* 2012;22(4):456-63.

Ferrandiz L, Ruiz-de-Casas A, Trakatelli M, de Vries E, Ulrich M, Aquilina S, Saksela O, Majewski S, Ranki A, Proby C, Magnoni C, Pitkänen S, Kalokasidis K, Siskou S, Hinrichs B, Altsitsiadis E, Stockfleth E, Moreno-Ramirez D; EPIDERM Group. Assessing physicians' preferences on skin cancer treatment in Europe. *Br J Dermatol* 2012;167(2):29-35.

Fitzpatrick TB. The Validity and Practicality of Sun-Reactive Skin Types I Through VI. *Arch Dermatol* 1988;124:869-871.

Fixler D, Ankri R, Kaplan I, Novikov I, Hirshberg A. Diffusion Reflection: A Novel Method for Detection of Oral Cancer. *J Dent Res* 2014;93(6):602-606.

Fleming CJ, Bryden AM, Evans A, Dawe RS, Ibbotson SH. A pilot study of treatment of lentigo maligna with 5% imiquimod cream. *Br J Dermatol* 2004;151(2):485-8.

Flotte TJ, Mihm MC Jr. Lentigo maligna and malignant melanoma in situ, lentigo maligna type. *Hum Pathol* 1999;30(5):533-6.

Foote JA, Harris RB, Giuliano AR, Roe DJ, Moon TE, Cartmel B, Alberts DS. Predictors for cutaneous basal- and squamous-cell carcinoma among actinically damaged adults. *Int J Cancer* 2001;95(1):7-11.

Forslund O, Ly H, Reid C, Higgins G. A broad spectrum of human papillomavirus types is present in the skin of Australian patients with non-melanoma skin cancers and solar keratosis. *Br J Dermatol* 2003;149(1):64-73.

Fotinos N, Campo MA, Popowycz F, Gurny R, Lange N. 5-Aminolevulinic acid derivatives in photomedicine: Characteristics, application and perspectives. Photochem Photobiol 2006;82(4):994-1015.

Fritsch C, Homey B, Stahl W, Lehmann P, Ruzicka T, Sies H. Preferential relative porphyrin enrichment in solar keratoses upon topical application of delta-aminolevulinic acid methylester. *Photochem Photobiol* 1998;68(2):218-21.

Frost CA, Green AC. Epidemiology of solar keratoses. *Br J Dermatol* 1994;131(4):455-64.

Frost C, Williams G, Green A. High incidence and regression rates of solar keratoses in a Queensland community. *J Invest Dermatol* 2000;115(2):273-7.

Fuchs A, Marmur E. The kinetics of skin cancer: progression of actinic keratosis to squamous cell carcinoma. *Dermatol Surg* 2007;33(9):1099-101.

Gaudi S, Meyer R, Ranka J, Granahan JC, Israel SA, Yachik TR, Jukic DM. Hyperspectral imaging of melanocytic lesions. *Am J Dermatopathol* 2014;36(2):131-6.

Gaudy-Marqueste C, Madjlessi N, Guillot B, Avril MF, Grob JJ. Risk factors in elderly people for lentigo maligna compared with other melanomas: a double case-control study. *Arch Dermatol* 2009;145(4):418-23.

Gniadecka M, Wulf HC, Nielsen OF, Christensen DH, Hercogova J. Distinctive molecular abnormalities in benign and malignant skin lesions: studies by Raman spectroscopy. *Photochem Photobiol* 1997;66(4):418-23.

Gniazdowska B, Ruëff F, Hillemanns P, Przybilla B. Allergic contact dermatitis from delta-aminolevulinic acid used for photodynamic therapy. *Contact Dermatitis* 1998;38(6):348-9.

Gordon LG, Rowell D. Health system costs of skin cancer and cost-effectiveness of skin cancer prevention and screening: a systematic review. *Eur J Cancer Prev* 2014. Electronic publication ahead of a print.

Green A, Williams G, Neale R, Hart V, Leslie D, Parsons P, Marks GC, Gaffney P, Battistutta D, Frost C, Lang C, Russell A. Daily sunscreen application and betacarotene supplementation in prevention of basal-cell and squamous-cell carcinomas of the skin: a randomised controlled trial. *Lancet* 1999;354(9180):723-9.

Guitera P, Pellacani G, Crotty KA, Scolyer RA, Li LX, Bassoli S, Vinceti M, Rabinovitz H, Longo C, Menzies SW. The impact of in vivo reflectance confocal microscopy on the diagnostic accuracy of lentigo maligna and equivocal pigmented and nonpigmented macules of the face. *J Invest Dermatol* 2010;130(8):2080-91.

Guitera P, Moloney FJ, Menzies SW, Stretch JR, Quinn MJ, Hong A, Fogarty G, Scolyer RA. Improving management and patient care in lentigo maligna by mapping with in vivo confocal microscopy. *JAMA Dermatol* 2013;149(6):692-8.

Gupta AK, Paquet M. Network meta-analysis of the outcome 'participant complete clearance' in nonimmunosuppressed participants of eight interventions for actinic keratosis: a follow-up on a Cochrane review. *Br J Dermatol* 2013;169(2):250-9.

Haedersdal M, Sakamoto FH, Farinelli WA, Doukas AG, Tam J, Anderson RR. Pretreatment with ablative fractional laser changes kinetics and biodistribution of topical 5-aminolevulinic acid (ALA) and methyl aminolevulinate (MAL). *Lasers Surg Med* 2014;46(6):462-9.

Hacioglu S, Saricaoglu H, Baskan EB, Uner SI, Aydogan K, Tunali S. The value of spectrophotometric intracutaneous analysis in the noninvasive diagnosis of nonmelanoma skin cancers. *Clin Exp Dermatol* 2013;38(5):464-9.

Harris AT. Spectral mapping tools from the earth sciences applied to spectral microscopy data. *Cytometry A* 2006;69(8):872-9.

Hazan C, Dusza SW, Delgado R, Busam KJ, Halpern AC, Nehal KS. Staged excision for lentigo maligna and lentigo maligna melanoma: A retrospective analysis of 117 cases. *J Am Acad Dermatol* 2008;58(1):142-8.

Heaphy MR Jr, Ackerman AB. The nature of solar keratosis: a critical review in historical perspective. *J Am Acad Dermatol* 2000;43(1):138-50.

Hedblad MA, Mallbris L. Grenz ray treatment of lentigo maligna and early lentigo maligna melanoma. *J Am Acad Dermatol* 2012;67(1):60-8.

Hemminki K, Zhang H, Czene K. Incidence trends and familial risks in invasive and in situ cutaneous melanoma by sun-exposed body sites. *Int J Cancer* 2003;104(6):764-71.

Hendi A, Brodland DG, Zitelli JA. Melanocytes in long-standing sun-exposed skin: quantitative analysis using the MART-1 immunostain. *Arch Dermatol* 2006;142(7):871-6.

Hewett J, Nadeau V, Ferguson J, Moseley H, Ibbotson S, Allen JW, Sibbett W, Padgett M. The application of a compact multispectral imaging system with integrated excitation source to in vivo monitoring of fluorescence during topical photodynamic therapy of superficial skin cancers. *Photochem Photobiol* 2001;73(3):278-82.

Hirst NG, Gordon LG, Scuffham PA, Green AC. Lifetime cost-effectiveness of skin cancer prevention through promotion of daily sunscreen use. *Value Health* 2012;15(2):261-8.

Holmes C, Foley P, Freeman M, Chong AH. Solar keratosis: epidemiology, pathogenesis, presentation and treatment. *Australas J Dermatol* 2007;48(2):67-74;75-6.

Horn M, Gerger A, Ahlgrimm-Siess V, Weger W, Koller S, Kerl H, Samonigg H, Smolle J, Hofmann-Wellenhof R. Discrimination of actinic keratoses from normal skin with reflectance mode confocal microscopy. *Dermatol Surg* 2008;34(5):620-5.

Huerta-Brogeras M, Olmos O, Borbujo J, Hernández-Núñez A, Castaño E, Romero-Maté A, Martínez-Sánchez D, Martínez-Morán C. Validation of dermoscopy as a real-time noninvasive diagnostic imaging technique for actinic keratosis. *Arch Dermatol* 2012;148(10):1159-64.

Hönigsmann H. History of phototherapy in dermatology. *Photochem Photobiol Sci* 2013;12(1):16-21.

Iorizzo LJ 3rd, Chocron I, Lumbang W, Stasko T. Importance of vertical pathology of debulking specimens during Mohs micrographic surgery for lentigo maligna and melanoma in situ. *Dermatol Surg* 2013;39:365-71.

Jolivot R, Vabres P, Marzani F. Reconstruction of hyperspectral cutaneous data from an artificial neural network-based multispectral imaging system. *Comput Med Imaging Graph* 2011;35(2):85-8.

Juzenas P, Juzeniene A. Reduction of cutaneous photosensitivity by application of ointment containing ferrous or cobaltous ions concomitant with the use of topical protoporphyrin IX precursors. *Photodiagnosis Photodyn Ther* 2010;7(3):152-7.

Juzeniene A, Juzenas P, Ma LW, Iani V, Moan J. Topical application of 5-aminolaevulinic acid, methyl 5-aminolaevulinate and hexyl 5-aminolaevulinate on normal human skin. *Br J Dermatol* 2006;155(4):791-9.

Kaçar N, Sanli B, Zalaudek I, Yildiz N, Ergin S. Dermatoscopy for monitoring treatment of actinic keratosis with imiquimod. *Clin Exp Dermatol* 2012;37(5):567-9.

Karam A, Simon M, Lemasson G, Misery L. The use of photodynamic therapy in the treatment of lentigo maligna. *Pigment Cell Melanoma Res* 2013;26(2):275-7.

Kaufmann R, Spelman L, Weightman W, Reifenberger J, Szeimies RM, Verhaeghe E, Kerrouche N, Sorba V, Villemagne H, Rhodes LE. Multicentre intraindividual randomized trial of topical methyl aminolaevulinate-photodynamic therapy vs. cryotherapy for multiple actinic keratoses on the extremities. *Br J Dermatol* 2008;158(5):994-9.

Kellner C, Bauriedl S, Hollstein S, Reinhold U. Simulated daylight photodynamic therapy with BF-200 ALA for actinic keratosis: assessment of the efficacy and tolerability in a retrospective study. *Br J Dermatol* 2014, electronic publication ahead of a print.

Kimyai-Asadi A, Katz T, Goldberg LH, Ayala GB, Wang SQ, Vujevich JJ, Jih MH. Margin involvement after the excision of melanoma in situ: the need for complete en face examination of the surgical margins. *Dermatol Surg* 2007;33(12):1434-9.

Kivisaari AK, Kallajoki M, Mirtti T, McGrath JA, Bauer JW, Weber F, Königová R, Sawamura D, Sato-Matsumura KC, Shimizu H, Csikós M, Sinemus K, Beckert W, Kähäri VM. Transformation-specific matrix metalloproteinases (MMP)-7 and MMP-13 are expressed by tumour cells in epidermolysis bullosa-associated squamous cell carcinomas. *Br J Dermatol* 2008;158(4):778-85.

Kivisaari A, Kähäri VM. Squamous cell carcinoma of the skin: Emerging need for novel biomarkers. *World J Clin Oncol* 2013;4(4):85-90.

Kleinpenning MM, Wolberink EW, Smits T, Blokx WA, van De Kerkhof PC, van Erp PE, Gerritsen RM. Fluorescence diagnosis in actinic keratosis and squamous cell carcinoma. *Photodermatol Photoimmunol Photomed* 2010;26(6):297-302.

Korde VR, Bonnema GT, Xu W, Krishnamurthy C, Ranger-Moore J, Saboda K, Slayton LD, Salasche SJ, Warneke JA, Alberts DS, Barton JK. Using optical coherence tomography to evaluate skin sun damage and precancer. *Lasers Surg Med* 2007;39(9):687-95.

Korshøj S, Sølvsten H, Erlandsen M, Sommerlund M. Frequency of sensitization to methyl aminolaevulinate after photodynamic therapy. *Contact Dermatitis* 2009;60(6):320-4.

Kozma B, Eide MJ. Photocarcinogenesis: an epidemiologic perspective on ultraviolet light and skin cancer. *Dermatol Clin* 2014;32(3):301-13.

Kraft S, Granter SR. Molecular pathology of skin neoplasms of the head and neck. *Arch Pathol Lab Med* 2014 ;138(6):759-87.

Kunishige JH, Brodland DG, Zitelli JA. Surgical margins for melanoma in situ. *J Am Acad Dermatol* 2012;66(3):438-44.

Kvaskoff M, Pandeya N, Green AC, Perry S, Baxter C, Davis MB, Mortimore R, Westacott L, Wood D, Triscott J, Williamson R, Whiteman DC. Site-specific determinants of cutaneous melanoma: a case-case comparison of patients with tumors arising on the head or trunk. *Cancer Epidemiol Biomarkers Prev* 2013;22(12):2222-31.

Lebwohl M, Shumack S, Stein Gold L, Melgaard A, Larsson T, Tyring SK. Long-term follow-up study of ingenol mebutate gel for the treatment of actinic keratoses. *JAMA Dermatol* 2013;149(6):666-70.

Lee JH, Won CY, Kim GM, Kim SY. Dermoscopic features of actinic keratosis and follow up with dermoscopy: a pilot study. *J Dermatol* 2014;41(6):487-93.

Liu Z, Wang H, Li Q. Tongue tumor detection in medical hyperspectral images. *Sensors* 2012;12(1):162-74.

Liutkeviciute-Navickiene J, Mordas A, Rutkovskiene L, Bloznelyte-Plesniene L. Skin and mucosal fluorescence diagnosis with different light sources. *Eur J Dermatol* 2009;19(2):135-40.

Longo C, Casari A, Beretti F, Cesinaro AM, Pellacani G. Skin aging: in vivo microscopic assessment of epidermal and dermal changes by means of confocal microscopy. *J Am Acad Dermatol* 2013;68(3):73-82.

Lui H, Zhao J, McLean D, Zeng H. Real-time Raman spectroscopy for in vivo skin cancer diagnosis. *Cancer Res* 2012;72(10):2491-500.

Maier T, Braun-Falco M, Laubender RP, Ruzicka T, Berking C. Actinic keratosis in the en-face and slice imaging mode of high-definition optical coherence tomography and comparison with histology. *Br J Dermatol* 2013;168(1):120-8.

Maisch T, Santarelli F, Schreml S, Babilas P, Szeimies RM. Fluorescence induction of protoporphyrin IX by a new 5-aminolevulinic acid nanoemulsion used for photodynamic therapy in a full-thickness ex vivo skin model. *Exp Dermatol* 2010;19(8):302-5.

Maldonado JL, Fridlyand J, Patel H, Jain AN, Busam K, Kageshita T, Ono T, Albertson DG, Pinkel D, Bastian BC. Determinants of BRAF mutations in primary melanomas. *J Natl Cancer Inst* 2003;95(24):1878-90.

Maltusch A, Röwert-Huber J, Matthies C, Lange-Asschenfeldt S, Stockfleth E. Modes of action of diclofenac 3%/hyaluronic acid 2.5% in the treatment of actinic keratosis. *J Dtsch Dermatol Ges* 2011;9(12):1011-7.

Malvehy J, Roldán-Marín R, Iglesias-García P, Díaz A, Puig S. Monitoring Treatment of Field Cancerisation with 3% Diclofenac Sodium 2.5% Hyaluronic Acid by Reflectance Confocal Microscopy: A Histologic Correlation. *Acta Derm Venereol 2014*, electronic publication ahead of a print.

Manyak MJ, Javitt M, Kang PS, Kreuger WR, Storm ES. The evolution of imaging in advanced prostate cancer. *Urol Clin North Am* 2006;33(2):133-46.

Marghoob AA, Swindle LD, Moricz CZ, Sanchez Negron FA, Slue B, Halpern AC, Kopf AW. Instruments and new technologies for the in vivo diagnosis of melanoma. *J Am Acad Dermatol* 2003;49(5):777-97.

Marks R, Foley P, Goodman G, Hage BH, Selwood TS. Spontaneous remission of solar keratoses: the case for conservative management. *Br J Dermatol* 1986;115(6):649-55.

Marks R, Rennie G, Selwood TS. Malignant transformation of solar keratoses to squamous cell carcinoma. *Lancet* 1988;1(8589):795-7.

Martin A, Tope WD, Grevelink JM, Starr JC, Fewkes JL, Flotte TJ, Deutsch TF, Anderson RR. Lack of selectivity of protoporphyrin IX fluorescence for basal cell carcinoma after topical application of 5-aminolevulinic acid: implications for photodynamic treatment. *Arch Dermatol Res* 1995;287(7):665-74.

Martin ME, Wabuyele MB, Chen K, Kasili P, Panjehpour M, Phan M, Overholt B, Cunningham G, Wilson D, Denovo RC, Vo-Dinh T. Development of an advanced hyperspectral imaging (HSI) system with applications for cancer detection. *Ann Biomed Eng 2006*;34(6):1061-8.[1]

Martin ME, Wabuyele M, Panjehpour M, Overholt B, DeNovo R, Kennel S, Cunningham G, Vo-Dinh T. An AOTF-based dual-modality hyperspectral imaging system (DMHSI) capable of simultaneous fluorescence and reflectance imaging. *Med Eng Phys* 2006;28(2):149-55. [2]

Mayer JE, Swetter SM2, Fu T3, Geller AC4. Screening, early detection, education, and trends for melanoma: Current status (2007-2013) and future directions: Part I. Epidemiology, high-risk groups, clinical strategies, and diagnostic technology. *J Am Acad Dermatol* 2014;71(4):599.

McKenna JK, Florell SR, Goldman GD, Bowen GM. Lentigo maligna/lentigo maligna melanoma: current state of diagnosis and treatment. *Dermatol Surg* 2006;32(4):493-504.

McLeod M, Choudhary S, Giannakakis G, Nouri K. Surgical treatments for lentigo maligna: a review. *Dermatol Surg* 2011;37(9):1210-28.

Memon AA, Tomenson JA, Bothwell J, Friedmann PS. Prevalence of solar damage and actinic keratosis in a Merseyside population. *Br J Dermatol* 2000;142(6):1154-9.

Micali G, Lacarrubba F, Nasca MR, Ferraro S, Schwartz RA. Topical pharmacotherapy for skin cancer: part II. Clinical applications. *J Am Acad Dermatol* 2014;70(6):979.

Mirzoyev SA, Knudson RM, Reed KB, Hou JL, Lohse CM, Frohm ML, Brewer JD, Otley CC, Roenigk RK. Incidence of lentigo maligna in Olmsted County, Minnesota, 1970 to 2007. *J Am Acad Dermatol* 2014;70(3):443-8.

Mittelbronn MA, Mullins DL, Ramos-Caro FA, Flowers FP. Frequency of pre-existing actinic keratosis in cutaneous squamous cell carcinoma. *Int J Dermatol* 1998;37(9):677-81.

Moan J, Ma LW, Iani V. On the pharmacokinetics of topically applied 5-aminolevulinic acid and two of its esters. *Int J Cancer* 2001;92(1):139-43.

Moan J, Ma LW, Juzeniene A, Iani V, Juzenas P, Apricena F, Peng Q. Pharmacology of protoporphyrin IX in nude mice after application of ALA and ALA esters. *Int J Cancer* 2003;103(1):132-5.

Mogensen M, Joergensen TM, Nürnberg BM, Morsy HA, Thomsen JB, Thrane L, Jemec GB. Assessment of optical coherence tomography imaging in the diagnosis of non-melanoma skin cancer and benign lesions versus normal skin: observer-blinded evaluation by dermatologists and pathologists. *Dermatol Surg* 2009;35(6):965-72.

Moloney FJ, Collins P. Randomized, double-blind, prospective study to compare topical 5-aminolaevulinic acid methylester with topical 5-aminolaevulinic acid photodynamic therapy for extensive scalp actinic keratosis. *Br J Dermatol* 2007;157(1):87-91.

Moncrieff M, Cotton S, Claridge E, Hall P. Spectrophotometric intracutaneous analysis: a new technique for imaging pigmented skin lesions. *Br J Dermatol* 2002 Mar;146(3):448-57.

Monheit G, Cognetta AB, Ferris L, Rabinovitz H, Gross K, Martini M, Grichnik JM, Mihm M, Prieto VG, Googe P, King R, Toledano A, Kabelev N, Wojton M, Gutkowicz-Krusin D. The performance of MelaFind: a prospective multicenter study. *Arch Dermatol* 2011;147(2):188-94.

Morrow DI, McCarron PA, Woolfson AD, Juzenas P, Juzeniene A, Iani V, Moan J, Donnelly RF. Hexyl aminolaevulinate is a more effective topical photosensitiser precursor than methyl aminolaevulinate and 5-aminolaevulinic acids when applied in equimolar doses. *J Pharm Sci* 2010;99(8):3486-98.

Morton C, Campbell S, Gupta G, Keohane S, Lear J, Zaki I, Walton S, Kerrouche N, Thomas G, Soto P; AKtion Investigators. Intraindividual, right-left comparison of topical methyl aminolaevulinate-photodynamic therapy and cryotherapy in subjects with actinic keratoses: a multicentre, randomized controlled study. *Br J Dermatol* 2006;155(5):1029-36.

Morton CA, Szeimies RM, Sidoroff A, Braathen LR. European guidelines for topical photodynamic therapy part 1: treatment delivery and current indications - actinic keratoses, Bowen's disease, basal cell carcinoma. *J Eur Acad Dermatol Venereol* 2013;27(5):536-44. [1]

Morton CA, Szeimies RM, Sidoroff A, Braathen LR. European guidelines for topical photodynamic therapy part 2: emerging indications--field cancerization, photorejuvenation and inflammatory/infective dermatoses. *J Eur Acad Dermatol Venereol* 2013;27(6):672-9. [2]

Moseley H. Total effective fluence: a useful concept in photodynamic therapy. *Lasers Med Sci.*1996;11;139-43.

Moseley H. Light distribution and calibration of commercial PDT LED arrays. *Photochem Photobiol Sci* 2005;4(11):911-4.

Moseley H, Allen JW, Ibbotson S, Lesar A, McNeill A, Camacho-Lopez MA, Samuel ID, Sibbett W, Ferguson J. Ambulatory photodynamic therapy: a new concept in delivering photodynamic therapy. *Br J Dermatol* 2006;154(4):747-50.

Muston D, Downs A, Rives V. An economic evaluation of topical treatments for actinic keratosis. *J Dermatolog Treat* 2009;20(5):266-75.

Nagaoka T, Nakamura A, Okutani H, Kiyohara Y, Sota T. A possible melanoma discrimination index based on hyperspectral data: a pilot study. *Skin Res Technol* 2012;18(3):301-10.

Nascimento JMP, Dias JMB. Vertex component analysis: A Fast algorithm to unmix hyperspectral data. *IEEE Trans Geosci Remote Sensing* 2005; 43 :898–910.

Neale R, Williams G, Green A. Application patterns among participants randomized to daily sunscreen use in a skin cancer prevention trial. *Arch Dermatol* 2002;138(10):1319-25.

Neidecker MV, Davis-Ajami ML, Balkrishnan R, Feldman SR. Pharmacoeconomic considerations in treating actinic keratosis. *Pharmacoeconomics* 2009;27(6):451-64.

Nestor MS, Zarraga MB. The incidence of nonmelanoma skin cancers and actinic keratoses in South Florida. *J Clin Aesthet Dermatol* 2012;5(4):20-4.

Novak B, Schulten R, Lübbert H. δ-Aminolevulinic acid and its methyl ester induce the formation of Protoporphyrin IX in cultured sensory neurones. *Naunyn Schmiedebergs Arch Pharmacol* 2011;384(6):583-602.

O'Connor AE, Gallagher WM, Byrne AT. Porphyrin and nonporphyrin photosensitizers in oncology: preclinical and clinical advances in photodynamic therapy. *Photochem Photobiol* 2009;85(5):1053-74.

Olsen EA, Abernethy ML, Kulp-Shorten C, Callen JP, Glazer SD, Huntley A, McCray M, Monroe AB, Tschen E, Wolf JE Jr. A double-blind, vehicle-controlled study evaluating masoprocol cream in the treatment of actinic keratoses on the head and neck. *J Am Acad Dermatol* 1991;24:738-43.

Osborne JE, Hutchinson PE. A follow-up study to investigate the efficacy of initial treatment of lentigo maligna with surgical excision. *Br J Plast Surg* 2002;55(8):611-5

Panasyuk SV, Yang S, Faller DV, Ngo D, Lew RA, Freeman JE, Rogers AE. Medical hyperspectral imaging to facilitate residual tumor identification during surgery. *Cancer Biol Ther* 2007;6(3):439-46.

Paraskevas LR, Halpern AC, Marghoob AA. Utility of the Wood's light: five cases from a pigmented lesion clinic.*Br J Dermatol* 2005;152(5):1039-44.

Pariser D, Loss R, Jarratt M, Abramovits W, Spencer J, Geronemus R, Bailin P, Bruce S. Topical methyl-aminolevulinate photodynamic therapy using red light-emitting diode light for treatment of multiple actinic keratoses: A randomized, double-blind, placebo-controlled study. *J Am Acad Dermatol* 2008;59(4):569-76.

Passos SK, de Souza PE, Soares PK, Eid DR, Primo FL, Tedesco AC, Lacava ZG, Morais PC. Quantitative approach to skin field cancerization using a nanoencapsulated photodynamic therapy agent: a pilot study. *Clin Cosmet Investig Dermatol* 2013;6:51-9.

Peng Q, Berg K, Moan J, Kongshaug M, Nesland JM. 5-Aminolevulinic acid-based photodynamic therapy: principles and experimental research. *Photochem Photobiol* 1997;65(2):235-51.

Petersen B, Wiegell SR, Wulf HC. Light protection of the skin after photodynamic therapy reduces inflammation: an unblinded randomized controlled study. *Br J Dermatol* 2014;171(1):175-8.[1]

Petersen B, Wulf HC. Application of sunscreen--theory and reality *Photodermatol Photoimmunol Photomed* 2014;30(2-3):96-101.[2]

Piacquadio DJ, Chen DM, Farber HF, Fowler JF Jr, Glazer SD, Goodman JJ, Hruza LL, Jeffes EW, Ling MR, Phillips TJ, Rallis TM, Scher RK, Taylor CR, Weinstein GD. Photodynamic therapy with aminolevulinic acid topical solution and visible blue light in the treatment of multiple actinic keratoses of the face and scalp: investigator-blinded, phase 3, multicenter trials. *Arch Dermatol* 2004;140(1):41-6.

Pommergaard HC, Burcharth J, Rosenberg J, Raskov H. Combination chemoprevention with diclofenac, calcipotriol and difluoromethylornithine inhibits development of non-melanoma skin cancer in mice. *Anticancer Res* 2013;33(8):3033-9.

Pralong P, Bathelier E, Dalle S, Poulalhon N, Debarbieux S, Thomas L. Dermoscopy of lentigo maligna melanoma: report of 125 cases. *Br J Dermatol* 2012;167(2):280-7.

Purdue MP, From L, Kahn HJ, Armstrong BK, Kricker A, Gallagher RP, McLaughlin JR, Klar NS, Marrett LD. Etiologic factors associated with p53 immunostaining in cutaneousmalignant melanoma. *Int J Cancer* 2005;117(3):486-93.

Pölönen I. Discovering knowledge in various applications with a novel hyperspectral imager. Dissertation, University of Jyväskylä 2013.

Quaedvlieg PJ, Tirsi E, Thissen MR, Krekels GA. Actinic keratosis: how to differentiate the good from the bad ones? *Eur J Dermatol* 2006;16(4):335-9.

Rajaram N, Reichenberg JS, Migden MR, Nguyen TH, Tunnell JW. Pilot clinical study for quantitative spectral diagnosis of non-melanoma skin cancer. *Lasers Surg Med. 2010;42(10):716-27.*

Reed JA, Shea CR. Lentigo maligna: melanoma in situ on chronically sun-damaged skin. *Arch Pathol Lab* Med 2011;135(7):838-41.

Ribeiro CF, Souza FH, Jordão JM, Haendchen LC, Mesquita L, Schmitt JV, Faucz LL. Photodynamic therapy in actinic cheilitis: clinical and anatomopathological evaluation of 19 patients. *An Bras Dermatol* 2012;87(3):418-23.

Ripley BD. Pattern recognition neural networks. Cambridge, UK: *Cambridge University Press*; 1996. pp 1–403.

Robinson JK. Use of digital epiluminescence microscopy to help define the edge of lentigo maligna. *Arch Dermatol* 2004;140(9):1095-100.

Robinson R. Economic evaluation and health care. What does it mean? *BMJ* 1993;307(6905):670-3.[1]

Robinson R. Cost-effectiveness analysis. *BMJ* 1993;307(6907):793-5.[2]

Rubel DM, Spelman L, Murrell DF, See JA, Hewitt D, Foley P, Bosc C, Kerob D, Kerrouche N, Wulf HC, Shumack S. Daylight photodynamic therapy with methyl aminolevulinate cream as a convenient, similarly effective, nearly painless alternative to conventional photodynamic therapy in actinic keratosis treatment: a randomized controlled trial. *Br J Dermatol* 2014;171(5):1164-71.

Rundle P. Treatment of posterior uveal melanoma with multi-dose photodynamic therapy. *Br J Ophthalmol* 2014;98(4):494-7.

Saari H, Aallos V-V, Holmlund C, Malinen J, Mäkynen J. Handheld hyperspectral imager. *Proc SPIE* 2010; 7680: 0-12.

Saari H, Pölönen I, Salo H, Honkavaara E, Hakala T, Holmlund C et al. Miniaturized hyperspectral imager calibration and uav flight campaigns. *Proc Spie* 2013; 8889:10-12

Salasche SJ. Epidemiology of actinic keratoses and squamous cell carcinoma. *J Am Acad Dermatol* 2000;42:4-7.

Samrao A, Cockerell CJ. Pharmacotherapeutic management of actinic keratosis: focus on newer topical agents. *Am J Clin Dermatol* 2013;14(4):273-7.

Sasaki Y, Niu C, Makino R, Kudo C, Sun C, Watanabe H, Matsunaga J, Takahashi K, Tagami H, Aiba S, Horii A. BRAF point mutations in primary melanoma show different prevalences by subtype. *J Invest Dermatol* 2004;123(1):177-83.

Schaefer I, Augustin M, Spehr C, Reusch M, Kornek T. Prevalence and risk factors of actinic keratoses in Germany-analysis of multisource data. *J Eur Acad Dermatol Venereol* 2014;28(3):309-13.

Schiffner R, Schiffner-Rohe J, Vogt T, Landthaler M, Wlotzke U, Cognetta AB, Stolz W. Improvement of early recognition of lentigo maligna using dermatoscopy. *J Am Acad Dermatol* 2000;42:25-32.

Schulten R, Novak B, Schmitz B, Lübbert H. Comparison of the uptake of 5-aminolevulinic acid and its methyl ester in keratinocytes and skin. *Naunyn Schmiedebergs Arch Pharmacol* 2012;385(10):969-79.

Senge MO, Brandt JC. Temoporfin (Foscan®, 5,10,15,20-tetra(m-hydroxyphenyl)chlorin)--a second-generation photosensitizer. *Photochem Photobiol* 2011;87(6):1240-96.

Sharfaei S, Juzenas P, Moan J, Bissonnette R. Weekly topical application of methyl aminolevulinate followed by light exposure delays the appearance of UV-induced skin tumours in mice. *Arch Dermatol Res* 2002;294(5):237-42.

Siddiqi AM, Li H, Faruque F, Williams W, Lai K, Hughson M, Bigler S, Beach J, Johnson W. Use of hyperspectral imaging to distinguish normal, precancerous, and cancerous cells. *Cancer* 2008;114(1):13-21.

Skalkos D, Gioti E, Stalikas CD, Meyer H, Papazoglou TG, Filippidis G. Photophysical properties of Hypericum perforatum L. extracts--novel photosensitizers for PDT. *J Photochem Photobiol B.* 2006;82(2):146-51.

Smits T, Robles CA, van Erp PE, van de Kerkhof PC, Gerritsen MJ. Correlation between macroscopic fluorescence and protoporphyrin IX content in psoriasis and actinic keratosis following application of aminolevulinic acid. *J Invest Dermatol* 2005;125(4):833-9.

Soergel P, Dahl GF, Onsrud M, Hillemanns P. Photodynamic therapy of cervical intraepithelial neoplasia 1-3 and human papilloma virus (HMV) infection with methylaminolevulinate and hexaminolevulinate--a double-blind, dose-finding study. *Lasers Surg Med* 2012;44(6):468-74.

Sotiriou E, Apalla Z, Vrani F, Lallas A, Chovarda E, Ioannides D. Photodynamic therapy vs. imiquimod 5% cream as skin cancer preventive strategies in patients with field changes: a randomized intraindividual comparison study. *J Eur Acad Dermatol Venereol* 2014. Electronic publication ahead of a print.

Stadelmeyer E, Heitzer E, Resel M, Cerroni L, Wolf P, Dandachi N. The BRAF V600K mutation is more frequent than the BRAF V600E mutation in melanoma in situ of lentigo maligna type. *J Invest Dermatol* 2014;134(2):548-50.

Stimpfle DW, Serra AL, Wüthrich RP, French LE, Braun RP, Hofbauer GF. Spectophotometric intracutaneous analysis: an investigation on photodamaged skin of immunocompromised patients. *J Eur Acad Dermatol Venereol* 2014, electronic publication ahead of a print.

Stockfleth E, Christophers E, Benninghoff B, Sterry W. Low incidence of new actinic keratoses after topical 5% imiquimod cream treatment: a long-term follow-up study. *Arch Dermatol* 2004;140(12):1542.

Stockfleth E. The paradigm shift in treating actinic keratosis: a comprehensive strategy. *J Drugs Dermatol* 2012;11(12):1462-7.

Stolz W, Schiffner R, Burgdorf WH. Dermatoscopy for facial pigmented skin lesions. *Clin Dermatol* 2002;20(3):276-8.

Suhonen R. Cutaneous cryosurgery. *Duodecim* 2005;121(10):1063-71.

Swetter SM, Boldrick JC, Jung SY, Egbert BM, Harvell JD. Increasing incidence of lentigo maligna melanoma subtypes: northern California and national trends 1990-2000. *J Invest Dermatol* 2005;125(4):685-91.

Szeimies RM, Stockfleth E, Popp G, Borrosch F, Brüning H, Dominicus R, Mensing H, Reinhold U, Reich K, Moor AC, Stocker M, Ortland C, Brunnert M, Hauschild A.Long-term follow-up of photodynamic therapy with a self-adhesive 5-aminolaevulinic acid patch: 12 months data. *Br J Dermatol* 2010;162(2):410-4.[1]

Szeimies RM, Radny P, Sebastian M, Borrosch F, Dirschka T, Krähn-Senftleben G, Reich K, Pabst G, Voss D, Foguet M, Gahlmann R, Lübbert H, Reinhold U. Photodynamic therapy with BF-200 ALA for the treatment of actinic keratosis: results of a prospective, randomized, double-blind, placebo-controlled phase III study. *Br J Dermatol* 2010;163(2):386-94.[2]

Szeimies RM, Torezan L, Niwa A, Valente N, Unger P, Kohl E, Schreml S, Babilas P, Karrer S, Festa-Neto C. Clinical, histopathological and immunohistochemical assessment of human skin field cancerization before and after photodynamic therapy. *Br J Dermatol* 2012;167(1):150-9.

Szepetiuk G, Piérard S, Pierard-Franchimont C, Caucanas M, Quatresooz P, Pierard GE. Recent trends in specular light reflectance beyond clinical fluorescence diagnosis. *Eur J Dermatol* 2011;21(2):157-61.

Tannous ZS, Lerner LH, Duncan LM, Mihm MC Jr, Flotte TJ. Progression to invasive melanoma from malignant melanoma in situ, lentigo maligna type. *Hum Pathol* 2000;31(6):705-8.

Tarstedt M, Rosdahl I, Berne B, Svanberg K, Wennberg AM. A randomized multicenter study to compare two treatment regimens of topical methyl aminolevulinate (Metvix)-PDT in actinic keratosis of the face and scalp. *Acta Derm Venereol* 2005;85(5):424-8.

Tessari G, Girolomoni G. Nonmelanoma skin cancer in solid organ transplant recipients: update on epidemiology, risk factors, and management. *Dermatol Surg* 2012;38(10):1622-30.

Thai KE, Fergin P, Freeman M, Vinciullo C, Francis D, Spelman L, Murrell D, Anderson C, Weightman W, Reid C, Watson A, Foley P. A prospective study of the use of cryosurgery for the treatment of actinic keratoses. *Int J Dermatol* 2004;43(9):687-92.

Themstrup L, Banzhaf C, Mogensen M, Jemec GB. Cryosurgery treatment of actinic keratoses monitored by optical coherence tomography: a pilot study. *Dermatology* 2012;225(3):242-7.

Themstrup L, Banzhaf CA2, Mogensen M3, Jemec GB2. Optical coherence tomography imaging of non-melanoma skin cancer undergoing photodynamic therapy reveals subclinical residual lesions. *Photodiagnosis Photodyn Ther* 2014;11(1):7-12.

Thompson SC, Jolley D, Marks R. Reduction of solar keratoses by regular sunscreen use. *N Engl J Med* 1993;329(16):1147-51.

Toender A, Kjær SK, Jensen A. Increased incidence of melanoma in situ in Denmark from 1997 to 2011: results from a nationwide population-based study. *Melanoma Res* 2014;24(5):488-95.

Togsverd-Bo K, Lerche CM, Poulsen T, Wulf HC, Haedersdal M. Photodynamic therapy with topical methyl- and hexylaminolevulinate for prophylaxis and treatment of UV-induced SCC in hairless mice. *Exp Dermatol* 2010;19(8):166-72.

Togsverd-Bo K, Lei U, Erlendsson AM, Taudorf EH, Philipsen PA, Wulf HC, Skov L, Haedersdal M. Combination of ablative fractional laser and daylight mediated photodynamic therapy for actinic keratosis in organ transplant recipients - a randomized controlled trial. *Br J Dermatol* 2015;172(2):467-74.

Traianou A, Ulrich M, Apalla Z, De Vries E, Bakirtzi K, Kalabalikis D, Ferrandiz L, Ruiz-de-Casas A, Moreno-Ramirez D, Sotiriadis D, Ioannides D, Aquilina S, Apap C, Micallef R, Scerri L, Pitkänen S, Saksela O, Altsitsiadis E, Hinrichs B, Magnoni C, Fiorentini C, Majewski S, Ranki A, Proby CM, Stockfleth E, Trakatelli M; EPIDERM Group. Risk factors for actinic keratosis in eight European centres: a case-control study. *Br J Dermatol* 2012;167:36-42.

Tsatsou F, Trakatelli M, Patsatsi A, Kalokasidis K, Sotiriadis D. Extrinsic aging: UV-mediated skin carcinogenesis. *Dermatoendocrinol* 2012;4(3):285-97.

Tschen EH, Wong DS, Pariser DM, Dunlap FE, Houlihan A, Ferdon MB; Phase IV ALA-PDT Actinic Keratosis Study Group. Photodynamic therapy using aminolaevulinic acid for patients with nonhyperkeratotic actinic keratoses of the face and scalp: phase IV multicentre clinical trial with 12-month follow up. *Br J Dermatol* 2006;155(6):1262-9.

Tyrrell J, Campbell S, Curnow A. Validation of a non-invasive fluorescence imaging system to monitor dermatological PDT. *Photodiagnosis Photodyn Ther* 2010;7(2):86-97. [1]

Tyrrell JS, Campbell SM, Curnow A. The relationship between protoporphyrin IX photobleaching during real-time dermatological methyl-aminolevulinate photodynamic therapy (MAL-PDT) and subsequent clinical outcome. *Lasers Surg Med* 2010;42(7):613-9.[2]

Ulrich C. Topical treatment of field cancerization. *Cancer Treat Res* 2009;146:439-46.

Ulrich C, Jürgensen JS, Degen A, Hackethal M, Ulrich M, Patel MJ, Eberle J, Terhorst D, Sterry W, Stockfleth E. Prevention of non-melanoma skin cancer in organ transplant patients by regular use of a sunscreen: a 24 months, prospective, case-control study. *Br J Dermatol* 2009;161(3):78-84.

Ulrich M, Krueger-Corcoran D, Roewert-Huber J, Sterry W, Stockfleth E, Astner S. Reflectance confocal microscopy for noninvasive monitoring of therapy and detection of subclinical actinic keratoses. *Dermatology* 2010;220(1):15-24.

van der Beek N, de Leeuw J, Demmendal C, Bjerring P, Neumann HA. PpIX fluorescence combined with auto-fluorescence is more accurate than PpIX fluorescence alone in fluorescence detection of non-melanoma skin cancer: an intra-patient direct comparison study. *Lasers Surg Med* 2012;44(4):271-6.

van der Pols JC, Williams GM, Pandeya N, Logan V, Green AC. Prolonged prevention of squamous cell carcinoma of the skin by regular sunscreen use. *Cancer Epidemiol Biomarkers Prev* 2006;15(12):2546-8.

Vatve M, Ortonne JP, Birch-Machin MA, Gupta G. Management of field change in actinic keratosis. *Br J Dermatol* 2007;157(2):21-4.

Vegter S, Tolley K. A network meta-analysis of the relative efficacy of treatments for actinic keratosis of the face or scalp in Europe. *PLoS One* 2014;9(6):e96829.

Venna SS, Lee D, Stadecker MJ, Rogers GS. Clinical recognition of actinic keratoses in a high-risk population: how good are we? *Arch Dermatol* 2005;141(4):507-9.

Warino L, Tusa M, Camacho F, Teuschler H, Fleischer AB Jr, Feldman SR. Frequency and cost of actinic keratosis treatment. *Dermatol Surg* 2006;32(8):1045-9.

Webber J, Kessel D, Fromm D. Side effects and photosensitization of human tissues after aminolevulinic acid. *J Surg Res* 1997;68(1):31-7.

Weinstock MA, Bingham SF, Cole GW, Eilers D, Naylor MF, Kalivas J, Taylor JR, Gladstone HB, Piacquadio DJ, DiGiovanna JJ. Reliability of counting actinic keratoses before and after brief consensus discussion: the VA topical tretinoin chemoprevention (VATTC) trial. *Arch Dermatol* 2001;137(8):1055-8.

Weinstock MA, Bingham SF, Digiovanna JJ, Rizzo AE, Marcolivio K, Hall R, Eilers D, Naylor M, Kirsner R, Kalivas J, Cole G, Vertrees JE; Veterans Affairs Topical Tretinoin Chemoprevention Trial Group. Tretinoin and the prevention of keratinocyte carcinoma (Basal and squamous cell carcinoma of the skin): a veterans affairs randomized chemoprevention trial. *J Invest Dermatol* 2012;132(6):1583-90.

Wennberg AM, Stenquist B, Stockfleth E, Keohane S, Lear JT, Jemec G, Mork C, Christensen E, Kapp A, Solvsten H, Talme T, Berne B, Forschner T. Photodynamic therapy with methyl aminolevulinate for prevention of new skin lesions in transplant recipients: a randomized study. *Transplantation* 2008;86(3):423-9.

Werner RN, Sammain A, Erdmann R, Hartmann V, Stockfleth E, Nast A. The natural history of actinic keratosis: a systematic review. *Br J Dermatol* 2013;169(3):502-18.

Wiegell SR, Stender IM, Na R, Wulf HC. Pain associated with photodynamic therapy using 5-aminolevulinic acid or 5-aminolevulinic acid methylester on tape-stripped normal skin. *Arch Dermatol* 2003;139(9):1173-7.

Wiegell SR, Haedersdal M, Philipsen PA, Eriksen P, Enk CD, Wulf HC. Continuous activation of PpIX by daylight is as effective as and less painful than conventional photodynamic therapy for actinic keratoses; a randomized, controlled, single-blinded study. *Br J Dermatol* 2008;158(4):740-6.

Wiegell SR, Haedersdal M, Eriksen P, Wulf HC. Photodynamic therapy of actinic keratoses with 8% and 16% methyl aminolaevulinate and home-based daylight exposure: a double-blinded randomized clinical trial. *Br J Dermatol* 2009;160(6):1308-14.

Wiegell SR, Fabricius S, Stender IM, Berne B, Kroon S, Andersen BL, Mørk C, Sandberg C, Jemec GB, Mogensen M, Brocks KM, Philipsen PA, Heydenreich J, Haedersdal M, Wulf HC. A randomized, multicentre study of directed daylight exposure times of 1½ vs. 2½ h in daylight-mediated photodynamic therapy with methyl aminolaevulinate in patients with multiple thin actinic keratoses of the face and scalp. *Br J Dermatol* 2011;164(5):1083-90.

Wiegell SR, Fabricius S, Gniadecka M, Stender IM, Berne B, Kroon S, Andersen BL, Mørk C, Sandberg C, Ibler KS, Jemec GB, Brocks KM, Philipsen PA, Heydenreich J, Hædersdal M, Wulf HC. Daylight-mediated photodynamic therapy of moderate to thick actinic keratoses of the face and scalp: a randomized multicentre study. *Br J Dermatol* 2012;166(6):1327-32.[1]

Wiegell SR, Wulf HC, Szeimies RM, Basset-Seguin N, Bissonnette R, Gerritsen MJ, Gilaberte Y, Calzavara-Pinton P, Morton CA, Sidoroff A, Braathen LR. Daylight photodynamic therapy for actinic keratosis: an international consensus: International Society for Photodynamic Therapy in Dermatology. *J Eur Acad Dermatol Venereol* 2012;26(6):673-9.[2]

Wiegell SR, Fabricius S, Heydenreich J, Enk CD, Rosso S, Bäumler W, Baldursson BT, Wulf HC. Weather conditions and daylight-mediated photodynamic therapy: protoporphyrin IX-weighted daylight doses measured in six geographical locations. *Br J Dermatol* 2013;168(1):186-91.

Wiegell SR, Petersen B, Wulf HC. Topical corticosteroid reduces inflammation without compromising the efficacy of photodynamic therapy for actinic keratoses: a randomized clinical trial. *Br J Dermatol* 2014;171(6):1487-92.

Wilson EC. Cost effectiveness of imiquimod 5% cream compared with methyl aminolevulinate-based photodynamic therapy in the treatment of non-hyperkeratotic, non-hypertrophic actinic (solar) keratoses: a decision tree model. *Pharmacoeconomics* 2010;28(11):1055-64.

Wiltz KL, Qureshi H, Patterson JW, Mayes DC, Wick MR. Immunostaining for MART-1 in the interpretation of problematic intra-epidermal pigmented lesions. *J Cutan Pathol* 2007;34(8):601-5.

Wulf HC, Philipsen P. Allergic contact dermatitis to 5-aminolaevulinic acid methylester but not to 5-aminolaevulinic acid after photodynamic therapy. *Br J Dermatol* 2004;150(1):143-5.

Wulf HC, Pavel S, Stender I, Bakker-Wensveen CA. Topical photodynamic therapy for prevention of new skin lesions in renal transplant recipients. *Acta Derm Venereol* 2006;86(1):25-8.

Youl PH, Youlden DR, Baade PD. Changes in the site distribution of common melanoma subtypes in Queensland, Australia over time: implications for public health campaigns. *Br J Dermatol* 2013;168(1):136-44.

Yudovsky D, Nouvong A, Pilon L. Hyperspectral imaging in diabetic foot wound care. *J Diabetes Sci Technol* 2010;4(5):1099-113.

Zalaudek I, Piana S, Moscarella E, Longo C, Zendri E, Castagnetti F, Pellacani G, Lallas A, Argenziano G. Morphologic grading and treatment of facial actinic keratosis. *Clin Dermatol* 2014;32(1):80-7.

Zane C, Facchinetti E, Rossi MT, Specchia C, Calzavara-Pinton PG. A randomized clinical trial of photodynamic therapy with methyl aminolaevulinate vs. diclofenac 3% plus hyaluronic acid gel for the treatment of multiple actinic keratoses of the face and scalp. *Br J Dermatol* 2014;170(5):1143-50.

Zonios G, Bykowski J, Kollias N. Skin melanin, hemoglobin, and light scattering properties can be quantitatively assessed in vivo using diffuse reflectance spectroscopy. *J Invest Dermatol* 2001;117(6):1452-7.